NETWORK-BASED DISCOVERY OF MOLECULAR TARGETED AGENT TREATMENTS IN HEPATOCELLULAR CARCINOMA

A THESIS SUBMITTED TO
THE GRADUATE SCHOOL OF INFORMATICS OF
THE MIDDLE EAST TECHNICAL UNIVERSITY

BY

RUMEYSA FAYETÖRBAY

IN PARTIAL FULFILLMENT OF THE REQUIREMENTS FOR THE DEGREE OF
MASTER OF SCIENCE
IN
BIOINFORMATICS

JANUARY 2020

Approval of the thesis:

NETWORK-BASED DISCOVERY OF MOLECULAR TARGETED AGENT TREATMENTS IN HEPATOCELLULAR CARCINOMA

Submitted by RUMEYSA FAYETÖRBAY in partial fulfillment of the requirements for the degree of **Master of Science in the Department of Bioinformatics, Middle East Technical University** by,

Prof. Dr. Deniz Zeyrek Bozşahin
Dean, **Graduate School of Informatics, METU** _____

Assoc. Prof. Dr. Yeşim Aydın Son
Head of Department, **Health Informatics, METU** _____

Assoc. Prof. Dr. Nurcan Tunçbağ
Supervisor, **Health Informatics, METU** _____

Examining Committee Members:

Prof. Dr. Tolga Can
Computer Engineering, METU _____

Assoc. Prof. Dr. Nurcan Tunçbağ
Health Informatics, METU _____

Assist. Prof. Dr. Aybar Can Acar
Health Informatics, METU _____

Assoc. Prof. Dr. Yeşim Aydın-Son
Health Informatics, METU _____

Assist. Prof. Dr. Ceren Sucularlı
Graduate School of Health Sciences, Hacettepe University _____

Date: **13.01.2020**

I hereby declare that all information in this document has been obtained and presented in accordance with academic rules and ethical conduct. I also declare that, as required by these rules and conduct, I have fully cited and referenced all material and results that are not original to this work.

Name, Last Name: RUMEYSA FAYETÖRBAY

Signature : _____

ABSTRACT

NETWORK-BASED DISCOVERY OF MOLECULAR TARGETED AGENT TREATMENTS IN HEPATOCELLULAR CARCINOMA

Fayetörbay, Rumeysa
MSc, Department of Bioinformatics
Supervisor: Assoc. Prof. Dr. Nurcan Tunçbağ

January 2020, 114 pages

Hepatocellular carcinoma (HCC) is one of the most-deadly cancers and the most common type of primary liver cancer. Multikinase inhibitor Sorafenib is one of FDA approved targeted agents in HCC treatment. PI3K/AKT/mTOR pathway is altered in about 51% of HCC; hence, understanding how Sorafenib and PI3K/AKT/mTOR pathway inhibitors act at signaling level is crucial for targeted therapies and to reveal the off-target effects. In this work, we use gene expression profiles (GEPs) of HCC cells (Huh7 and Mahlavu) which were treated with seven different agents and their combination. Our aim is to reveal the important targets and modulators in agent treatments by inferring the dysregulation of Interactome. In other words, we search for the mechanism of action of the agents in a network context beyond the list of genes. For this purpose, we use the DeMAND (Detecting Mechanism of Action based on Network Dysregulation) algorithm developed by Califano Lab. DeMAND compares GEPs and assesses the change in the individual interactions from weighted interactome obtained from STRING database. As a result, we reconstructed 18 agent-specific networks from each GEPs. Each gene and interaction within these networks have a value signifies how strongly these genes are affected from the chemical network perturbation. Then, we found enriched pathways in each network. We initially compared the networks of single agents and their combination; i.e. PI3Ki-α, Sorafenib and their combined treatment. Then, we compared all networks simultaneously. The simultaneous comparison of the reconstructed networks at gene and pathway levels shows that several pathways and proteins are commonly affected across agent treatments (e.g., Wnt, HIF-1, Notch pathways and MCM proteins, mTOR). On the other hand, some pathways are only affected in a specific agent treatment (e.g., SNARE interactions).

Keywords: Hepatocarcinoma Network Reconstruction, Therapeutic Agents, DeMAND Network Modelling Algorithm, Omics Data Integration, Targeted Cancer Therapy

ÖZ

HEPATOSELLÜLER KARSİNOMDA HEDEFE YÖNELİK MOLEKÜLER AJAN TEDAVİLERİNİN AĞA DAYALI KEŞFİ

Fayetörbay, Rumeysa
Yüksek Lisans, Biyoenformatik Yüksek Lisans Programı
Tez yöneticisi: Doç. Dr. Nurcan Tunçbağ

Ocak 2020, 114 sayfa

Hepatosellüler karsinom en ölümcül kanserlerden biridir ve en sık görülen primer karaciğer kanseri türüdür. Multikinaz inhibitörü Sorafenib, hepatosellüler kanser tedavisindeki FDA onaylı hedeflenmiş ajanlardan biridir. PI3K/AKT/mTOR yolağı hepatosellüler karsinomun yaklaşık % 51'inde değiştirilir, bu yüzden Sorafenib ve PI3K/AKT/mTOR yolağı inhibitörlerinin sinyal verme seviyesinde nasıl etki ettiğinin anlaşılması, hedefe yönelik terapiler için çok önemlidir ve yan etkilerini (hedef dışı etkiler) ortaya çıkarır. Bu çalışmada biz yedi farklı ajan ve onların kombinasyonu ile tedavi edilen hepatosellüler karsinom hücrelerinin (Huh7 ve Mahlavu) gen ekspresyon profillerini (GEP) kullanıyoruz. Amacımız, ajan tedavilerindeki önemli hedefleri ve modülatörleri moleküler etkileşimlerin düzensizliğini anlayarak ortaya çıkarmaktır. Başka bir deyişle, biz ajanların etki mekanizmasını genler listesinin haricinde bir ağ kaynağında araştırıyoruz. Bu amaçla Califano Lab tarafından geliştirilen DeMAND (Ağ bozulmasına dayalı etki mekanizması belirleme) algoritmasını kullanıyoruz. DeMAND, GEP karşılaştırır ve STRING veri tabanından elde edilen ağırlıklı interaktomdaki özgün etkileşimlerin değişimini değerlendirir. Sonuç olarak, herbir gen ekpresyon profilinden ajana özel 18 ağ yeniden oluşturduk. Bu ağlar içindeki her gen ve etkileşimin değeri bu genlerin kimyasal ağ bozulmasından ne kadar fazla etkilendiğini gösterir. Daha sonra, biz her bir ağda zenginleştirilmiş yolaklar bulduk. İlk olarak tek ajan tedavilerinin ağlarını ve bu ajanların kombinasyonunu karşılaştırdık; yani PI3Ki-α, Sorafenib ve bunların birleştirilmiş tedavi şeklini. Ardından, tüm ağları eşzamanlı olarak karşılaştırdık. Yeniden yapılandırılmış ağların gen düzeyinde ve yolak seviyesinde eşzamanlı karşılaştırması ajan tedavilerinde çeşitli yolak ve proteinlerin yaygın olarak etkilendiğini göstermektedir (örneğin, Wnt, HIF-1, Notch yolakları ve MCM proteinleri, mTOR). Öte yandan, bazı yolaklar sadece belirli bir ajan tedavisinde etkilenir (örneğin, SNARE interaksiyonları).

Anahtar Sözcükler: Hepatosellüler Karsinom Yeniden Ağ Kurma, Tedavi Ajanları, DeMAND Ağ Modelleme Algoritması, Omik Veri Bütünleşmesi, Hedefe Yönelik Kanser Terapisi

To my beloved mother

and my dear family,

ACKNOWLEDGMENTS

First and foremost, I would like to express my deepest gratitude to my supervisor, Assoc. Prof. Dr. Nurcan Tunçbağ for her continuous trust, belief, support, patience and valuable advices which enable to enlighten my academic journey. I will always be grateful for giving me the chance of being a member of her research group. I am also eternally grateful to my previous advisor, Prof. Dr. Rengül Çetin-Atalay not only for sharing her data, but also her enthusiasm and guidance. I am greatly indebted to her. This thesis study would not have been possible without these two precious academic advisors.

Besides, I would like to thank my thesis committee members Prof. Dr. Tolga Can, Assoc. Prof. Dr. Yeşim Aydın-Son, Assist. Prof. Dr. Aybar Acar and Assist. Prof. Dr. Ceren Sucularlı for their valuable time, criticism and advices. I would also like to thank to all of the people who contributed significantly to me throughout my studies, including my professors at METU. Particularly, I owe sincere special thanks to Prof. Dr. Tolga Can, my role model, who has an endless support and great ideas all the time. I consider myself lucky to take his course.

In addition to my professors, I would also like to thank all of my friends who believe in me, specifically Ayşegül Tombuloğlu, Ozan Koçak, Deniz Barer, Hacer Bilü, Burak Demiralay, Sema Zabcı for their friendship and encouragement which is priceless. Additionally, I owe special thanks to Prof. Dr. Sevgi Beşışık, for her intellect and great efforts. I really appreciate her time and consideration, and always admire her. This accomplishment would not have been possible without her.

Last but not least, I would like to thank my beloved family. I appreciate everything you have done. My beautiful mother, you are my angel, soulmate, best friend and everything. Without your endless motivation and energy, I could not write even a single sentence. My dear father, without your support and valuable advices, I could not have succeeded. And my one and only sister, source of joy and happiness, thank you for everything sweetheart, indeed. Ultimately, every single one of you deeply touched my heart and soul. Nothing would be possible without you. Many thanks!

TABLE OF CONTENTS

LIST OF TABLES

LIST OF FIGURES

LIST OF ABBREVIATIONS

Akti-1/2	Akt Inhibitor VIII
Akti-2	Akt Inhibitor XII
AMPK	5' AMP-activated Protein Kinase
CaM	Calmodulin, Calcium-modulated protein
DeMAND	Detecting Mechanism of Action by Network Dysregulation
EBV	Epstein-Barr Virus
EGF	Epidermal Growth Factor
FDA	U.S. Food and Drug Administration
GEP	Gene Expression Profile
GO	Gene Ontology
HBV	Hepatitis B Virus
HCC	Hepatocellular Carcinoma
HCV	Hepatitis C Virus
HHV	Human Herpes Virus
HIF-1	Hypoxia-Inducible Factor 1
HIV	Human Immunodeficiency Virus
HPV	Human Papilloma Virus
HTLV	Human T-cell Lymphotropic Virus
IGF	Insulin-Like Growth Factor
KLD	Kullback-Leibler Divergence
KLD.p	P-value of Kullback-Leibler Divergence
MAPK	Mitogen-Activated Protein Kinase
MCM	Minichromosome Maintenance Protein Complex
MoA	Mechanism of Action
mTOR	Mechanistic Target of Rapamycin
NASH	Non-Alcoholic Steatohepatitis
ORA	Overrepresentation Enrichment Analysis
PDGFR	Platelet-Derived Growth Factor Receptor
PI3K	Phosphoinositide 3-Kinases
PI3Ki-α	Phosphoinositide 3-Kinases Alpha Isoform Inhibitor
PPI	Protein-Protein Interaction
SHH	Sonic Hedgehog
VEGF	Vascular Endothelial Growth Factor
WHO	World Health Organization

CHAPTER 1

INTRODUCTION

Cancer is a general term for diseases that are responsible for the uncontrolled division and proliferation in the cells. Through the invasion, nearby tissues might be adversely affected. Previously known carcinogenesis factors are infectious carcinogens (HIV, HPV, EBV, HBV, HCV, HHV, HTLV, *helicobacter pylori*, etc.), physical carcinogenic agents (radiation and UV light), and chemical carcinogenic agents (tobacco smoking, arsenic, benzene, asbestos, acetaldehyde, aflatoxins, etc.) (Blackadar, 2016; Plummer et al., 2016). Cancer is one of the top causes of death globally. According to the World Health Organization (WHO) reported fact sheet, almost 10 million deaths were occurred due to the cancer in 2018. Liver cancer has the fourth highest cancer-related mortality in the WHO 2018 report (with nearly 800.000 deaths). In addition to the statistics of liver cancer, the incidence rate of the liver cancer alters diversely from distinct regions of the world and the highest frequency of prevalence is detected in Eastern Asia (L. Lin et al., 2019).

Roughly, a cancer which originates from hepatocytes is identified as primary liver cancer. The most common type of primary hepatic malignancy is hepatocellular carcinoma (HCC). There are several factors that increase the risk of HCC including the infection of hepatitis B or hepatitis C virus, cirrhosis, excessive alcohol, aflatoxins, inherited liver diseases (Hemochromatosis, Wilson's disease, etc.), nonalcoholic fatty liver disease, type II diabetes and obesity (Balogh et al., 2016). Treatments of hepatoma depend mainly on the stage of the disease, age of the individual, and the general health condition of the patient. As treatment options, there are some different techniques including surgery, chemotherapy, radiation, liver transplantation, immunotherapy, and targeted therapy. The classic chemotherapeutic agents are doxorubicin, cisplatin and 5-fluorouracil in liver cancer. Although a single agent or combination of these agents decrease the size of the tumor, tumor come back again in a period of time (S. Lin, Hoffmann, & Schemmer, 2012; Park et al., 2006). As Balogh et al. claimed that, one of the recent methods in hepatoma treatment is targeted therapy which is used to target specific molecules in cancerous cells. It is different from chemotherapy in the aspect of healthy cell damage. Chemotherapy attacks the cancer systemically, destroying both healthy normal cells and tumorigenic cells that divides quickly. Unlike chemotherapy, targeted therapy blocks the growth of cancerous cells by interfering with proteins that are acting in the processes of tumor progression and

proliferation of cancer. Hence, targeted therapy aims to have fewer off-target effects that decrease the given harm to the normal body cells (Balogh et al., 2016).

Sorafenib, Nexavar as a trade name, is one of the FDA approved targeted drugs used in HCC treatment. It is a multikinase inhibitor drug that primarily inhibits Raf, LIMK, VEGFR and PDGFR kinases (Lai et al., 2018). Due to the repressing functional activity of Raf and other receptor tyrosine kinases by suppressing phosphorylation of Raf/MEK/ERK pathway, Sorafenib is an efficient alternative while targeting cell proliferation and angiogenesis (Adnane, Trail, Taylor, & Wilhelm, 2006). Yet, tumor recurrence in most of the patients is arose due to increasingly proliferative signals; hence, other targeted drugs in combination with Sorafenib is a necessity.

In order to compensate for the inhibited pathway, cancerous cells may upregulate alternative existing pathways as in the case of PI3K/AKT/mechanistic target of rapamycin (mTOR) signalling pathway. This proliferative pathway is much altered in primary liver cancer cells (Gedaly et al., 2012). The upregulation of angiogenic signals have significant roles in the acquired resistance to Sorafenib; thus, understanding how Sorafenib and its combination with PI3K/AKT/mTOR pathway inhibitors act is vital for targeted drug therapies and to reveal the off-target effects of the drugs.

From the pharmacological point of view, mechanism of action (MoA) of a compound describes the biochemical reactions that interactor and effector proteins interact, enabling to produce the pharmacological effect of the drug. To determine on-target and off-target effects of a drug, MoA interrogation questioning is indispensable (Scannell, Blanckley, Boldon, & Warrington, 2012). Whether there is a significant progress in characterization of MoA, drug discovery pipelines' productions will be considerably arisen (Woo et al., 2015). In the aspect of drug response, MoA is critical to detect the interaction dysregulation of a drug in a network–based content beyond the list of genes.

DeMAND (Detecting Mechanism of Action based on Network Dysregulation) is a network modelling algorithm to identify the targets and modulators by inferring the dysregulation of Interactome subsequent molecular targeted therapeutic perturbation. As an alternative to differential gene expression analysis, DeMAND searches for the MoA of the drugs, inhibitors of drugs and their combination in a network contextual perspective. The algorithm compares GEPs before and after the drug perturbation, and determines the alteration in the individual interactions from STRING Interactome (Woo et al., 2015).

In this thesis study, our main purpose is to reconstruct drug specific networks from GEPs, and to identify significant targets in treatments of molecular targeted agents following the dysregulation of Interactome. Toward this aim, small molecule inhibitors that are targeting the cascade of PI3K/AKT/mTOR, including pan-PI3K inhibitors, isoform-specific PI3K inhibitor, and isoform-specific or non-specific AKT inhibitors, and mTOR inhibitor were analyzed. We used gene expression profiles (GEPs) of Huh7 and Mahlavu cells that were treated with multiple distinct drugs,

inhibitors and their combination. Both Huh7 and Mahlavu cells were derived from HCC cell lines used in this work. Huh7 is a well-differentiated liver cell. However, Mahlavu hepatoma cells are poorly-differentiated.

In our study, 18 drug specific networks were reconstructed by using DeMAND approach. Each gene and interaction within these networks corresponds to a certain value that demonstrates the level of response to the compound perturbation. Addition to network reconstruction and analyses, enriched pathways were analyzed in each network. The networks obtained from both single drug and combination of the drugs were compared at gene and pathway levels by applying functional enrichment analyses. As a result, some pathways/proteins were only affected from a specific drug; whereas, the majority of the pathways are commonly affected from drug treatments.

This thesis is divided into the following chapters:

In Chapter 2, we primarily provided the literature review including the information about HCC, Huh7 and Mahlavu cell lines, and the survival rate of liver cancer. Furthermore, we gave detailed information about PI3K/AKT/mTOR pathway, drugs and inhibitors, protein-protein interaction databases, and DeMAND algorithm.

In Chapter 3, we described the experimental dataset and interactome used in this study. In addition to the input of our network modeling algorithm, DeMAND analysis, functional enrichment analysis, network visualization criteria were given in detail throughout this chapter.

In Chapter 4, we initially gave the statistical outcomes of our reconstructed hepatocarcinoma networks provided by our network modeling algorithm, DeMAND. Apart from the statistical results, literature targets of drug treatments/inhibitors are stated to identify target genes and to check the presence of these genes in the reconstructed networks. For determining common characteristics between Sorafenib-related multiple networks and identifying potential similarities, overlapping genes are analyzed. Additionally, we demonstrated all hepatoma networks and several resulting functional analyses outcomes of this study that elucidate the inclusion of the reconstructed networks in pathways and in significant terminology insights to reveal fundamental biological signatures in the light of the literature support.

Finally, we conclude our thesis study in Chapter 5 with a general overview and discuss several of the striking substantial results supporting with literature. These outcomes are based on our direct findings from our analyses (Chapter 4). Additionally, we suggest potential several candidate targeted agents to improve our targeted therapy approach as our future direction.

CHAPTER 2

LITERATURE REVIEW

2.1 Comprehending the Underlying Systems Biology of Silent Killer, Hepatocellular Carcinoma

Cancer is a major cause of death worldwide with 9.6 million deaths reported in 2018. Lung, colorectal, stomach, liver and breast cancer are the most observed types of cancer-related deaths (WHO 2018 reported facts). According to the cancer statistics in 2018, the incidence of liver cancer continues to increase in females; whereas, no substantial difference observed in males (Siegel, Miller, & Jemal, 2018). This incidence considerably augments more than other cancer types for both sexes (Siegel, Miller, & Jemal, 2019).

HCC is the most common type of hepatocarcinoma cells that are malignant tumors of the liver. Hepatocarcinoma has multiple distinct etiology. Different factors that increase the risk of HCC are including the viral infection (HBV and HCV), alcohol, nonalcoholic fatty liver disease (e.g. non-alcoholic steatohepatitis (NASH)), cirrhosis, autoimmune disorders, cholestatic disorders, metabolic disorders (e.g. Iron metabolism disorder- Hemochromatosis, Wilson's disease), and obesity (Balogh et al., 2016; Pellicoro, Ramachandran, Iredale, & Fallowfield, 2014). As a treatment option, chemotherapy demonstrates low level of impact because of the heterogeneity of hepatocarcinoma (El-Serag, 2011). In order to better understand hepatoma, D'Alessandro et al. suggested using gene expression and proteomics profiling data with network models from the perspective of systems biology approach (D'Alessandro, Meyer, & Klingmüller, 2013). Additionally, there is a very recent study that identify potential hepatocarcinoma drug targets with network-based analysis and machine-learning based model, support vector machine (SVM). Concisely, Tong et al. initially map distinct genes to both human protein-protein interaction network and cellular signaling network. Following the mapping process, statistical analyses of networks were evaluated and developed a new methodology that predict drug target hepatoma genes. SVM-based analysis to build drug target hepatoma predictor is done regarding the dependency scores of networks (Tong, Zhou, & Wang, 2019).

There are two hepatocarcinoma cell lines used in this work. Huh7 is a well-differentiated liver cell line. In 1982, it was initially isolated from a liver tumor in a Japanese man (Pridgeon et al., 2016). Huh7, epithelial-like malignant, cells are

morphologically similar to the healthy liver cells. Their differences from the hepatocytes are their smaller size and structural organization. Well-differentiated Huh7 expression is observed in the early stage of HCC and might be rarely in the advanced levels (Yuzugullu et al., 2009). Mahlavu is a poorly-differentiated liver cell line. It was taken from a human genome. Surprisingly, it is mainly made up of L1 repeat elements (HHCM NCBI, 2019). On the contrary, poorly differentiated Mahlavu cells have low cytoplasm and variable structure. The expression of Mahlavu is detected in the advanced levels of HCC proliferation (Keskin et al., 2013; Yuzugullu et al., 2009).

2.2 The Survival Rate of Primary Liver Cancer

According to the American Cancer Society, the five-year survival percent ratio for liver cancer is approximately 18%. The percentage depends on the stage and the region of the liver cancer. Whether the cancerous region is limited to a certain location within the liver, the percentage is approximately 31% for the next 5 years. Surgical operations are the first options when the cancerous part is only in the liver and the tumor size is feasible. If the cancer is expanded to other places or organs, the overall rate is decreased dramatically for the following 5 years (American Cancer Society Facts Report in 2019).

Sorafenib is the first systemic agent approved by the FDA in hepatocarcinoma treatment (when HCC cannot be treated with surgery) and extends the survival rate up to 10.7 months (in European and United States regions) and 6.5 months (in Pacific Asia) (Cheng, Hsu, Shen, Shao, & Hsu, 2014). Since Sorafenib has wide range of targets, systematic mechanism of action is poorly understood. It primarily inhibits Raf, LIMK, VEGFR and PDGFR kinases. Additionally, it blocks tumor proliferation and angiogenesis and induces apoptosis in tumorigenic cells. The alteration is about 40% in PI3K/AKT/mTOR pathway for primary liver cancer (L. Liu et al., 2006). As a result, understanding how Sorafenib and its combination with PI3K/AKT/mTOR pathway inhibitors act is vital for targeted drug therapies and to reveal the side effects of the drugs.

2.3 Detecting Mechanism of Action by Network Dysregulation, DeMAND Algorithm

In order to reveal the significant targets and modulators, the dysregulation of Interactome is analyzed across different drug treatments. In the aspect of drug response, mechanism of action (MoA) is crucial to detect the interaction of a drug dysregulation in a network–based content. Basically, DeMAND is an algorithm to model networks of molecular interactions for specific cell lines. As required inputs for DeMAND, gene expression profiles obtained from drug and control samples and a molecular interaction network is necessary. The algorithm compares GEPs

before and after the molecular targeted agent perturbation and tests the edge dysregulation in the Interactome. Similarly, the change that corresponds to all of the interactions from STRING database (as Interactome) is calculated. In order to assess the edge dysregulation, the probability density difference before and after drug perturbation is calculated by using Kullback-Leibler divergence (KLD). Statistical significance for each interaction is determined by the shuffling of gene pairs. The combined dysregulation of interactions for each gene is detected by the p-values of all of the interactions. Molecular targeted therapeutic agent specific networks from each GEPs are reconstructed. The output of DeMAND contains a gene list and their level of dysregulation with the corresponding statistical significances in the reconstructed network (Woo et al., 2015).

There are multiple known methods to detect mechanism of action in the literature. Although experimental detection of MoA is labor-intensive and less informative, affinity purification and chromatography assay are leading of this technique (Aebersold & Mann, 2003; Ito et al., 2010; Woo et al., 2015). Together with the previously mentioned experimental techniques, various computational methods are presented. Virtual screening, chemical-based computational approach, seek promising candidates which bind to drug targets (Miller, 2002; Rollinger, Stuppner, & Langer, 2008). Similarity ensemble approach (SEA) is one of the chemoinformatics-based methods. Predicted false-positive result rates are much higher than the optimal for the technique (Lounkine et al., 2012). With the help of omics data taking into account, after the drug perturbation, gene expression profiles which set differentially expressed genes to the corresponding MoA are presented. One of the substantial disadvantages of the method might be unaltered level of expression of mRNA while subjected to drug despite changing activity of protein (subsequent to perturbation of drug) (Lamb et al., 2006; Woo et al., 2015).

By performing reverse engineering techniques, network-based methods are developed as leading methods for MoA characterization. To summarize, there are 2 common mechanisms of network-based methodologies, namely creating a reversely engineered regulatory network, and deducing evaluation of dysregulated edges after agent perturbations. One of the current studies of network-based approaches is mode-of-action by network identification, MNI algorithm. This algorithm build a molecular interaction network by using reverse-engineered network model (in particular, multiple linear regression models) to whole-genome expression profiles. Subsequently, gene expression array data are identified by the linear models to detect the targeted genes and cascade inclusion (Bernardo et al., 2005; Woo et al., 2015).

Another network-based method is the interactome dysregulation enrichment analysis, IDEA algorithm. Basically, regulatory interaction network is created by Bayesian evidence integration approach. In order to detect drug MoA, the alteration of all interactions provided by microarray expression profiles in the molecular network is examined. The statistical significance of the alteration of dysregulated network perturbation is calculated by mutual information. The targets

of the drugs are deduced from the algorithm while checking for the dysregulated interactions of the genes in the network. To detect the phenotype of tumor, this algorithm is also performed. As a limitation, the systems biology-related algorithm need to have sample size more than 100 which makes it unsuitable to choose for most of the datasets (Mani et al., 2008; Woo et al., 2015).

2.4 Targeting Raf/MEK/ERK Pathway and Parallel Alternative Signaling Cascade, PI3K/AKT/mTOR Pathway

Genomic analysis is occurred for examining hepatocarcinoma cells which reveal some of the pathways have abnormalities (D'Alessandro et al., 2013) and these aberrancies observed in the pathways may cause hepatocarcinogenesis (Whittaker, Marais, & Zhu, 2010). Hanahan and Weinderberg highlighted that the aberrancies which are detected in cascades (especially, kinase signaling pathways) lead to provoke multiple hallmarked phenotypes of cancer, namely angiogenesis, survival, invasion and metastasis, motility, responses due to DNA damage, and proliferation (Gross, Rahal, Stransky, Lengauer, & Hoeflich, 2015; Hanahan & Weinberg, 2011). In one of the recent studies, Castelli et al. highlighted that PI3K/AKT/mTOR pathway is one of the most changed signaling cascades in hepatocarcinoma with 51% aberrancy rate. Additionally, Ras-mediated/Raf/MEK/ERK signaling pathway is another altered cascade that has shown 43% aberrance ratio in HCC cases (Castelli, Pelosi, & Testa, 2017).

PI3Ks (Phosphatidylinositol-4,5-bisphosphate 3-kinases) are kinases that are associated with cellular processes such as proliferation, cell growth, differentiation, cell survival, motility and so on (Zhu, Ke, Xu, & Jin, 2019). There are three different classes of PI-3 kinases as Class I, Class II and Class III. PI3Ks phosphorylate the 3'position hydroxyl group of the inositol ring of phosphoinositides. There are two subunits of Class I PI-3 kinases; regulatory and catalytic subunits as p85 and p110, respectively. The catalytic isoforms of Class I PI3Ks have 4 isoforms PI3Kα, PI3Kβ, PI3Kδ, and PI3Kγ. Activation of tyrosine kinase receptor via growth factors promotes PI3K activation. PI3K phosphorylates PIP2 (Phosphatidylinositol 4,5-bisphosphate) to PIP3 (Ptdlns(3,4,5)P3). PTEN (Phosphatase and tensin homolog) is a tumor suppressor that regulates dephosphorylating of PIP3 to PIP2 (Davis, Lehmann, & Li, 2015; Jean & Kiger, 2014).

AKT (also known as Protein kinase B) is a serine/threonine protein kinase that is included in the diverse cellular functions such as proliferation, cell growth, apoptosis, cell survival, etc. Following the recruitment to the plasma membrane, AKT is phosphorylated and gets activated. AKT is comprised of three isoforms; AKT1, AKT2, and AKT3 (Abeyrathna & Su, 2015; Szymonowicz, Oeck, Malewicz, & Jendrossek, 2018). mTOR is the abbreviation of mechanistic target of rapamycin (originally mammalian target of rapamycin) that is a serine/threonine

protein kinase regulates several processes including cell proliferation, survival, growth, transcription, motility, etc. mTOR is a member of PI3K-related kinases. mTOR has two different intracellular complexes as mTOR complex 1 (mTORC1) and mTOR complex 1 (mTORC2), respectively. In cancer, mTOR deregulation is observed (Abeyrathna & Su, 2015; Saxton & Sabatini, 2017).

PI3K/AKT/mTOR signaling pathway is a crucial signal transduction cascade that regulates several physiological processes, namely cellular growth, proliferation, anabolic reactions, survival, cell cycle, motility, glucose metabolism (Gerson, Caimi, William, & Creger, 2018; H. Q. Liu et al., 2019). In addition to the critical processes, this significant pathway is activated by the following compounds such as insulin, SHH, IGF, CaM and EGF. On the other hand, PTEN inactivates the signaling pathway by dephosphorylating PIP3 into PIP2. Other inhibitors of this signaling cascade are Hb9 (transcription factor), GSK3ß, respectively (Xie et al., 2019). PTEN acts as a tumor suppressor for the downstream of the PI3K/AKT signalling cascade. Very briefly, activation of tyrosine kinase receptor via growth factors promotes PI3K activation. PI3K phosphorylates PIP2 and converting it into PIP3. Following the translocation mechanisms to the plasma membrane, AKT is phosphorylated and turns into activated form. mTORC1, downstream effector protein of AKT, is stimulated by phosphorylation of AKT (Chamcheu et al., 2019).

Raf/MEK/ERK signaling pathway is another significantly altered cascade that has a role in hepatocarcinogenesis. This pathway regulates several various processes, namely cell survival, differentiation, apoptosis, proliferation, and cellular senescence (Knight & Irving, 2014; Wen et al., 2019; Yang & Liu, 2017). From the perspective of hallmarks of cancer, Maurer et al clarify that Raf kinases contribution with Ras-mediations and aberrations in Raf (B-raf and C-raf activations) lead to the transformation of hepatotumorigenesis (Maurer, Tarkowski, & Baccarini, 2011). Further, Sorafenib is an essential drug which targets the cascade of Raf/MEK/ERK. It primarily inhibits Raf kinases, in particular B-Raf and C-Raf, and blocking the activity of the other cell surface kinase receptors PDGFR, IGFR, VEGFR. As a consequence, the physiological processes of angiogenesis and tumor growth is both suppressed by multikinase inhibitor, Sorafenib (Yang & Liu, 2017).

2.5 Molecular Targeted Therapeutic Agents and Multiple Inhibitor Compounds Used in This Hepatocellular Carcinoma Study

Except Sorafenib, there are novel therapeutic hepatocarcinoma drug agents (in particular, Regorafenib, Lenvatinib, Cabozantinib, Ramucirumab) which are utilized in the treatment process (Kudo, 2019). Yet, the alteration of the survival rate is insubstantial. Thereby, there is an imperative necessity for newly developed effective drug targets during the treatment stages of hepatocarcinoma (Tong et al., 2019).

Sorafenib is a derivative of phenylurea and nicotinamide (NAM). The mechanism of action of Sorafenib is as a protein kinase inhibitor (Wilhelm et al., 2004). It basically inhibits tyrosine kinase, a phosphate group from ATP is taken to other amino acids (serine/threonine), through elimination of its signal transferring into the tumors. It is a multikinase inhibitor that is included in the physiological processes of tumor angiogenesis, and tumor apoptosis (Kudo et al., 2016). It inhibits intracellular kinases (e.g: Raf, B-Raf, C-Raf), cell surface kinases LIMK, VEGFR, PDGFR, KIT, FLT-3, and RET kinases. It further targets tumor cell proliferation and tumor growth. It is involved in the treatment of certain cancers including renal cell carcinoma (primary kidney cancer), radioactive iodine therapy-refractory differentiated thyroid carcinoma, and hepatocellular carcinoma. Sorafenib is an essential drug that simultaneously targets the cascade of Raf/MEK/ERK (Adnane et al., 2006; Iavarone et al., 2011; Lencioni et al., 2014). The most common off-target effects of Sorafenib is fatigue, nausea, abdominal pain, diarrhea, hand-foot skin reaction, and hypertension. Heart attack and liver failure might be arisen as severe reactions of Sorafenib (Karovic, Shiuan, Zhang, Cao, & Maitland, 2016).

Sirolimus, Rapamune as a trade name, was firstly used as an antifungal agent. Dr. Surendra Sehgal has isolated it from *Streptomyces hygroscopius* samples in 1972. The active compound was known as Rapamycin due to the native name of the founding island as Rapa Nui (Sehgal, 2003). In addition to the founding and historical information, it has antiproliferative and antineoplastic properties because of suppression of the target of rapamycin, mTOR. It prevents renal transplant rejection. It is also involved in the treatment of such a rare disease, lymphangioleiomyomatosis. The mechanism of action of Sirolimus is an mTOR inhibitor immunosuppressant (Koul & Mehfooz, 2019; Zhan et al., 2018). It basically inhibits activation of T cells that has a role in antigenic and cytokine production (Sehgal, 2003). It binds to FK-binding protein 12 abbreviated as FKBP-12, to produce a complex (Koul & Mehfooz, 2019). The immunosuppressant complex binds to mTOR, and decreasing the activating of mTOR. As a result, the proliferation of cytokine-driven T cell is blocked and cell cycle is arrested at the G1 phase and no transition is observed from G1 to S phase (Sehgal, 2003). Some of the most adverse effects of Sirolimus in lymphangioleiomyomatosis is chest pain, nausea, headache, myalgia, abdominal pain, acne, diarrhea, dizziness, and nasopharyngitis. Some of the most adverse reactions of Sirolimus in preventing of renal transplant rejection is urinary tract infection, thrombocytopenia, anemia, fever, edema, abdominal pain, hypertension, nausea, headache, and arthralgia (Rapamune Sirolimus FDA accessible data).

Wortmannin is a fungal steroid compound that is isolated from *Penicillium funiculosum*. It has an impact upon several pathways by inhibiting PI3Ks. The irreversible inhibition mechanism of PI3Ks is through a covalent bond between the target and the inhibitor; thus, Wortmannin is a covalent inhibitor of PI3Ks. It is a highly cell permeable metabolite. It is a pan-PI3K inhibitor that targets PI3K-

related proteins including PI4K, ATM, DNA-PK, and ATR. It also blocks the proliferation of lymphocytes (Deane & Fruman, 2004).

LY294002, (2-4-morpholinyl-8-phenlchromone), is a synthetic cell permeable inhibitor of PI3K. It was obtained as a pan-PI3K inhibitor by Eli Lily. It acts as a reversible inhibitor and it is a stable compound. LY294002 is less potent than the previous PI3K inhibitor, Wortmannin. After the decreasing level of PI3K by LY294002, the arrest of the cell cycle is induced and subsequently occurring the apoptosis (Mcnamara & Degterev, 2011). Furthermore, it inhibits the BET bromodomain proteins (BET inhibitors) including BRD2, BRD3, and BRD4. It also blocks the proliferation of B-cells and T-cell lymphocytes (Dittmann et al., 2014).

Akti-1/2, abbreviation of AKT Inhibitor 1/2, also known as AKT Inhibitor VIII, is an allosteric reversible inhibitor that targets AKT1 and AKT2. AKT Inhibitor VIII promotes apoptosis and inhibits cell growth, and survival in human hepatoma cells. Additionally, Akti-1-2 is isozyme-selective and it is cell permeable (Gilot, Giudicelli, Lagadic-Gossmann, & Fardel, 2010; Nitulescu et al., 2016; Zhang, Yang, Qu, Zhou, & Jiang, 2016).

Akti-2, also known as AKT Inhibitor XII, is an allosteric inhibitor that specifically targets AKT2. Akti-2 is isozyme-selective and it is cell permeable. The blocking is dependent upon the domain of pleckstrin homology, which binds phosphatidylinositols. These domains play significant roles in intracellular signaling (Gilot et al., 2010; Nitulescu et al., 2016).

PI3Ki-α is an isoform specific PI3K inhibitor that targets PI3Ki-α. PIK3CA, PIK3CB, PIK3CD, and PIK3CG are the cell signaling genes of PI3K. These genes encode distinct PI3K isoforms as PI3K-α, PI3K-β, PI3K-δ, and PI3K-γ, respectively. Class I PI-3 kinases have two subunits regulatory and catalytic subunits as p85 and p110. From the point of cancer approach and its progress, PI3Ki-α has a high priority because of the occurring mutations in PI3KCA gene and raised expression level of p110α protein in cancerous cells (Yadav et al., 2016).

2.6 Protein-Protein Interaction Databases

Proteins are essential macromolecules that are involved in several cellular mechanisms including replication, cell signalling, metabolic reactions, transcription, signal transduction, developmental control, and so on. Detecting the interactions of the proteins helps to identify the activity of protein, its function, and its role in various biological processes. The whole collection of the interactions of the proteins in a cell is called Interactome.

The increasing number of protein-protein interaction (PPI) data that are obtained from both experiments (high-throughput and low-throughput experiments) and in

silico based predictions are stored into the databases. PPI data are analyzed through various methods including protein microarray, yeast two-hybrid system, X-ray crystallography, co-immunoprecipitation, nuclear magnetic resonance spectroscopy, sequence-based and structure-based techniques, and so on. The number of public PPI databases is more than 130 and most of the databases store distinct type of characteristics of PPI (Taghizadeh, Safari-Alighiarloo, & Tavirani, 2015).

Search Tool for the Retrieval of Interacting Genes/Proteins, also known as STRING, is a database that retrieves and integrates different kinds of information from several PPI resources for many organisms. A score between 0 and 1 which indicates confidence score of each PPI is assigned to the associations of the proteins. STRING database covers 24.6 M proteins from 5090 organisms; over 2.0 M interactions in version 11.0. STRING is composed of seven evidence channels including the experiments, the curated databases, the text-mining, the co-expression, the neighborhood, the fusion, and the co-occurrence (Szklarczyk et al., 2018).

The experimental data of STRING is obtained from the databases including BIND, BioGRID, DIP, HPRD, IntAct, MINT, and PID (Szklarczyk et al., 2018). BIND, known as Biomolecular Interaction Network Database, is a specialized database which deposits both biomolecular interactions and complexes and also the cascades (Bader, Betel, & Hogue, 2003). Moreover, Biological General Repository for Interaction Datasets, abbreviated as BioGRID, is a curated database that stores PPI, the interactions of genetic, and chemical for multiple organisms (Stark et al., 2006). Additionally, DIP, Database of Interacting Proteins, is a curated biological database which archives PPI obtained from the experiments (Xenarios et al., 2000). Besides, Human Protein Reference Database, abbreviated as HPRD, is a curated database on human proteomic data that mainly includes PPI, post-translational modifications, and so on (Keshava Prasad et al., 2009). Further, IntAct, contains both curated and direct data, is a particular database which deposits the information of PPI and the analysis of these interactions (Kerrien et al., 2012). Also, Molecular Interaction Database, shortly MINT, is a storage of curated molecular interactions including PPI in distinct representations (Licata et al., 2012). In addition to these databases, PID, abbreviated version of Pathway Interaction Database, is a curated database that primarily collects the regulatory cellular mechanisms, signalling processes and cascades in humans (Schaefer et al., 2009).

The curated data is collected from BioCyc, GO, KEGG, and Reactome (Szklarczyk et al., 2018). BioCyc is a curated microbial database collection that supplies the information of the cascades and also contributes as a reference to genome. As of December 2019, there are 14,735 databases within BioCyc. The database has 3 major tiers based on the manually curation and determines variety of tools, the software of analysis and visualization (Karp et al., 2018). Furthermore, GO (Gene Ontology) is a well-known resource which comprehensively aims to provide gene, the biological terms of the gene and the corresponding functional annotation of the

gene product across all species. The obtained biological terminology is used to enable the data interpretation for the enrichment analysis (Carbon et al., 2019). In addition, KEGG (Kyoto Encyclopedia of Genes and Genomes) is a curated database that is used for the analysis of high-throughput data, pathways, biological visualization, drug, chemical compound, disease, etc. through the collection of databases and analysis tools. According to Kanehisa et al., the integrated database is categorized into four major groups including systems information, genomic information, chemical information, and health information, respectively (Kanehisa, Sato, Furumichi, Morishima, & Tanabe, 2019). Together with these databases, Reactome is a curated open-access database. Given that the pathways, visualization, and interactive analysis tools are the major elements in Reactome, the database supplies the information of multiple cell events including transcriptional regulation, replication, transportation, cell cycle, signal transduction, motility, metabolism, immunity, apoptosis, and many others (Fabregat et al., 2018).

Table 2.1: List of protein-protein interaction databases (As of December 2019).

PPI Database	**# of Total Proteins**	**# of Total Interactions**	**Organism**
BioGRID	72,690	693,825	70
HPRD	30,047	41,327	1 (Human)
GO	1,433,391	---	4522
IntAct	114,235	601,388	> 9
KEGG	29,196,304	---	6269
MINT	26,344	131,695	647
Reactome	94,262	---	16

Some of the unidentified numbers of databases are indicated with dashes.

CHAPTER 3

MATERIALS AND METHODS

In this chapter, we concisely detail the methodology of our study that is comprised of our dataset which we used to reconstruct molecular targeted therapeutic agents treated hepatocarcinoma networks and explain the underlying sections of the integrative network modelling.

3.1 Overview of the Pipeline

The parallel alternative PI3K/AKT/mTOR signaling pathway and the unchanged survival ratio of hepatocarcinoma leads to designing a molecular targeted therapy in which targeted therapeutic agents with the combination of well-known multikinase inhibitor Sorafenib are imperatively needed. In this study, we analyzed small molecule inhibitors which are targeting the cascade of PI3K/AKT/mTOR, namely pan-PI3K inhibitors, isoform-specific PI3K inhibitor, isoform-specific or non-specific AKT inhibitors, mTOR inhibitor through a network-based modelling approach. We developed an integrative understanding for the most effective PI3K/AKT/mTOR inhibitors that can reduce hepatic tumor growth alone or in combination with Sorafenib by using microarray and interactome data with a network-based perspective which is outlined in Figure 3.1. The hepatoma microarray dataset is generated by Cancer Systems Laboratory (CanSyL). We initially performed both steps of pre-processing and quality control by using Affymetrix related Bioconductor packages. Further, to normalize the array dataset, RMA algorithm is used to determine the optimal expression values. Subsequently, in order to reveal the significant targets in distinct molecular targeted agents by inferring the dysregulation of the Interactome, we reconstructed multiple hepatocarcinoma networks treated with the different drugs/inhibitors or the combination of them by DeMAND network modelling algorithm. Apart from the reconstruction of hepatoma networks for both HCC cell lines, we start to analyze the initial networks and detect significant edges by adjusting threshold to 0.05 for KLD.p values in the edge lists. From the perspective of nodes in the network, we seek to know how much of them appear as significant by assigning p-value threshold to 0.05. Unless these criteria are valid for nodes and edges, we eliminate these insignificant nodes and edges. To take a step further, we applied an additional filtering where the set of significantly regulated genes (p-value<0.005) were added to a set. Next, we searched for the direct interaction of the significant nodes in G. Whether both partners of the edges contain significant nodes with respect to the

additional filtering, thereafter, we directly added the edges to the largest connected component. Afterwards, if one partner of the edge is significant and the other partner is insignificant then the first neighbors of the insignificant node is checked if at least 3 neighbors are significant then that edge is also added to the filtered network. The last step is to find the largest connected component which is our final optimal network (See Figure 3.1).

3.2 Datasets

3.2.1 Gene Expression Profiling

We utilized the gene expression profiles dataset that is designed for the treatment of hepatoma cell lines (specifically, Huh7 and Mahlavu) with Sorafenib, PI3K/AKT/mTOR signalling pathway inhibitors and the combination of Sorafenib with several PI3K/AKT/mTOR pathway inhibitors in this work. Cytotoxic activities of PI3K/AKT/mTOR signalling pathway inhibitors in hepatocellular carcinoma cell lines were analyzed by using RT-CES assay. Apart from that, the IC_{50} values at 72 hours of incubation of Huh7 and Mahlavu cells were determined by Cancer Systems Laboratory (CanSyL) (See Table 3.1).

Table 3.1: The IC_{50} values at 72 hours of hepatoma cells had calculated and the array experiment concentrations for drugs and inhibitors were specified.

Molecular Targeted Agents	**Molecular Targets**	**Huh7 IC_{50}**	**Mahlavu IC_{50}**	**Array Experiment Concentration**
Sorafenib	B-Raf VEGFR PDGFR	10 µM	10 µM	10 µM
LY294002	PI3K	10 µM	10 µM	10 µM
Wortmannin	PI3K	10 µM	10 µM	10 µM
Rapamycin	mTOR	0.1 µM	0.1 µM	0.1 µM
PI3Ki-α	PI3Ki-α	0.1 µM	0.1 µM	0.1 µM
Akti-1-2	Akt1 Akt2	10 µM	10 µM	10 µM
Akti-2	Akt2	10 µM	8 µM	10 µM

.cel files were the signals obtained from the microarray Affymetrix chips. By using R, raw cel files were analyzed. For the purpose of the quality control, preprocessing and gene expression analysis processes, mostly used Bioconductor Packages such as Affy, Biobase, Affxparser, Affyio, Annotate, Oligo, AnnotationDbi, Limma are primarily chosen. In order to have the data in a normalized form, the algorithm Robust multi-array average (RMA) is used for determining the expression values.

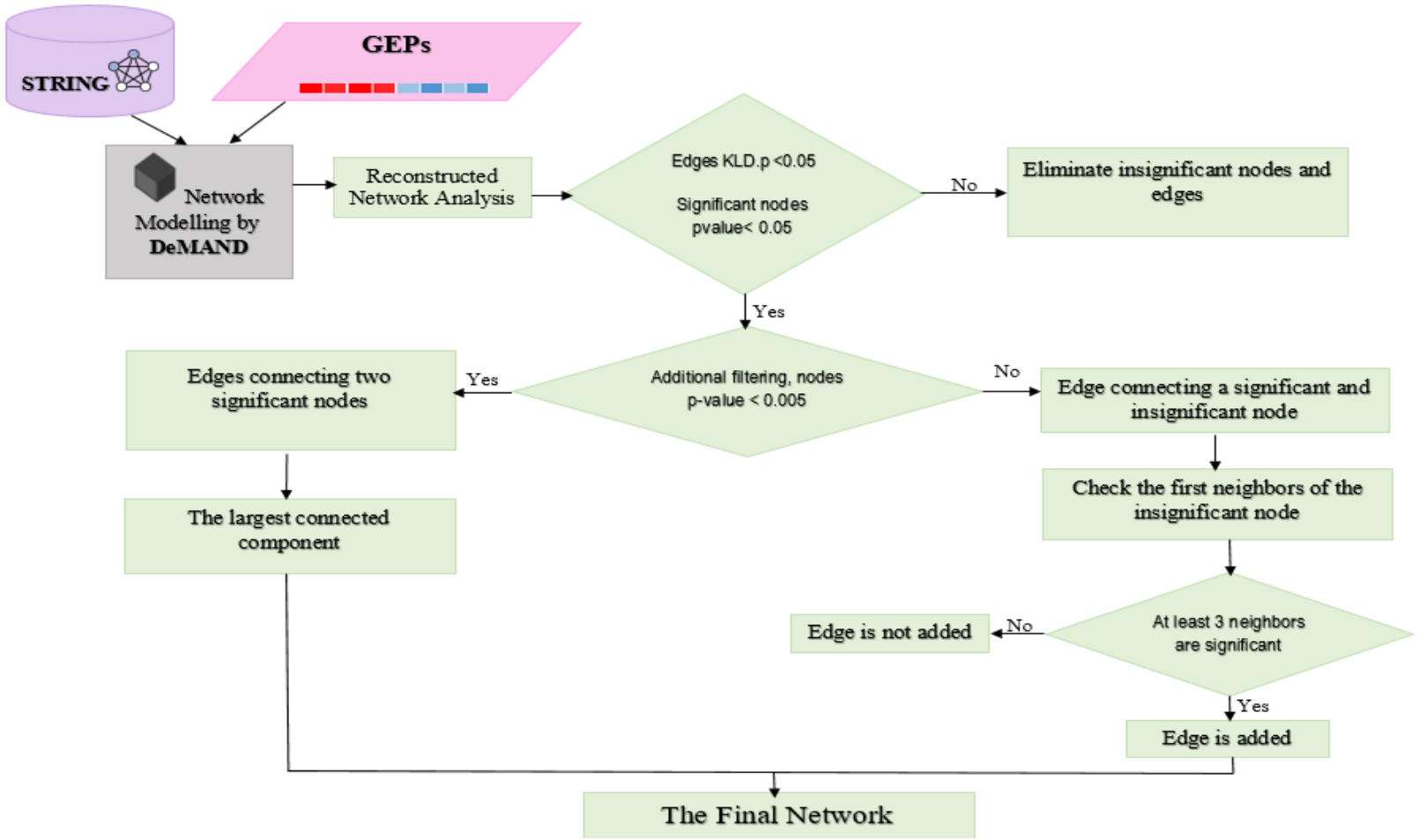

Figure 3.1: The flowchart representation of our methodology.

There were two liver malignant tumorigenic hepatocytes used in this work. Deliberately, these two hepatocarcinoma cell lines with differential PI3K/AKT pathway activities were selected. Huh7 cell line has normoactive pathway. On the other hand, due to tumor suppressor PTEN deletion, Mahlavu cell line has a hyperactive pathway. Huh7 is a well-differentiated hepatocarcinoma cell line (Buontempo et al., 2011). Also, Huh7 HCC cells have a mutation in p53 (Brito et al., 2012; Iwao & Shidoji, 2014). Huh7, epithelial-like malignant, cells are alike to the phenotypes of hepatocytes (Keskin et al., 2013; Yuzugullu et al., 2009). Their differences from the hepatocytes are that they tend to be smaller. Well-differentiated Huh7 expression is related to the early stage of hepatocarcinoma (Yuzugullu et al., 2009). Contrarily, Mahlavu is a poorly-differentiated liver cell line (Buontempo et al., 2011). Its cells have inadequate level of cytoplasm and variable structure. Poorly-differentiated Mahlavu is associated with the late stages of hepatocarcinoma (Yuzugullu et al., 2009).

For each cell line, there were 30 samples. Human Genome (HG) U133 Plus 2.0 Array Affymetrix was used. There were 10 different experiments (for a single hepatoma cell line). 1 out of 10 experiments was DMSO as a control. Per a single experiment, 3 replicates were carried out. A single treatment with a drug or a single treatment with PI3K/AKT/mTOR signalling pathway inhibitors or combined treatment of Sorafenib and several PI3K/AKT/mTOR inhibitors were applied to the samples. 60 samples were used in total (See Tables 3.2 and 3.3).

In the beginning of the sample, letter H represented Huh7 cell line and letter M symbolized Mahlavu cell line. Following the cell line indication letter, the abbreviation of the name of the treatment was written. Before .cel file extension, the numbers 1, 2, 3 represented the three replicates for each sample (See Tables 3.2 and 3.3).

Table 3.2: Huh7 dataset which we have used in this study. The names of the samples, cell lines and the treatment of each sample are indicated.

Sample File	Cell Line	Treatment
H-DMSO-1,2,3.CEL	Huh7	Control DMSO
H-AKTi2-1,2,3.CEL	Huh7	Akti-2
H-PI3Ka-1,2,3.CEL	Huh7	PI3Kialpha
H-SOR-1,2,3.CEL	Huh7	Sorafenib
H-SOR-AKTi2-1,2,3.CEL	Huh7	Sorafenib and Akti-2
H-SOR-PI3Ka-1,2,3.CEL	Huh7	Sorafenib and PI3Kialpha
H-A12-1,2,3.CEL	Huh7	Akti-1-2
H-LY-1,2,3.CEL	Huh7	LY294002
H-Rapa-1,2,3.CEL	Huh7	Rapamycin
H-Wort-1,2,3.CEL	Huh7	Wortmannin

Table 3.3: Mahlavu dataset that we have used in this study. The names of the samples, cell lines and the treatment of each sample are demonstrated.

Sample file	Cell Line	Treatment
M-DMSO-1,2,3.CEL	Mahlavu	Control DMSO
M-AKTi2-1,2,3.CEL	Mahlavu	Akti-2
M-PI3Ka-1,2,3.CEL	Mahlavu	PI3Kialpha
M-SOR-1,2,3.CEL	Mahlavu	Sorafenib
M-SOR-AKTi2-1,2,3.CEL	Mahlavu	Sorafenib and Akti-2
M-SOR-PI3Ka-1,2,3.CEL	Mahlavu	Sorafenib and PI3Kialpha
M-A12-1,2,3.CEL	Mahlavu	Akti-1-2
M-LY-1,2,3.CEL	Mahlavu	LY294002
M-Rapa-1,2,3.CEL	Mahlavu	Rapamycin
M-Wort-1,2,3.CEL	Mahlavu	Wortmannin

Collectively, we used gene expression profiles (GEPs) of Huh7 and Mahlavu hepatocarcinoma cells that were treated with multiple different therapeutic agents (drugs, inhibitor compounds and their combined versions). Small molecule inhibitors targeting the cascade of PI3K/AKT/mTOR, namely pan-PI3K inhibitors, isoform-specific PI3K inhibitor, and isoform-specific or non-specific AKT inhibitors, mTOR inhibitor, and were analyzed beyond the list of the genes (See Figure 3.2).

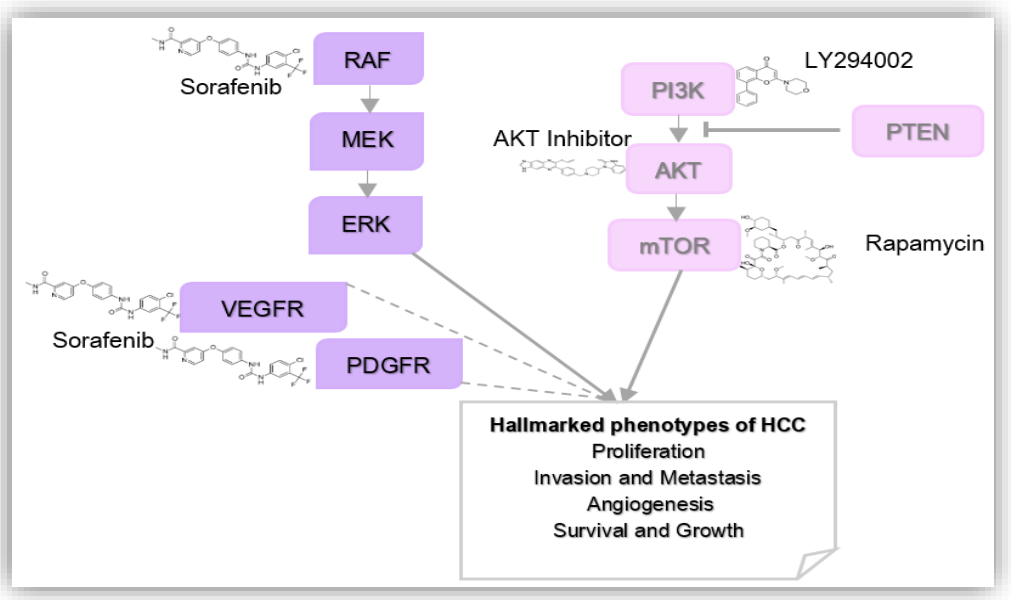

Figure 3.2: The illustrative diagram of molecular targeted agents in Raf/MEK/ERK pathway and PI3K/AKT/mTOR cascade are depicted. Three targets of Sorafenib and small molecule inhibitors targeting PI3K/AKT/mTOR pathway are demonstrated.

3.2.2 Interactome

The weighted interactome used in this analysis is obtained from Search Tool for the Retrieval of Interacting Genes/Proteins (STRING). The database combined different kind of information from several protein-protein interaction resources for many organisms. A score between 0 and 1 which indicates confidence score of each PPI is assigned to the associations of the proteins. The number of protein-protein interactions in interactome of our study is 79.160. These experimentally validated molecular interactions are taken from STRING v9.1. STRING database covers 5,214,234 proteins from 1133 organisms, and 332,235,675 interactions in version 9.1 (Franceschini et al., 2013).

3.3 Network Modelling with DeMAND Algorithm

3.3.1 Theoretical and Algorithmic Backgrounds of DeMAND

In this thesis study, we mainly focused on elucidating the significant molecular targets across treatments with multiple targeted agents by inferring the dysregulation of the Interactome. In other words, we revealed the mechanism of action of molecular targeted therapeutic agents in the context of different HCC networks beyond the list of genes. Toward this purpose, we reconstructed multiple hepatocarcinoma networks treated with different molecular targeted agents to develop a further understanding of the gene perturbation level and compared the significantly enriched biological responses predominantly in the aspects of cellular state.

DeMAND is a Bioconductor package that is developed by Califano Lab. It is a combination of experimental and computational methods. Very concisely, DeMAND algorithm reveals the mechanism of action of targeted therapeutic agents through the dysregulation of the Interactome. In other words, DeMAND searches for the mechanism of action of the molecular targeted therapeutic agents in a network context as an alternative to differential gene expression analysis. It integrates the possible interactions between each entity using a reference interactome to obtain an analysis beyond a gene list. We used String interactome for the network reconstruction in our study. From a pharmacological perspective, mechanism of action (MoA) of a compound briefly specifies a biochemical process in which a molecular targeted therapeutic agent exerts its therapeutic effects. According to Scannell et al, in order to determine both on-target and off-target effects of the agents, the interrogation of MoA is indispensable (Scannell et al., 2012). Wehling mentioned that throughout the phases of clinical trials the majority of drugs turns out to be unsuccessful because of these 2 main reasons, insufficient efficacy and potential toxicity (Wehling, 2009). As a consequence, whether there is a significant progress in characterization of MoA, the production of drug discovery pipelines is constitutively activated (Woo et al., 2015).

The primarily required inputs for the network modeling algorithm are GEPs (control sets and molecular targeted agents treated perturbed sets) as the dataset and the molecular interaction network (obtained from a weighted interactome, STRING). From an algorithmic perspective, to run DeMAND, the fundamental objects within certain criteria are experimental data provided from GEPs (N>=6, N indicates the number of the expression signatures), annotation based on the data, interactome, case index (to index the molecular targeted therapeutic agents treated samples), and control index (to index the control samples) (Woo et al., 2015). In this network modelling approach, N is quite low if we compare it to the other network-based genomics methods that makes it advantageously preferable for small or average-numbered of datasets.

Network-based genomics methods for MoA characterization have sample size more than 100 and initial knowledge of the pathways are required beforehand (Bansal, Gatta, & di Bernardo, 2006; Mani et al., 2008; Woo et al., 2015). Integrative analyses with pathways and subsets of gene interactions are carried out by these methods. In our study, we have 20 hepatocarcinoma profiles and 2 of them are standing as controls (treated with DMSO). The low number of samples prevents using previously mentioned network-based genomics methods. In our dataset, there is not any priorly provided information of pathways that makes these methods unsuitable, unlike DeMAND algorithm (Woo et al., 2015).

Following providing the inputs, the essential principle of DeMAND algorithm is comparisons of GEPs from treatments of molecular targeted agents versus from control samples for all of the targeted therapeutic agents. Except for GEPs comparison, the dysregulated edges are primarily identified within STRING and the level of dysregulation are calculated. To detect the statistical significance of edges, very briefly, 2-dimensional probability distribution for all the edges before and after perturbation within STRING is assessed. By applying Kullback-Leibler divergence (KLD), the level of alteration in these previously mentioned 2-dimensional probability distribution is evaluated. In addition to detecting the dysregulated edges, all the genes are subsequently inspected as if to their connected edges are among the dysregulated interactions. The output of DeMAND algorithm is a list of genes that are belonging to network incorporating with the corresponding p-values evaluated by both Fisher's and Brown's methods. These p-values demonstrate the level of dysregulated interactions around the genes in the network. Additionally, DeMAND algorithm provides a reconstructed network in which 2 nodes and their perturbed connection is indicated. The statistical significance of the corresponding level of edge dysregulation is also provided (KLD and KLD.p (p-value of KLD)) in this reconstructed network (Woo et al., 2015).

To analyze the initial reconstructed networks, we detected significant edges by adjusting threshold to 0.05 for KLD.p values in the edge lists. From the perspective of nodes in the network, we sought to know how much of them appear as significant by assigning p-value threshold to 0.05. Each gene and interaction within these networks had a value signifies how strongly these genes were affected from the perturbation of molecular targeted therapeutic agents. Using only a p-value threshold gave a hairball-like network G (V, E)

and needed more filtering to come up with a better network. In addition to the significance of edges, DeMAND algorithm gives also the significance of the nodes. Therefore, we applied an additional filtering in which the set of significantly regulated genes (p-value<0.005) were added to a set. Then, we searched for the direct interaction of the significant nodes in G. Afterwards, if one partner of the edge was significant and the other partner was insignificant then the first neighbors of the insignificant node would be checked if at least 3 neighbors were significant then that edge would also be added to the filtered network. The last step was to find the largest connected component which would be the final network to be analyzed further. The reconstructed network analysis was performed with NetworkX package in Python.

3.3.2 Statistical Background of DeMAND Algorithm

DeMAND modelling algorithm inputs a molecular interactome $\mathcal{E}$ and a group of gene expression profiles, GEP in which each pair of genes interact within this network. A probability distribution is formed by the expression of genes under certain conditions, and, for non-linearity, a molecular targeted therapeutic agent perturbed group GEP^p and a control group (in our case, DMSO-treated) GEP^c, which consist of the calculations of N genes and M_p and M_c samples, the summation of priorly defined both samples constituting M samples, are created.

As a brief summary, probability distribution functions at the integer point (k,l) for the samples of molecular targeted therapeutic agent perturbation and control, respectively, are constructed through each molecular interaction $G_i \leftrightarrow G_j$ in the network to determine the joint probability distribution of the gene expressions E_i and E_j for the genes G_i and G_j, respectively, where $1 \leq i, j \leq N$, $1 \leq (k,l) \leq M$ and $1 \leq m \leq M$. The discrete probability distributions are stated as the following distributions (**Distribution 1** and **Distribution 2**).

$$P_i{}^{p}{}_j\,(k,) \propto \Sigma_{m\in Mp}\,(k - E_{im},- E_{jm},,) \tag{1}$$

$$P_i{}^{c}{}_j\,(k,) \propto \Sigma_{m\in Mc}\,(k - E_{im},- E_{jm},,) \tag{2}$$

where $\sigma \approx 1.06\cdot \hat{\sigma} \cdot M^{-1/6}$ with σ_i and σ_j being the standard deviations of Gaussian function and dataset's standard deviation is given as $\hat{\sigma}$.

Of the priorly defined the distributions of the probability for the samples of control and molecular targeted therapeutic agent perturbation, Kullback-Leibler divergence (KLD), which implies the amount of deprived information due to an approximation, is computed as below to measure the divergence of one of the distributions from the other one (**Equation 3**):

$$(P_i{}^{c}{}_j \backslash P_i{}^{p}{}_j) = \Sigma_{k=1}^{M}\Sigma_{l=1}^{M} P_i{}^{c}{}_j\,(k,)\,\log\left(\frac{P_{ij}^{c}(k,l)}{P_{ij}^{p}(k,l)}\right) \tag{3}$$

In order to assure that the distance between the distributions is symmetric, a measure of dysregulation for the edges in the network is calculated as the following equation (**Equation 4**).

$$(P_i{}^c{}_j, P_i{}^p{}_j) = \frac{KLD(P_{ij}^c \backslash P_{ij}^p) + KLD(P_{ij}^p \backslash P_{ij}^c)}{2} \quad (4)$$

In addition to the KLD calculations, to determine the significance of dysregulation of the edges in the network statistically, the p-value of KLD, which is denoted Pv_{ij}, is found.

Apart from the edge dysregulation, the dysregulation of genes is also computed by taking all the connected edges of a single gene G_i into consideration. For this purpose, the p-values of these interactions, in other words connected edges, are incorporated by Fisher's method. The combined p-values form a chi-square distribution with $2k$ degrees of freedom. Here, k stands for the number of merged interactions in the following distribution, as shown (**Distribution 5**):

$$x^2 = \Sigma_{Gi \leftrightarrow Gj \in \mathcal{E}-} 2 \log Pv_{ij} \quad (5)$$

To improve the approach of gene dysregulation, as a gene might have multiple edges (interactions) that connect itself to other nodes within a network, the resulting p-values of these interactions are not statistically independent, which is a requirement for the application of Fisher's method. Therefore, an altered version of Brown's method is used to formulate the variance of the chi-square in the following distribution (**Variance 6**).

$$\sigma^2(X^2) = 4k + \Sigma_{i=1}^{k} \Sigma_{j=i+1}^{k} \varphi(\rho_{ij}) \quad (6)$$

Here, ρ_{ij} signifies the related connection among the residual parameters of the genes i and j and the following function as below (**Function 7**):

$$\varphi(\rho_{ij}) = \begin{cases} \rho_{ij}(3.25 + 0.75\rho_{ij}) & 0 \leq \rho_{ij} \leq 1 \\ \rho_{ij}(3.27 + 0.71\rho_{ij}) & -0.5 \leq \rho_{ij} \leq 0 \end{cases} \quad (7)$$

Thereafter, the new assigned degrees of freedom for the chi-square distribution after integrating the Function 7 is as the following equation (**Equation 8**):

$$df = \frac{8k^2}{\sigma^2(X^2)} \quad (8)$$

The associated connection between interactions is calculated via the related link among residuals by relying on the hypothesis that the residuals of two independent interactions will not be connected, and a possible connection among the residuals suggests a mutual gene within these interactions. Hence, the derived p-value indicates the statistical significance of the gene G_i's dysregulation in the network.

3.4 Overrepresentation Enrichment Analysis

In order to have a knowledge on the functional enrichment terms, WebGestaltR package was used as a bioinformatics resource; such that, Gene Ontology terms (GO Biological Process, GO Molecular Function, GO Cellular Function), and pathway information via pathway databases as Reactome and KEGG were obtained (Liao, Wang, Jaehnig, Shi, & Zhang, 2019). We provided one column multiple text files for all the corresponding situations in the reconstructed hepatocarcinoma networks as our input.

The significance was assigned to 0.05 which was the threshold value for the False Discovery Rate (FDR), the organism was human, standing as "hsapiens" and the enrichment method was specified as ORA. Apart from the several essential parameters of WebGestaltR, negative logarithms of the corresponding p-values with base 10 were calculated and added as a new column into the generated matrix (also known as newly adjusted p-values). Each column represented to the adjusted p-values of the corresponding drug and/or PI3K/AKT/mTOR signalling pathway inhibitors and each row corresponded to the different enrichment term. To further analyze the overall results, several heatmaps/plots were drawn to easily visualize the built data matrix.

3.5 Network Visualization with Cytoscape

18 reconstructed hepatoma networks were visualized in Cytoscape (3.7.0). For the node shapes, triangles represented more significant nodes as their p-values were smaller than the p-values of circular nodes. Aside from the shape of the nodes, color of the nodes was assigned according to the expression level value. For specifying node colors, overexpressed genes were indicated by red color and downregulated genes were displayed by dark blue color. Whether the expression value of an individual node was 0, white color was depicted for the node in the optimized network figure. In addition to the node shapes and colors, node size was adjusted with respect to DyNet Rewiring Score (Dn-Score). When Dn-Score was close to 0, the size of the node was much smaller. Except for the properties of the nodes, edge color was arranged with respect to the Kld.p values (calculated by DeMAND). For this purpose, dark red color was set to the more significant edges (having less Kld.p values). In addition to the edge color, maximum edge width was appointed to less Kld.p values of edges.

Each network was clustered by clusterMaker2 application plug-in. As concepts of network partition, Community clustering (GLay) algorithm was applied to all the reconstructed networks of both hepatocarcinoma cell lines. In order to detect the most significant nodes in multiple reconstructed hepatocarcinoma networks, we applied to measure the betweenness centrality value of the corresponding important nodes.

CHAPTER 4

RESULTS AND DISCUSSION

In this chapter, our results of network-based analysis of molecular targeted agent treatments in hepatocellular carcinoma are presented. Initially, we detail the statistical evidences of our reconstructed HCC networks provided by our model, DeMAND. Following that, literature targets of drug treatments/inhibitors are stated to identify target genes and to check the presence of these genes in the reconstructed networks. For determining common characteristics between Sorafenib-related multiple networks and identifying potential similarities, overlapping genes are analyzed. As a concluding perspective, we demonstrate several resulting outcomes of this study that elucidate the inclusion of the reconstructed networks in pathways and in significant terminology insights to reveal fundamental biological signatures.

4.1. Reconstruction of Molecular Targeted Agent Treated Multiple Networks in Hepatocarcinoma

4.1.1 The Obtained Outputs of DeMAND Algorithm and Statistical Interpretation of the Reconstructed HCC Networks

From a pharmacological point of view, mechanism of action (MoA) of a compound specifies a biochemical process in which a drug exerts its therapeutic effects. According to Scannell et al, in order to determine on-target and off-target effects, the interrogation of MoA is indispensable (Scannell et al., 2012). Throughout the phases of clinical trials, the majority of drugs turns out to be unsuccessful because of these 2 main reasons, insufficient efficacy and potential toxicity (Wehling, 2009). Hence, if there is a significant progress in characterization of MoA, drug discovery pipelines' productions will be arisen (Woo et al., 2015).

Lately, network-based methods for MoA characterization have been developed (Bansal et al., 2006; Mani et al., 2008). Integrative analyses with pathways and subsets of gene interactions are carried out by these methods. As a limitation, the methods need to have sample size more than 100 and initial knowledge of the pathways are required beforehand (Woo et al., 2015). In our study, we have 20 samples and 2 of them are standing as controls. The low number of samples prevents using previously mentioned network-based

methods. In our dataset, there is not any priorly provided information of pathways that makes these methods unsuitable, unlike DeMAND algorithm. DeMAND searches for the mechanism of action of the drugs in a network context as an alternative to differential gene expression analysis. It integrates the possible interactions between each entity using a reference interactome to obtain an analysis beyond a gene list. In this study, we used String interactome for the network reconstruction (Woo et al., 2015).

This study aims for the analyzing of drugs, inhibitors and their combinations in HCC through network-based modelling approach (DeMAND). In this work, we have used the microarray (Human Genome U133 Plus 2.0 Affymetrix Array) dataset which has been designed for the treatment of hepatocarcinoma cell lines with Sorafenib, PI3K/AKT/mTOR signalling pathway inhibitors and the combination of Sorafenib with some of PI3K/AKT/mTOR pathway inhibitors. For this purpose, we have 20 array sample outputs with different treatments, including DMSO as a control for both cell lines. Thereafter, we compare each treatment with control DMSO and generate 9 different networks for each HCC cell line. The cell lines are Huh7 and Mahlavu, respectively. All experiments are done in three replicates to be reliable and precise. The weighted context-free interactome (containing only protein-protein interactions) used in our analysis is obtained from STRING database. The number of experimentally validated protein-protein interactions in the network is 79.160 (Franceschini et al., 2013).

As an example, the first network of Huh7 cell line is treated with Akti-2 agent. The initial reconstructed network is composed of 1387 nodes and 1942 edges. Within p-value threshold 0.05, the number of observed nodes is obtained as 465 upon single treatment with Akti-2 in Huh7 network. If we further adjust p-value threshold to 0.01, the number of significant nodes is obtained as 332 within the same Huh7 network. In addition to the p-value thresholds, when we assign FDR cutoff to 0.05, we obtain 261 significant nodes upon single treatment with Akti-2. If we further adjust FDR cutoff to 0.01, there are 204 nodes detected in this Huh7 network. From the perspective of Mahlavu cell line, Akti-2 treated network includes 1240 nodes and 1938 edges. Within p-value cutoff 0.05, there are 633 nodes detected as significant in this network. When we set the p-value cutoff to 0.01 in the network, there are 475 significant nodes. Apart from the p-value cutoffs, when FDR threshold is set to 0.05, the number of significant nodes in the network is 373. Within FDR threshold 0.01, there are 258 nodes observed as significant Akti-2 treated Mahlavu network (See Table 4.1).

Furthermore, the sixth reconstructed Huh7 network which is treated with Sorafenib, the well-known targeted drug of hepatocarcinoma, is composed of 1487 nodes and 1770 edges. Within p-value threshold 0.05, the number of observed nodes in this network is obtained as 459. Whether we further set p-value threshold to 0.01, the number of significant nodes is decreased to 164. Other than the p-value thresholds, when we adjust FDR cutoff to 0.05, we obtain only 24 nodes in this Huh7 network. Within FDR cutoff 0.01, there are only 3 significant nodes identified in the network. For Mahlavu cell line, Sorafenib treated network has 1215 nodes and 1607 edges. Within p-value threshold 0.05, the number of significant nodes is obtained as 768. When we further decreased the p-value

cutoff to 0.01, this network contains 429 significant nodes. Except for the p-value thresholds, when FDR cutoff is set to 0.05, the number of nodes is decreased to 237. Within FDR cutoff 0.01, there are 113 nodes observed as significant upon single treatment with Sorafenib in Mahlavu network (See Table 4.1).

Table 4.1: The corresponding numbers of the each filtered network belonging to HCC.

Molecular Targeted Therapeutic Agents	**# of Nodes**	**# of Edges**	**# of Nodes at p-value 0.05**	**# of Nodes at p-value 0.01**	**# of Nodes at FDR 0.05**	**# of Nodes at FDR 0.01**
Huh7 Akti-2	1387	1942	465	332	261	204
LY294002	1302	2067	692	552	468	319
Akti-1-2	1340	1851	471	341	265	207
PI3kialpha	1661	2291	726	288	51	12
Rapamycin	1131	1600	639	496	403	280
Sorafenib	1487	1770	459	164	24	3
Sorafenib-Akti2	1523	1910	553	191	25	6
Sorafenib-PI3kialpha	1409	1606	547	197	25	0
Wortmannin	1226	1704	614	456	372	234
Mahlavu Akti-2	1240	1938	633	475	373	258
LY294002	1201	1455	443	328	254	193
Akti-1-2	1250	1966	636	481	382	261
PI3kialpha	1184	1509	715	352	130	53
Rapamycin	1167	1468	446	319	240	194
Sorafenib	1215	1607	768	429	237	113
Sorafenib-Akti2	1346	1786	707	294	70	18
Sorafenib-PI3kialpha	1214	1750	797	509	383	203
Wortmannin	1032	1646	684	480	347	220

In order to have a better network, we further apply an additional filtering. Following that, Akti-2 treated Huh7 network contains 342 nodes and 815 edges (See Figures 4.1). Within the p-value threshold 0.05, the number of observed nodes is decreased to 218 and likewise, the edge numbers, 349. Whether we apply stricter p-value threshold, 0.01, we obtain 214 significant nodes in Huh7 network. Aside from the p-value thresholds, when we adjust FDR cutoff to 0.05, we obtain 199 nodes and 298 edges. Within FDR cutoff 0.01, there are 167 significant nodes and 231 edges detected in Akti-2 treated Huh7 network. For Mahlavu cell line, the initial reconstructed network treated with Akti-2 contains 390 nodes and 910 edges (See Figure 4.3). Within p-value threshold 0.05, the total numbers of significant nodes and edges are 347 and 737, respectively. When we further decrease the p-value cutoff to 0.01, Akti-2 treated Mahlavu network has 343 significant node. In addition to the p-value cutoffs, when FDR cutoff is set to 0.05, the number of nodes is decreased to 317 and similarly, the edge numbers, 663. Within FDR cutoff 0.01, there are 242 nodes and 551 edges observed as significant upon single treatment with Akti-2 in Mahlavu network (See Table 4.2).

Additionally, Sorafenib treated Huh7 network includes 104 nodes and 144 edges (See Figure 4.5). Within p-value threshold 0.05, the total numbers of observed nodes and edges in this network is obtained as 77 and 50, respectively. Whether we use stricter threshold, at p-value threshold 0.01, the number of significant nodes is decreased to 69. Apart from the p-value thresholds, when we assign FDR cutoff to 0.05, the network has only 19 nodes and these nodes are not connected to each other with edges. Within FDR cutoff 0.01, there are only 3 separated nodes without any edges identified in the network. For Mahlavu cell line, Sorafenib treated contains 304 nodes and 624 edges (See Figure 4.8). Within p-value cutoff 0.05, the number of significant nodes is obtained as 301 and there are 614 significant edges. When we further decrease the p-value cutoff to 0.01, the number of nodes in the network is decreased to 286. Other than the p-value cutoffs, when FDR cutoff is set to 0.05, the numbers of significant nodes and edges in the network are 210 and 370, respectively. Within FDR cutoff 0.01, there are 105 nodes and 132 edges observed as significant upon single treatment with Sorafenib in Mahlavu network (See Table 4.2).

Table 4.2: The corresponding numbers of the each filtered network belonging to HCC.

Molecular Targeted Agents	**# of Nodes**	**# of Edges**	**# of Nodes at p-value 0.05**	**# of Edges at pvalue 0.05**	**# of Nodes at p-value 0.01**	**# of Nodes at FDR 0.05**	**# of Edges at FDR 0.05**	**# of Nodes at FDR 0.01**	**# of Edges at FDR 0.01**
Huh7 Akti-2	342	815	218	349	214	199	298	167	231
LY294002	505	1298	444	1051	432	421	971	303	775
Akti1-2	334	778	225	365	218	202	309	168	241
PI3kialpha	222	467	185	322	149	46	10	12	0
Rapamycin	431	904	381	703	378	357	661	268	535
Sorafenib	104	144	77	50	69	19	0	3	0
Sorafenib-Akti2	139	227	118	152	96	19	1	4	0
Sorafenib-PI3kialpha	107	142	88	72	79	19	1	0	0
Wortmannin	383	797	327	569	326	311	542	215	400
Mahlavu									
Akti-2	390	910	347	737	343	317	663	242	551
LY294002	287	539	216	272	204	181	194	158	175
Akti1-2	402	943	355	755	351	323	684	243	559
PI3kialpha	271	505	263	477	229	115	114	49	20
Rapamycin	259	532	201	302	188	177	221	155	201
Sorafenib	304	624	301	614	286	210	370	105	132
Sorafenib-Akti2	229	416	223	396	185	65	42	17	4
Sorafenib-PI3kialpha	428	964	423	948	411	364	799	202	409
Wortmannin	369	809	360	779	355	311	674	210	466

4.1.2 Visual Illustrations of the Clustered Versions of the Reconstructed Multiple HCC Networks Representative Images

After reconstructing the hepatocarcinoma networks, 18 networks were initially drawn in Cytoscape, to display the optimized network figures. The instructions of the drawing network image is shown in the legend of the each figure. For the node properties, color of the nodes is assigned according to the expression level value. To be more specific, highly expressed genes are displayed by red color; conversely, downregulated genes are displayed by dark blue color. The color intensity shows the corresponding value of the gene expression level of each individual node. Whether the expression value of an individual node is 0, white color will be depicted for the node in the network image. Size of the node is adjusted according to the DyNet Rewiring Score (Dn-Score). Whether Dn-Score is close to 0, the size of the node will be much smaller. As a node shape, a triangular node is more significant due to having less p-values than the circular-shaped nodes. In addition to the properties of the nodes, edge color is arranged with respect to the Kld.p values (calculated by DeMAND). Dark red color is set to the more significant edges (having less Kld.p values). Maximum edge width is appointed to less Kld.p values of edges.

After visualizing networks, each network was clustered by clusterMaker2 application. As concepts of network partition, Community clustering (GLay) algorithm was applied to all the reconstructed networks of both hepatoma cell lines. As an example network image, Akti-2 agent treated Huh7 network have 13 different clusters in the clustered version (See Figure 4.1). The following figures (Figure 4.1- 4.10, Appendix A.1-8) are corresponding clustered network images of Huh7 and Mahlavu cell lines, respectively. The number of nodes, edges and clusters in the networks are stated. Afterwards, we used this clusters to draw scatter plots of significant networks and further analyses in the following sections.

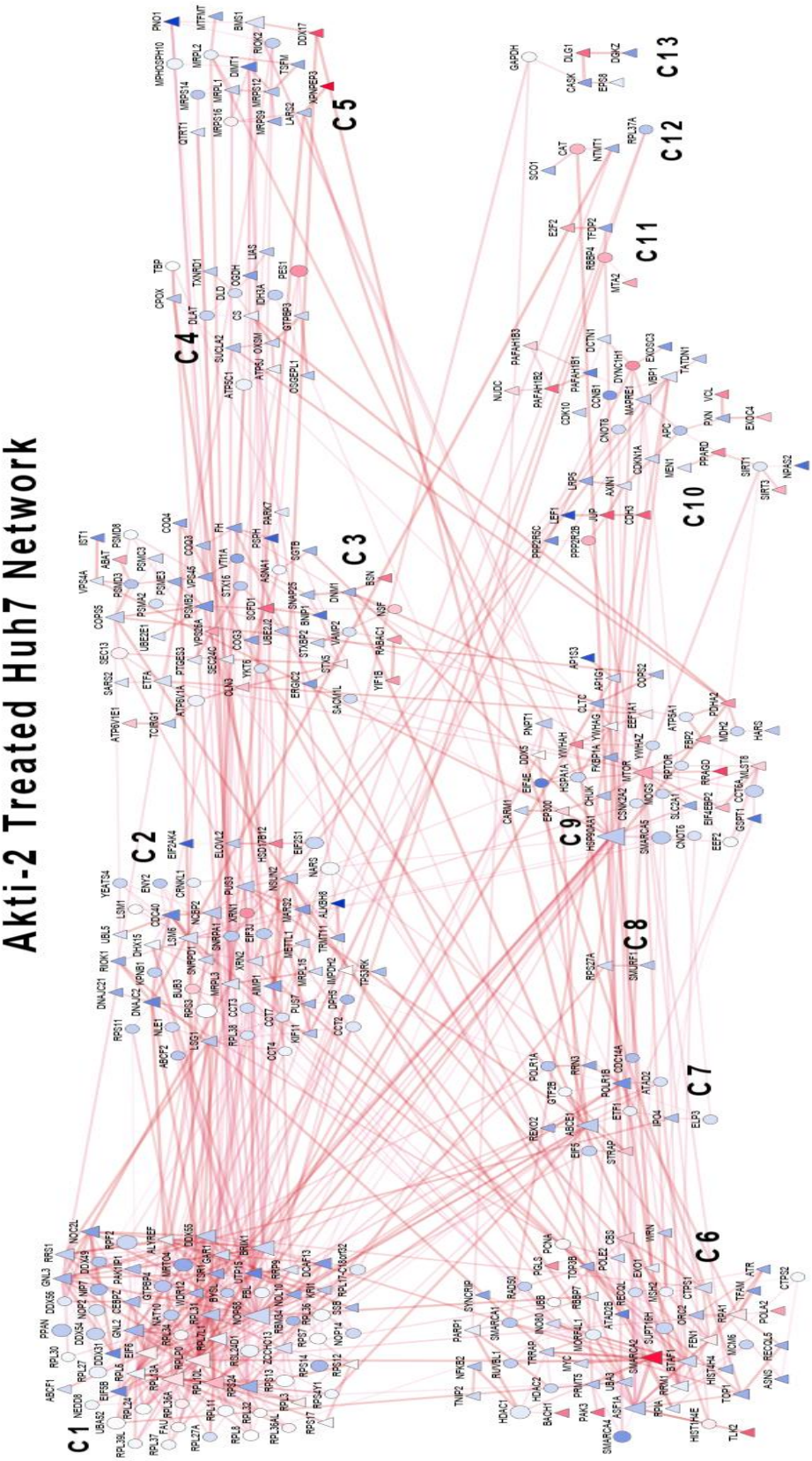

Figure 4.1: Visual representation of the clustered version of Akti-2 treated Huh7 network. Total number of nodes in this network is 342, also the number of edges is 815. The network is separated into 13 distinct clusters. Triangles represent more significant nodes as their p-values are smaller than the p-values of circular nodes. Overexpressed genes are indicated by red color and downregulated genes are displayed by dark blue color.

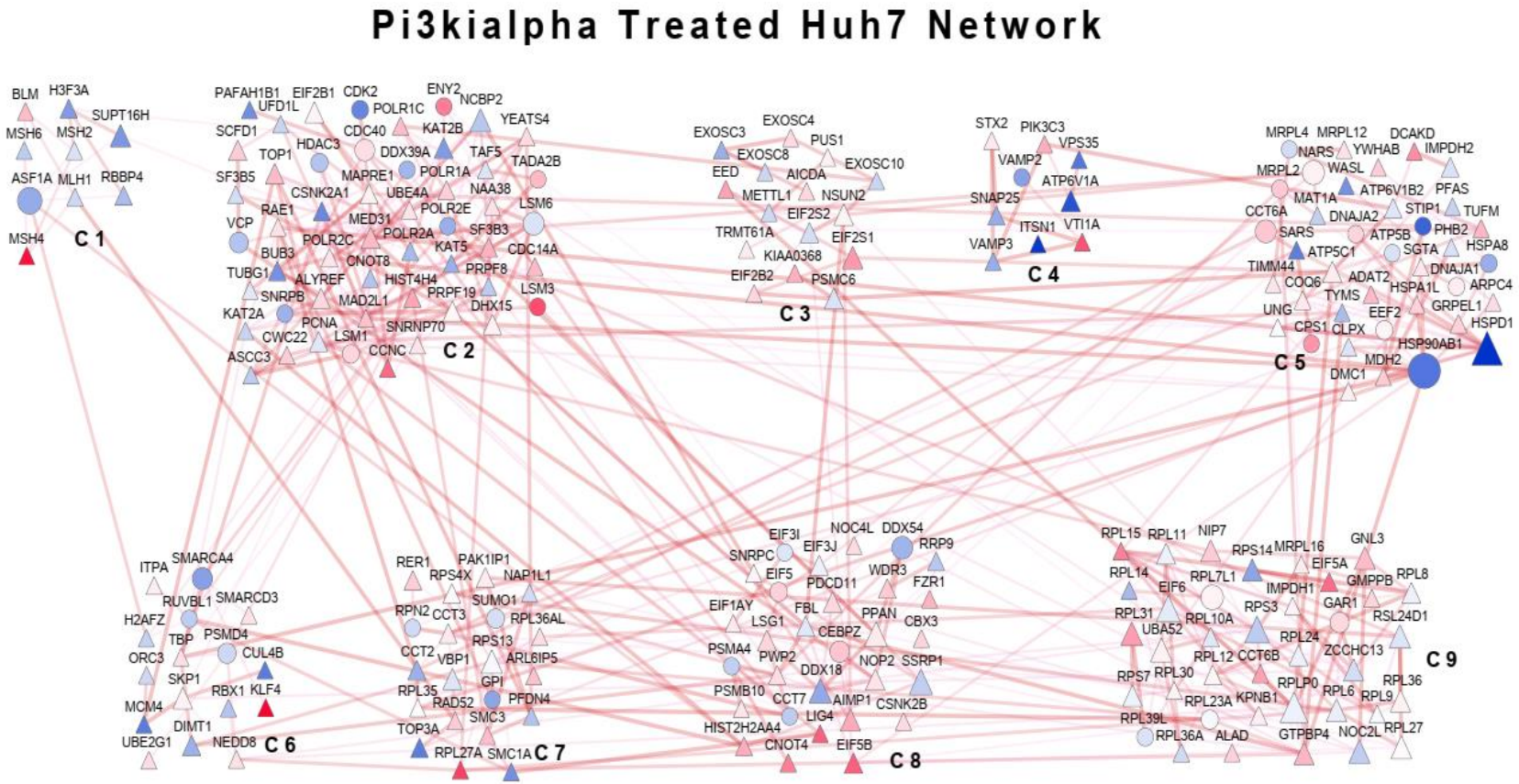

Figure 4.2: Visual illustration of the clustered version of Pi3kialpha treated Huh7 network. The network is divided into 9 different clusters. Total number of nodes in this network is 222, also the number of edges is 467. Node size is adjusted with respect to Dn-Score. If Dn-Score is close to 0, the size of the node will be much smaller. Edge color is arranged with respect to the Kld.p values (calculated by DeMAND). Dark red color is set to the more significant edges (having less Kld.p values). Maximum edge width is appointed to less Kld.p values of edges.

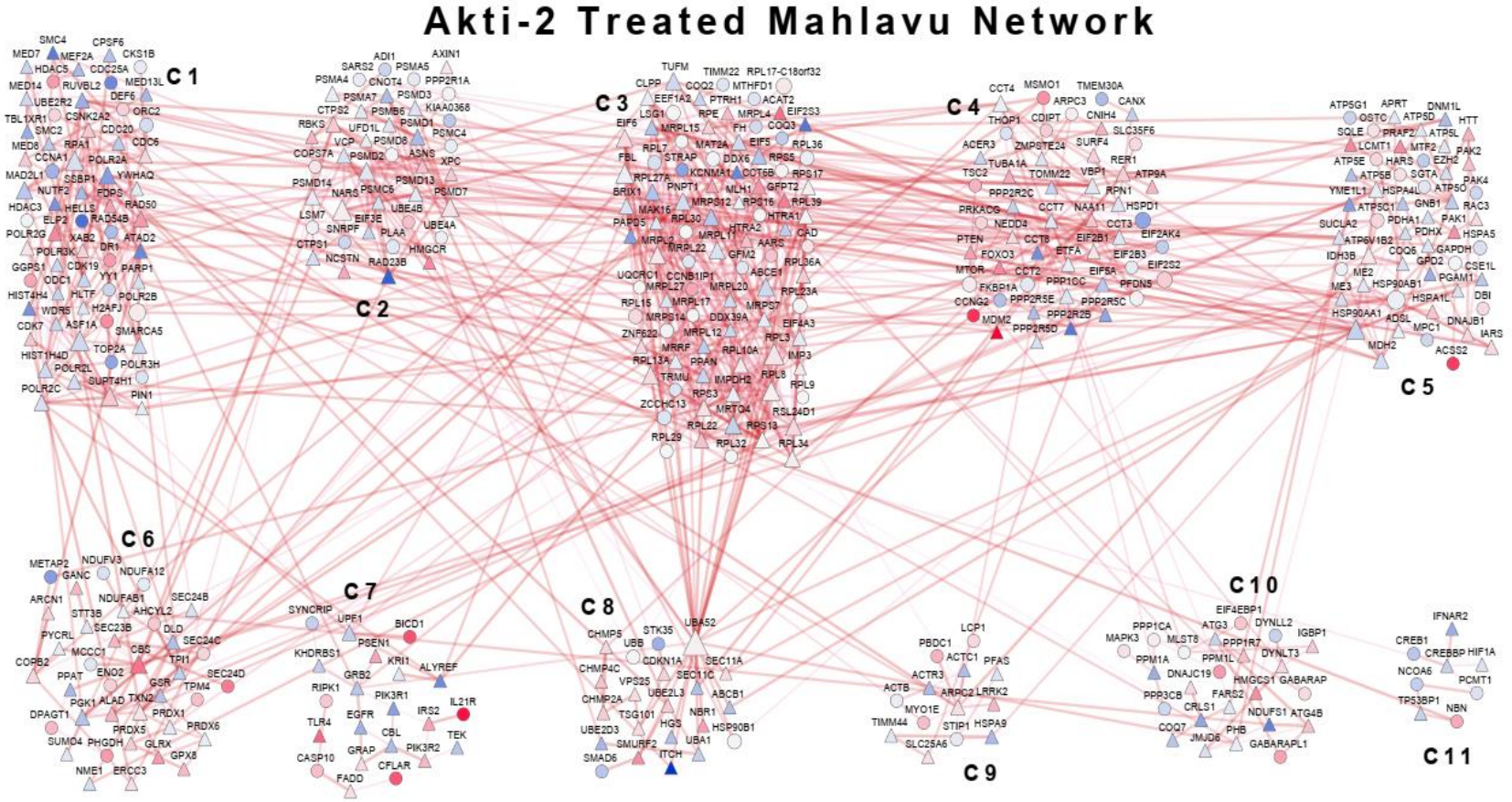

Figure 4.3: Visual representational image of the clustered version of Akti-2 treated Mahlavu network. Total number of nodes in this network is 390 also the number of edges is 910. The network is separated into 11 distinct clusters. Triangles represent more significant nodes as their p-values are smaller than the p-values of circular nodes. Overexpressed genes are indicated by red color and downregulated genes are displayed by dark blue color.

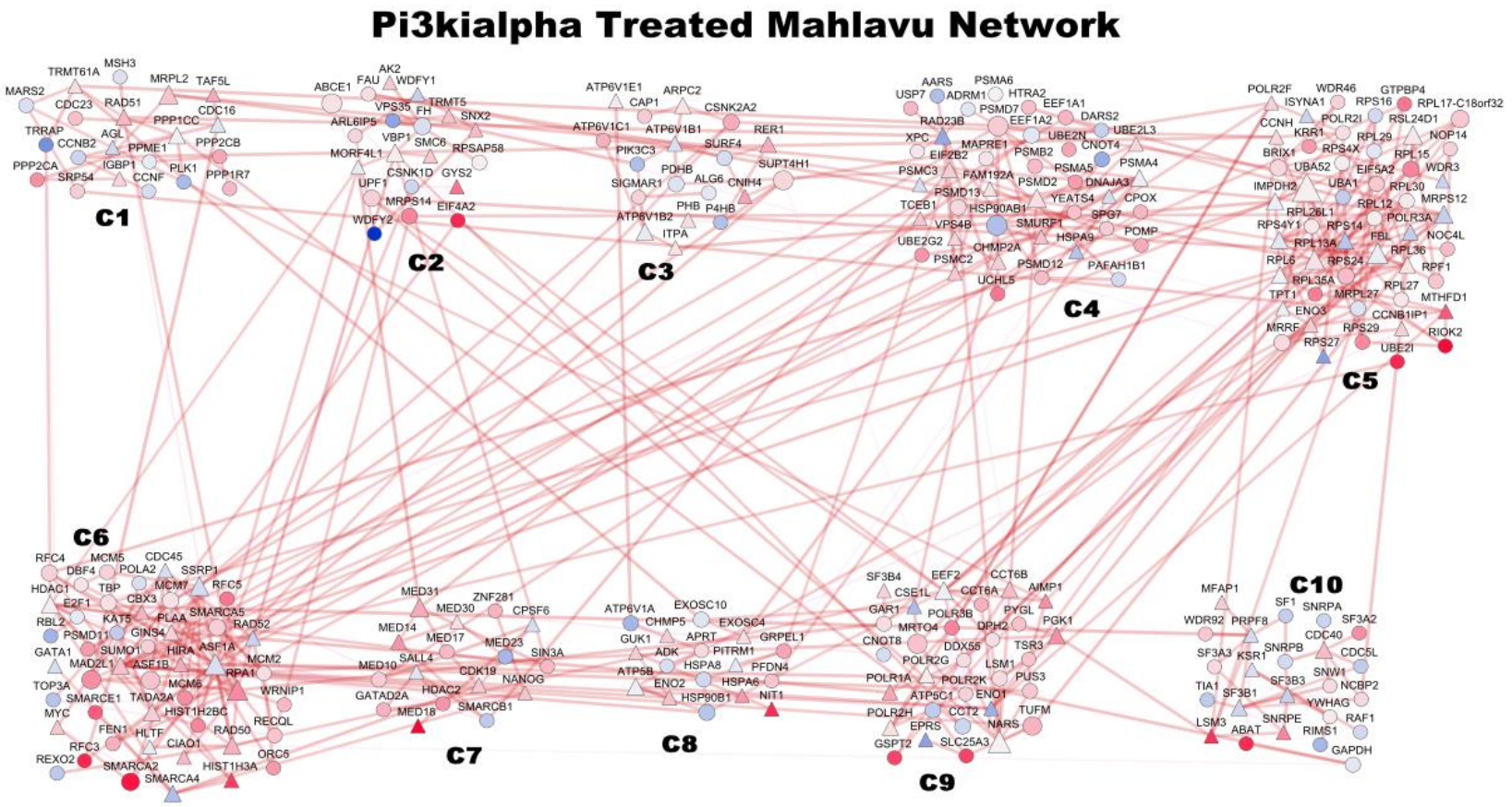

Figure 4.4: Visual illustration of the clustered version of Pi3kialpha treated Mahlavu network. The network is divided into 10 different clusters. Total number of nodes in this network is 271, also the number of edges is 505. Node size is adjusted with respect to Dn-Score. If Dn-Score is close to 0, the size of the node will be much smaller. Overexpressed genes are indicated by red color and downregulated genes are displayed by dark blue color. Dark red edge color is set to the more significant edges (having less Kld.p values). Maximum edge width is appointed to less Kld.p values of edges.

4.1.2.1 Pathway Analyses of Molecular Targeted Agents, Akti-2 and PI3Kia

HPV infection, WNT and HIF-1 signalling pathways are enriched in a single treatment with Akti-2 in Huh7 cells. Multiple studies have shown that HIF and WNT pathways are associated with each other. In fact, HIF causes abnormal signalling of WNT pathway, and that correlates a crosstalk between these cascades (Bogaerts, Heindryckx, Vandewynckel, Van Grunsven, & Van Vlierberghe, 2014; Khalaf et al., 2018). Multiple clusters are enriched in several distinct KEGG pathways of cancers, namely gastric, endometrial, colorectal, breast, prostate cancers, acute myeloid leukemia, basal cell carcinoma which might be associated with off-target effects. The analyzed figure of this network is in Appendix section.

Protein transport is enriched in a treated with a single agent, PI3Ki-α in Huh7 cells. The first cluster has also KEGG enrichment terms in platinum drug resistance, and its correlated result, colorectal cancer which may be included in off-target effects. Additionally, synaptic vesicle cycle and SNARE interactions in vesicular transport are enriched in Cluster 4 which indicate a relation with nervous system, and is likely to be another off-target effect. The analyzed image of this network may be observed in Appendix.

Several virus infections are detected, namely EBV, HPV, *helicobacter pylori*, vibrio cholera infection in a single treatment with PI3Ki-α in Mahlavu cells. Progesterone-mediated oocyte maturation is another functional KEGG enrichment term as a member of endocrine system. Energy metabolism and genetic information processing (including DNA repair mechanisms) are significantly enriched KEGG terminologies. The analyzed network figure might be observed in Appendix.

In addition to the previously mentioned virus infections, HIV-1 and Kaposi sarcoma-associated herpesvirus infections are also detected. Hepatitis B, hepatitis C, non-alcoholic fatty liver disease are enriched terms that might probably cause HCC. Several signal transduction pathways are enriched, including AMPK, FoxO, Ras, JAK-STAT, HIF-1, NF-kappa B, VEGF signalling pathways, and immune system responses, namely natural killer cell mediated cytotoxic activity, B cell receptor, T cell receptor, chemokine, Toll-like receptor signalling pathways. Aside from the off-target effects in the previous clustered versions of the reconstructed networks, melanoma, glioma, pancreatic cancer, chronic myeloid leukemia, and renal cell carcinoma are standing as off-target effects in a single treatment with Akti-2 for Mahlavu cell line.

4.1.2.2 Gene Ontology Biological Process Analyses of Molecular Targeted Agents, Akti-2 and PI3Kia

Multiple clusters (specifically, clusters 1, 4, 5) are enriched in protein transport (parent term, transport), negative regulation of cell cycle (mostly the following child terms, negative regulations of mitotic cell cycle, cell cycle process). Second cluster is composed of many RNA processing terms, as well. Additionally, RNA metabolic process is

significantly enriched parent term for Cluster 3. First cluster also consists of apoptotic signalling pathway as a significantly enriched GO biological process functional term. Cluster 9 includes translation-related multiple child terms in Huh7 cells treated with PI3Ki-α as a single agent. Although PI3Ki-α is used at very low doses, it demonstrates an effective behaviour as our conclusion.

All clusters are enriched in various different categorical terms for biological process. First cluster is mostly enriched in localization related child terms. Cluster 4 includes several enrichment terms related to cellular metabolic process. Sixth cluster comprises of chromosome organization terms, and the second cluster consists of RNA metabolic process terms. Additionally, third cluster is enriched in transport-related GO biological process functional enrichment terms. Organelle organization and cell growth are induced as enrichment terms in Huh7 cells treated with a single agent, Akti-2.

All clusters are enriched in various different categorical functional terms for GO biological process in Mahlavu cells treated with Akti-2 inhibitor. Protein dephosphorylation is an enrichment term that is found in several clusters. Third cluster consists of translation and localization associated terminologies. Cluster 8 is enriched in transport, immune responses (i.e, regulation of immune response), dephosphorylation, viral life cycle. Seventh cluster is enriched in apoptotic process related terms, including regulation of apoptotic signalling pathway, leukocyte apoptotic process, cell death, and so on. Several off-target biological processes are demonstrated in Cluster 7, namely immune system process (child terms, leukocyte migration, cell differentiation, etc.), hematopoietic or lymphoid organ development (i.e., hemopoiesis), inflammatory response, and cytokine production.

All clusters are enriched in various different categorical terms for GO biological process. Multiple clusters (mostly, third cluster) are enriched in protein transport-related terms (parent term, transport). Cluster 10 consists of RNA metabolic processes (i.e., RNA processing). Sixth cluster is mostly enriched in DNA repair mechanisms. In addition to these, Cluster 9 is enriched in transcription-related processes in Mahlavu cells treated with PI3Ki-α as a single agent.

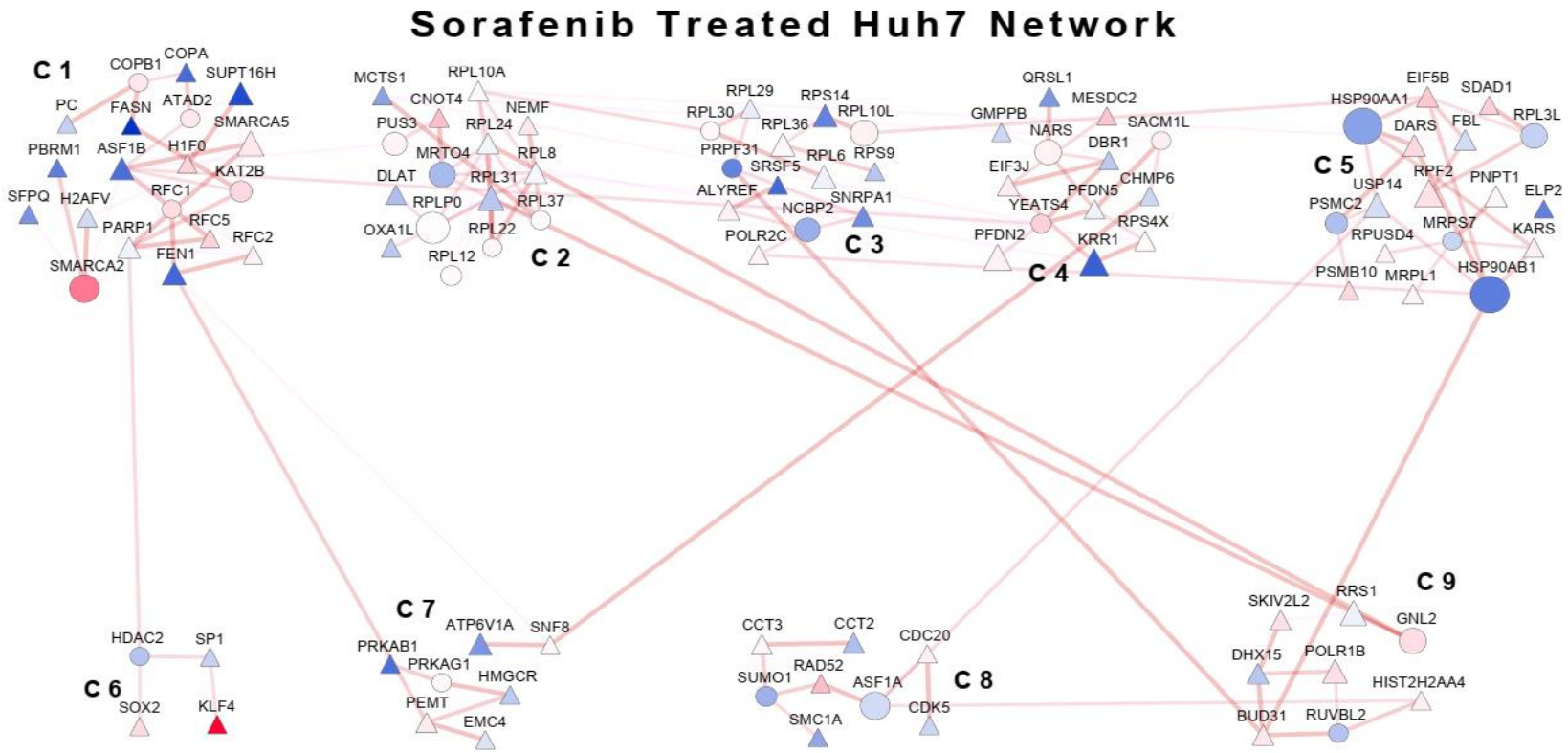

Figure 4.5: Visually depicted network illustration of the clustered version of Sorafenib treated Huh7 network. The network is separated into 9 distinct clusters. Total number of nodes in this network is 104, also the number of edges is 144. Node size is adjusted with respect to Dn-Score. If Dn-Score is close to 0, the size of the node will be much smaller. Edge color is arranged with respect to the Kld.p values. Dark red color is set to the more significant edges (having less Kld.p values). Maximum edge width is appointed to less Kld.p values of edges.

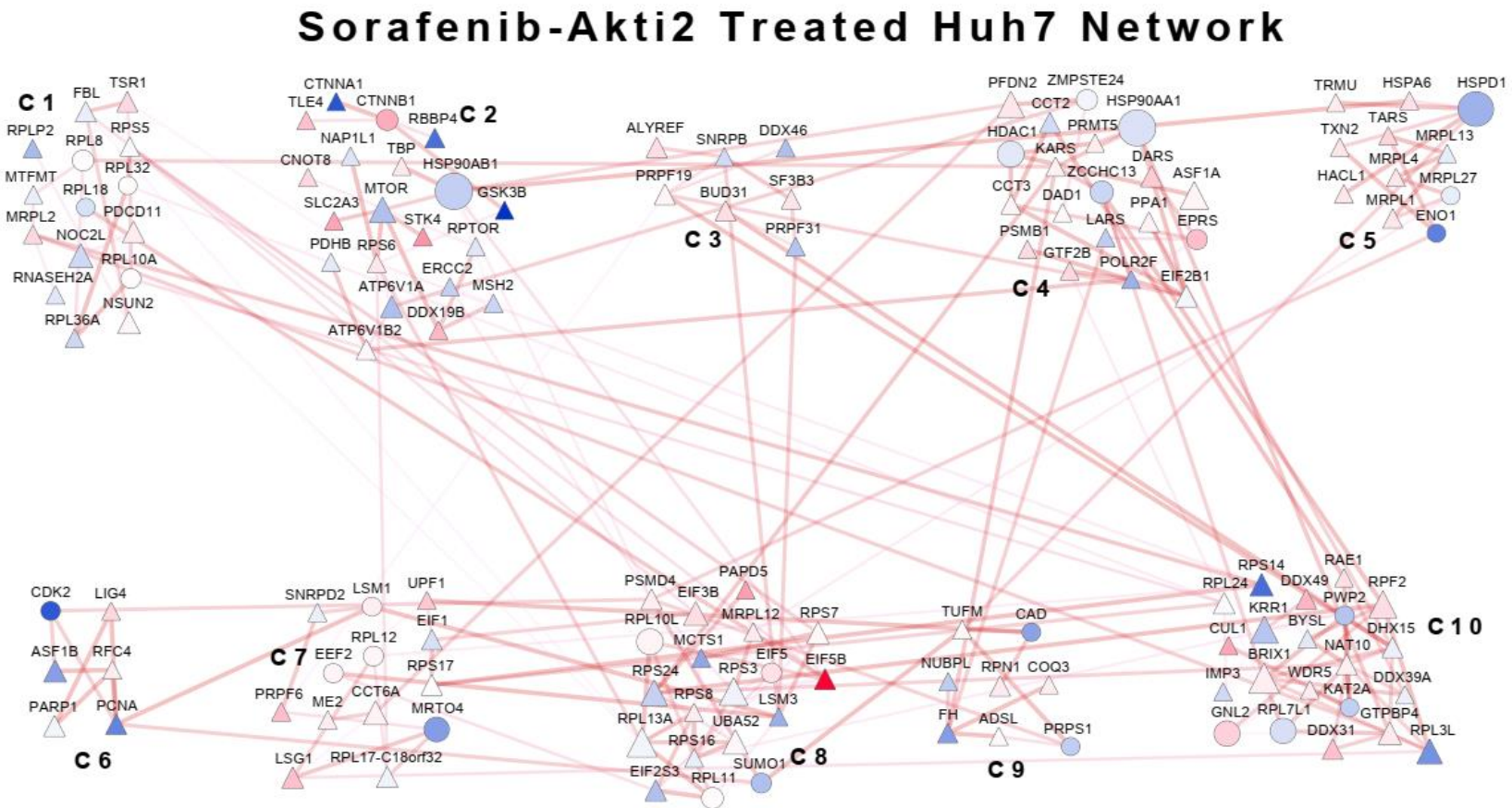

Figure 4.6: Visual network image of the clustered version of Sorafenib-Akti2 treated Huh7 network. Total number of nodes in this network is 139, also the number of edges is 227. The network is grouped into 10 different clusters. Color of the nodes is assigned according to the expression level value. Overexpressed genes are indicated by red color and downregulated genes are displayed by dark blue color. If expression value is 0, node color will be white. The color intensity shows the corresponding value of the gene expression level of each individual node.

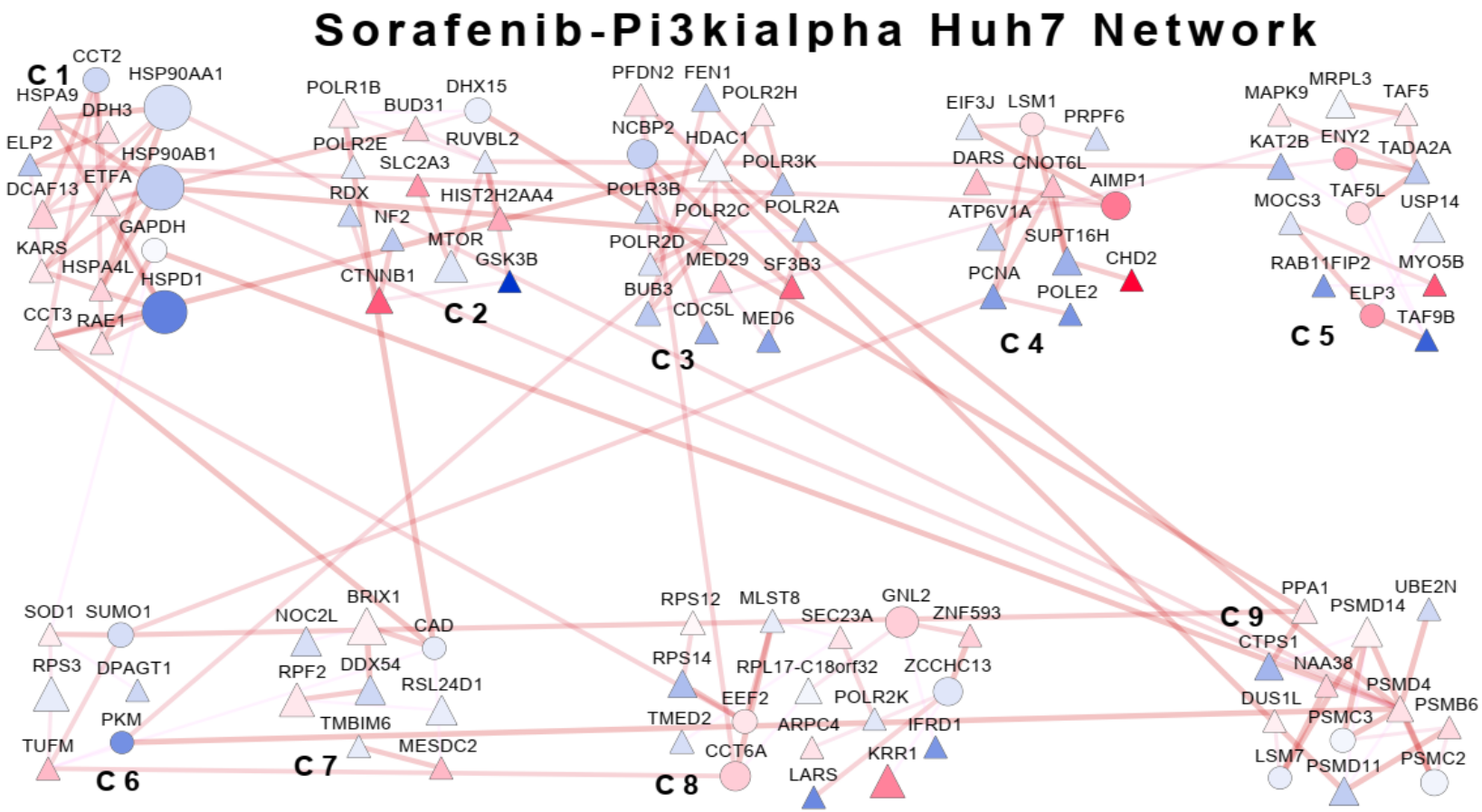

Figure 4.7: Visual representational figure of the clustered version of Sorafenib-Pi3kialpha treated Huh7 network. The network is grouped into 9 distinct clusters. Total number of nodes in this network is 107, also the number of edges is 142. Node size is adjusted with respect to DyNet Rewiring Score (Dn-Score). If Dn-Score is close to 0, the size of the node will be much smaller. Triangles represent more significant nodes as their p-values are smaller than the p-values of circular nodes.

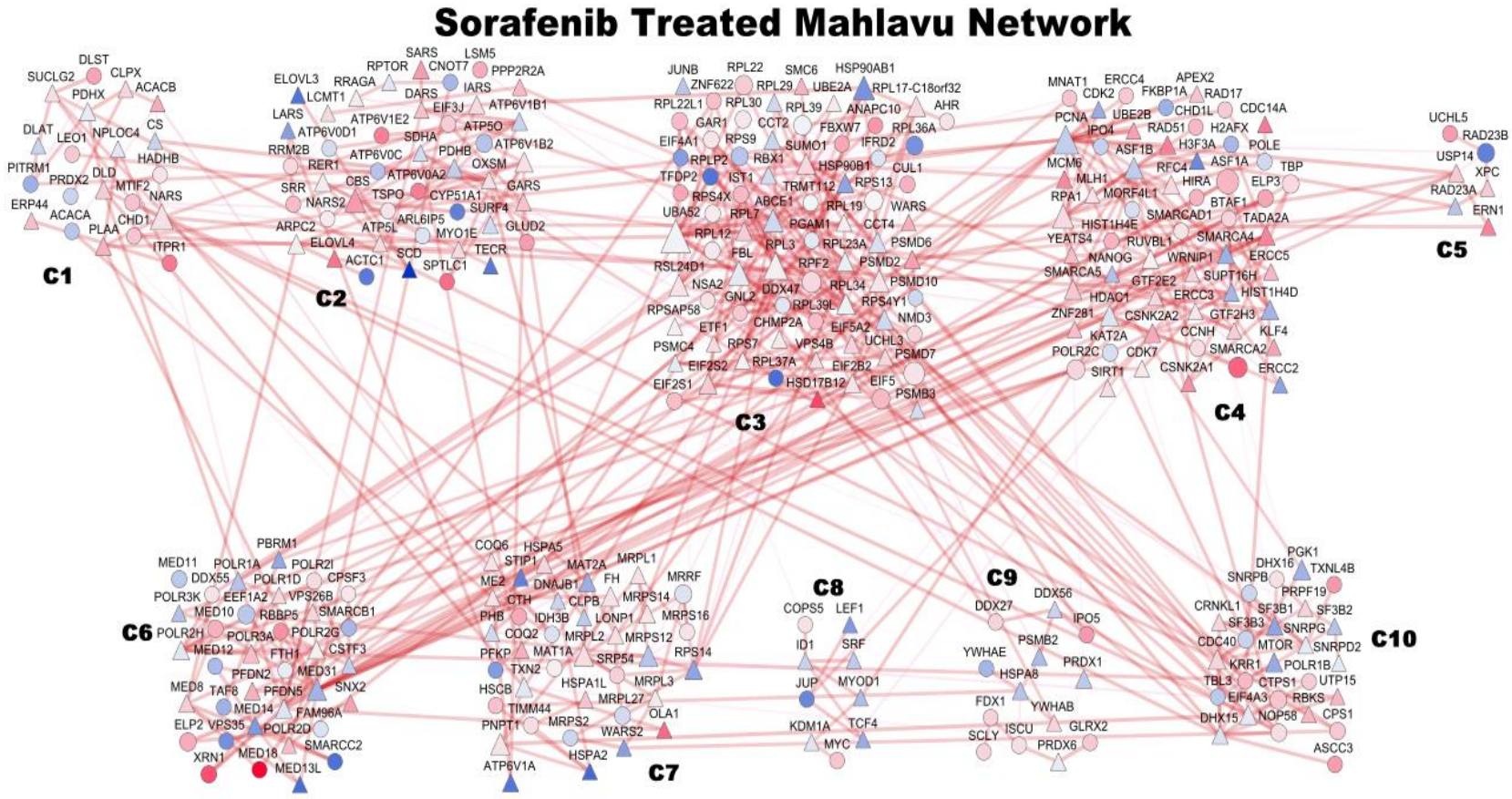

Figure 4.8: Visual illustration of the clustered version of Sorafenib agent treated Mahlavu network. Total number of nodes in this network is 304, and the number of edges is 624, as well. The network is grouped into 10 different clusters. Node size is adjusted with respect to Dn-Score. If Dn-Score is close to 0, the size of the node will be much smaller. Edge color is arranged with respect to the Kld.p values. Dark red color is set to the more significant edges (having less Kld.p values). Maximum edge width is appointed to less Kld.p values of edges.

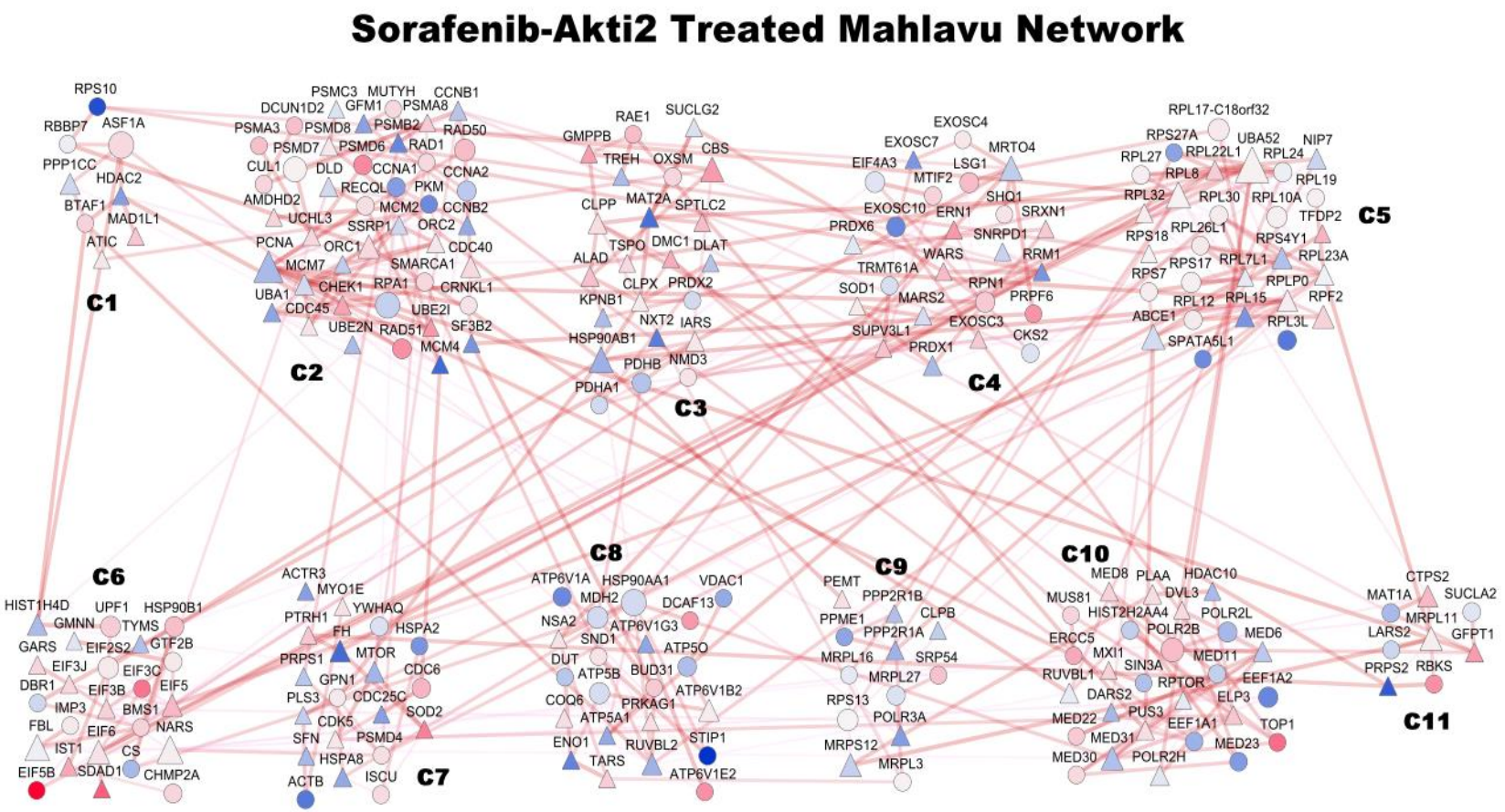

Figure 4.9: Visual depicted image of the clustered version of Sorafenib-Akti2 treated Mahlavu network. Total number of nodes in this network is 229, and the number of edges is 416. The network is grouped into 11 different clusters. Color of the nodes is assigned according to the expression level value. Overexpressed genes are indicated by red color and downregulated genes are displayed by dark blue color. If expression value is 0, node color will be white. The color intensity shows the corresponding value of the gene expression level of each individual node.

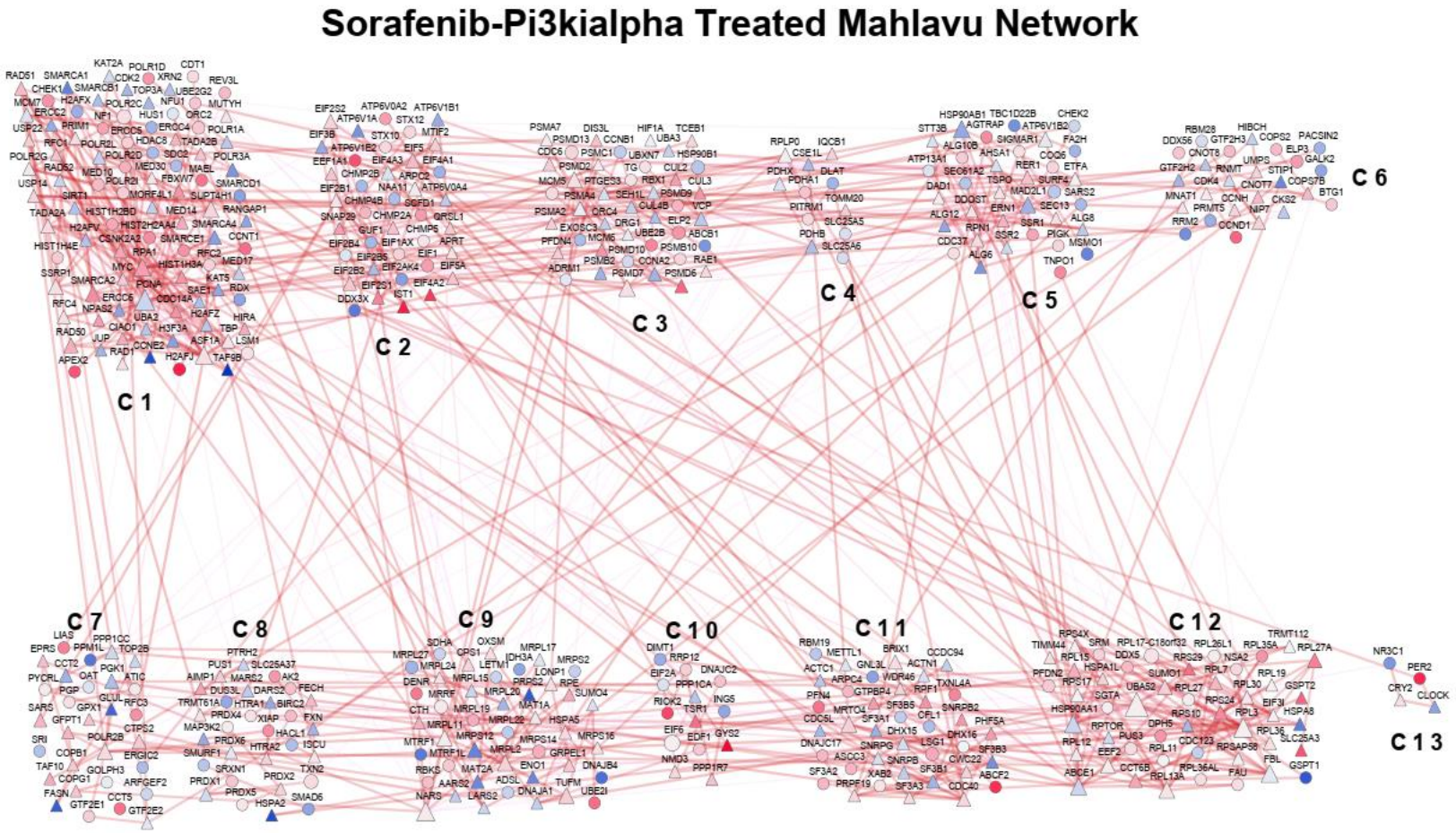

Figure 4.10: Visual illustrational image of the clustered version of Sorafenib-Pi3kialpha treated Mahlavu network. Total number of nodes in this network is 428, and the number of edges is 964. The network is separated into 13 different clusters. Triangles represent more significant nodes as their p-values are smaller than the p-values of circular nodes. Overexpressed genes are indicated by red color and downregulated genes are displayed by dark blue color.

4.1.2.3 Overrepresentation Analyses of the Clusters in Sorafenib-Related Multiple Networks

Hereafter, we compare the common aspects and distinct features of only Sorafenib-related multiple reconstructed hepatoma networks. To do this, we first divide heterogeneous networks into the different clusters that comprise ultimately more similar nodes and assign the same FDR threshold value to all of the networks. Afterwards, negative logarithm base 10 was applied to the p-values of the genes in all clusters. Consequently, by doing this analysis, our objective is to clarify hidden significant terminology more precisely and elucidate functional enrichment terms that dispose of background effect of the whole unclustered version of the network.

4.1.2.3.1 KEGG Pathway Analyses of the Clustered Multiple Hepatocarcinoma Networks

Only 3 significant KEGG pathway enrichment terms for a single treatment with Sorafenib in Huh7 network are exhibited in the heatmap (See Appendix B.3). In Figure 4.11a, 7 different KEGG functional enrichment terms are displayed for the same network in the plot. Although Sorafenib-treated Huh7 network comprises 9 distinct clusters, 4 different clusters are presented in the plot. The reason is that several clusters do not have an enrichment score and corresponding functional enrichment term within the specific cutoff or very few gene numbers in the clusters are insufficient to have an enriched term. AMP activated kinase (AMPK) signalling pathway, one of the enriched significant cascade of cluster 7, modulates several processes, namely energy stability, embryonic development, biogenesis of mitochondria, cellular growth and autophagy (Hardie, 2011). As Ferretti et al. claimed that, the level of AMPK molecular activity is sharply depleted in hepatoma tumors, by considering this, AMPK is known to incorporate in hepatoma cells (Ferretti et al., 2019).

In Figure 4.11b, human papillomavirus infection is one of the significantly enriched pathway belonging to Cluster 2 in combined treatment of Sorafenib and Akti-2. Blackadar stated that HPV is one of the infectious carcinogens (Blackadar, 2016). Insulin signalling pathway is another functionally enrichment term as a member of endocrine system. The second Huh7 cluster in combined treatment of Sorafenib and Akti-2 is also enriched in endometrial and prostate cancers which may be included in off-target effects.

In Figure 4.11c, previous studies highlighted that EBV is involved in HCV infection which may result in hepatocarcinogenesis (Abdel Sammad, El-Bassuoni, & Talaat, 2013; W. Li et al., 2004). Cluster 2 in combined Huh7 treatment of Sorafenib and PI3Ki-α is enriched in colorectal, breast and gastric cancers which might be related to off-target effects. In addition to the enriched terminologies, after comparing all Sorafenib-related Huh7 networks, negative regulations of DNA repair, MAPK activity, and DNA replication are detected in the combination of Sorafenib and PI3Ki-α.

In Figure 4.12a, several virus associations are detected, including viral carcinogenesis, HPV, *helicobacter pylori* infection in a single agent treatment with Sorafenib in Mahlavu cells. Also, lipid, carbohydrate and energy metabolisms, DNA repair mechanisms and replication, signal transduction (in particular, mTOR signalling) are significantly enriched. Gastric and thyroid cancers, fanconi anemia pathway and acute myeloid leukemia are enrichment terms that may be included in off-target effects. Additionally, a recent study mention that DNA repair mechanisms (in our case, nucleotide excision, base excision, mismatch repairs) and DNA replication are supported in Fanconi anemia pathway (Rodríguez & DAndrea, 2017) that is a correlation with our finding results.

In Figure 4.12b, several virus infections are detected, namely HBV, *helicobacter pylori*, vibrio cholera infection in combined treatment with Sorafenib and Akti-2 in Mahlavu cells. Progesterone-mediated oocyte maturation is another functionally enrichment term as a member of endocrine system. Carbohydrate and energy metabolisms, cell growth (specifically, cellular senescence, and cell cycle) are significantly enriched. Lipid metabolism is negatively regulated in the combined agents of Sorafenib and Akti-2 in Mahlavu cells.

In Figure 4.12c, several distinct Mahlavu clusters are enriched in virus associations, namely viral carcinogenesis, EBV, *helicobacter pylori*, vibrio cholera infection and alcoholism is another significant term in combined treatment with Sorafenib and PI3Ki-α. Apoptosis is the most significant functional term. Lipid metabolism is negatively regulated in the combination of agents, Sorafenib and PI3Ki-α in Mahlavu cells.

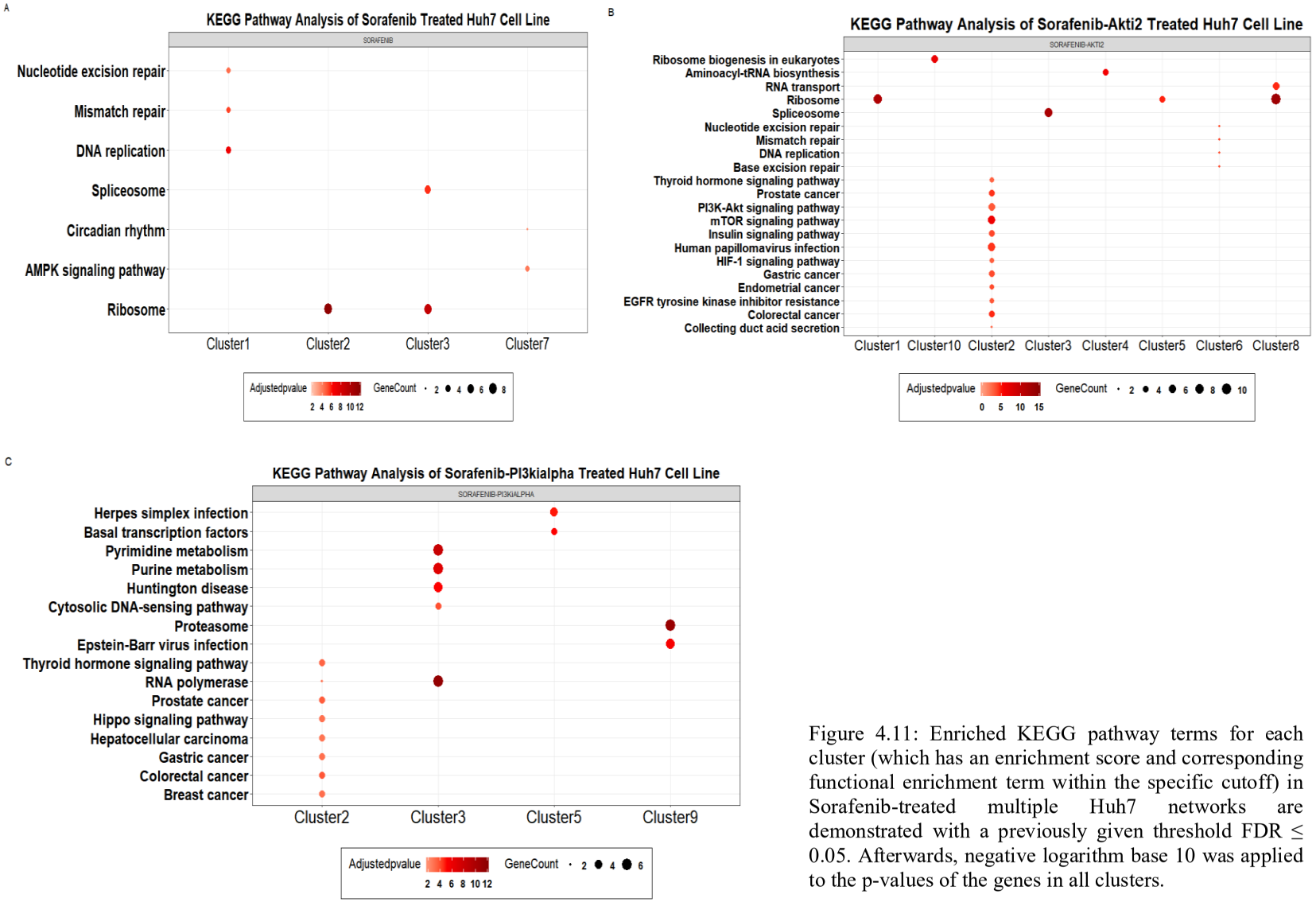

Figure 4.11: Enriched KEGG pathway terms for each cluster (which has an enrichment score and corresponding functional enrichment term within the specific cutoff) in Sorafenib-treated multiple Huh7 networks are demonstrated with a previously given threshold FDR $\leq$ 0.05. Afterwards, negative logarithm base 10 was applied to the p-values of the genes in all clusters.

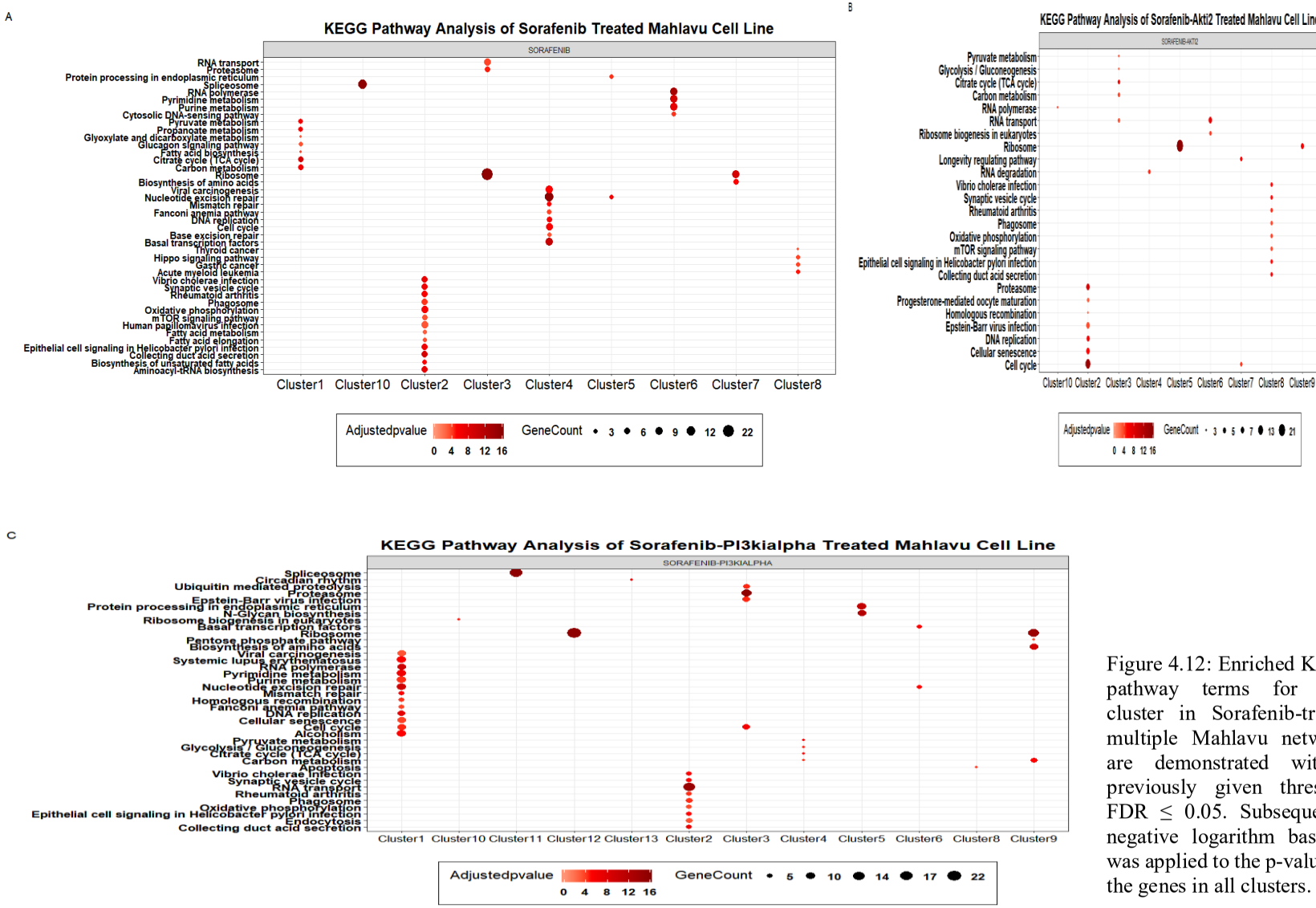

Figure 4.12: Enriched KEGG pathway terms for each cluster in Sorafenib-treated multiple Mahlavu networks are demonstrated with a previously given threshold FDR $\leq$ 0.05. Subsequently, negative logarithm base 10 was applied to the p-values of the genes in all clusters.

4.1.2.3.2 GO Biological Process Analyses of the Clustered Multiple Hepatocarcinoma Networks

Cluster 1 is enriched in several GO biological process enrichment terms, namely cellular component organizations (chromatin, chromosome, organelle organizations), primary metabolic processes (nucleic acid metabolic process), and DNA damage and repair mechanisms (cellular response to DNA damage and stimulus, nucleotide-excision repair). Second cluster is enriched in mainly translation-associated events and localization. In addition to the functional enrichment term categories given in Cluster 2, third cluster comprises the significant processes such as RNA processing, macromolecule metabolic process and transport. Cluster 5 significantly enriched in cellular component organization, RNA processing and gene expression in a treatment with Sorafenib as a single Huh7 agent (See Figure 4.13).

Cluster 6 is significantly enriched in DNA damage and repair mechanisms and regulation of macromolecule metabolic process. Second cluster includes the functional terms, namely negative regulation of cell cycle (child terms, negative regulation of mitotic cell cycle and cell cycle arrest), regulation of programmed cell death (specifically, regulation of apoptotic signalling pathway), RNA metabolic process, and cell death (in particular, neuron death) in a combined treatment with Sorafenib and Akti-2 in Huh7 cell line (See Figure 4.14).

Cluster 1 is enriched in cellular response to stress, response to stimulus, regulation of biological quality (specifically, regulation of protein stability), cellular process (in particular, protein folding), establishment of protein localization, and protein-containing complex assembly. In this context, Sauzay and her colleagues highlighted that Sorafenib may get involved in the processes of chaperoning and protein folding in Huh7 cell line (Sauzay et al., 2018). One of the enrichment terms in second cluster is regulation of organelle organization (child term, regulation of cytoskeleton organization). Fifth and ninth clusters is enriched in 3 distinct significant terms, including cellular protein modifications (protein acylation, peptidyl-lysine modification), macromolecule modification (covalent chromatin modification), and cellular protein modification processes (post-translational protein modification, protein modification by small protein removal) and protein catabolic process, respectively. Significantly enriched genes are belonging to protein biosynthesis and protein modification following Sorafenib treated hepatoma cells (Cervello et al., 2012), correlating with our results. Third cluster is significantly enriched in response to organic substance, RNA processing, RNA biosynthetic process, negative regulation of DNA repair and gene expression in a combined treatment with Sorafenib and PI3Ki-α in Huh7 cell line (See Figure 4.15).

.

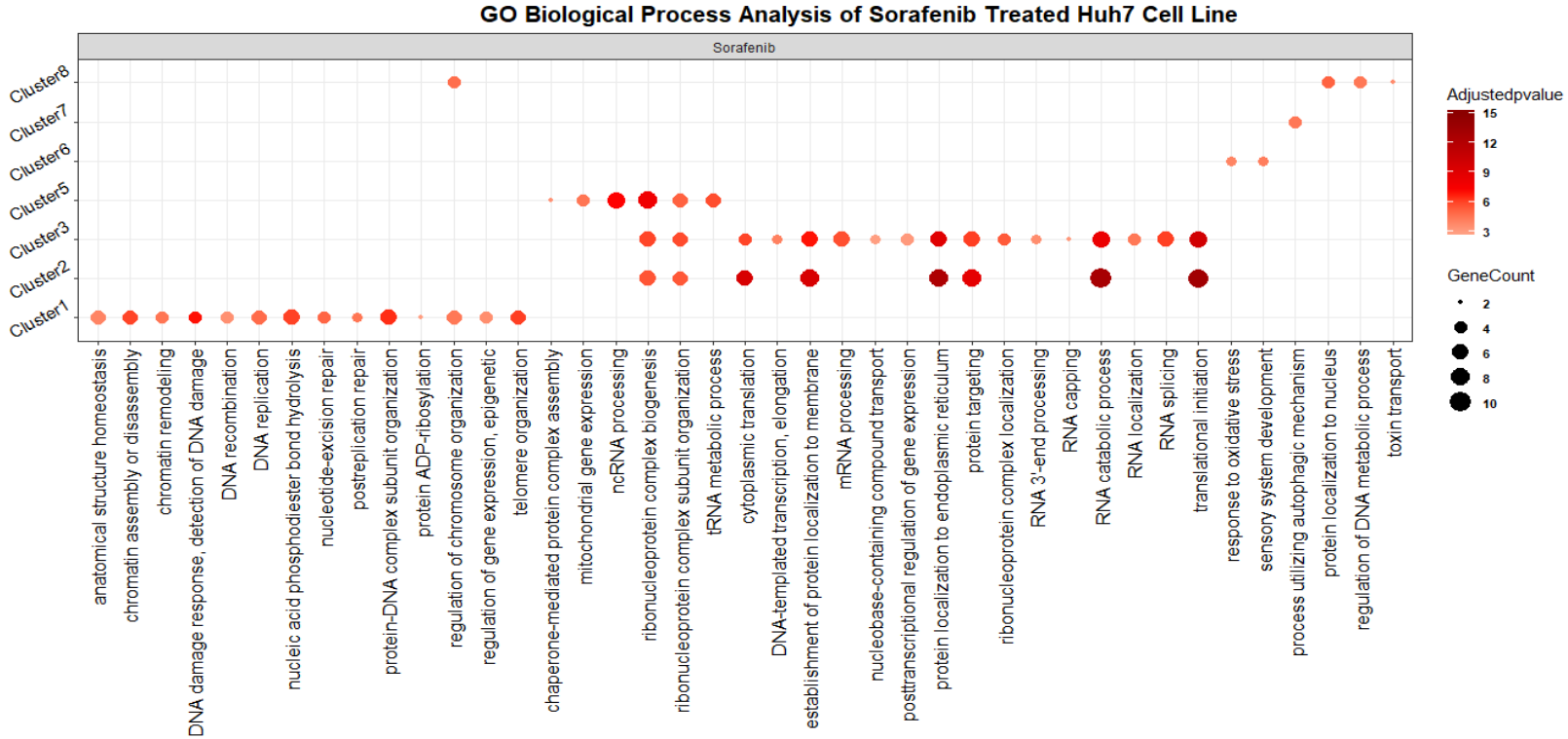

Figure 4.13: Enriched GO biological process terms for each cluster (which has an enrichment score and corresponding functional enrichment term within the specific cutoff) in Sorafenib-treated Huh7 network are demonstrated with a previously given threshold FDR ≤ 0.05. Afterwards, negative logarithm base 10 was applied to the p-values of the genes in all clusters. The color intensity, based on adjusted p-values, depicts the level of significancy of the corresponding functional enrichments. GeneCount refers to the number of genes involved in the associated biological process enrichment category.

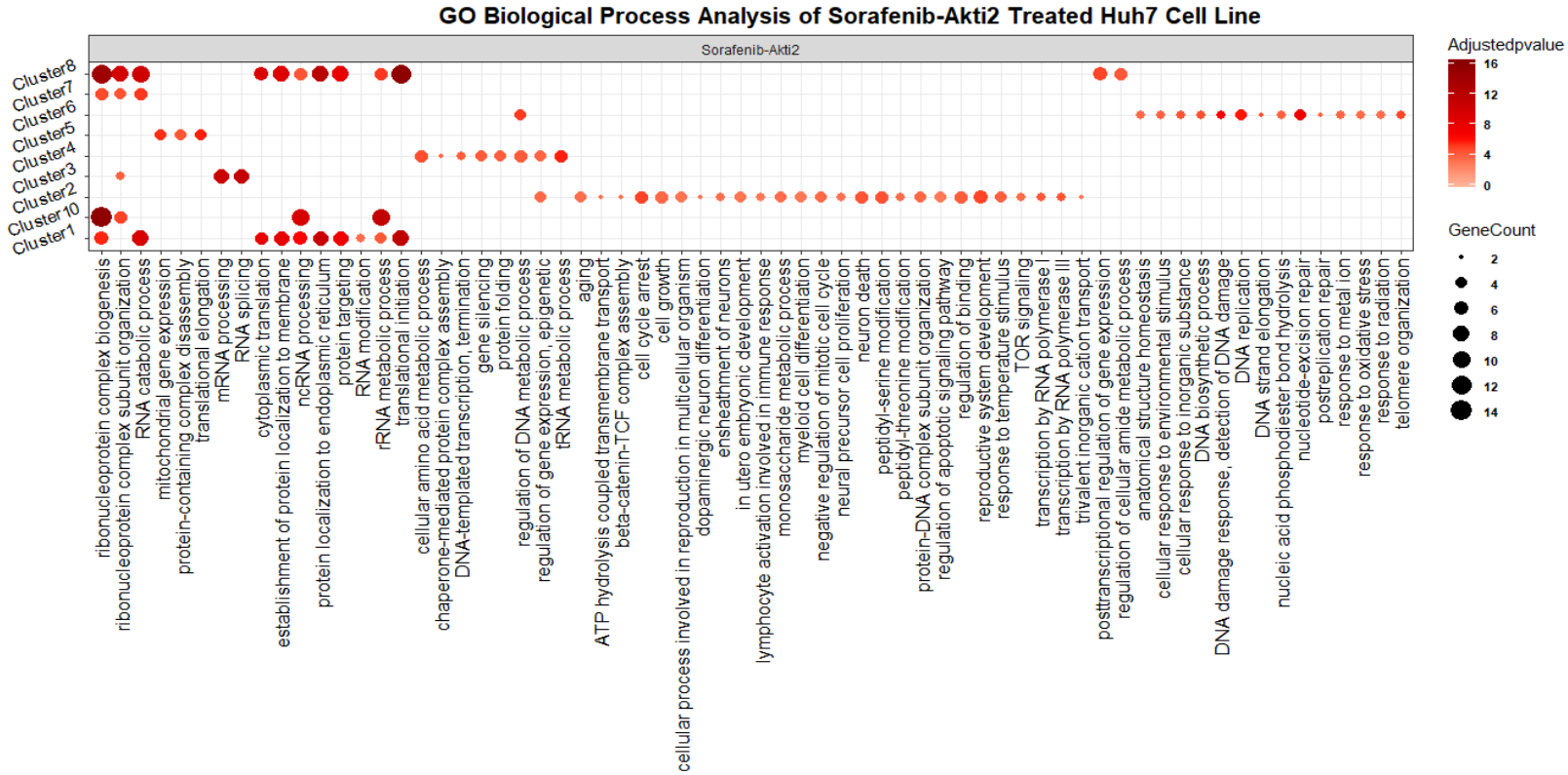

Figure 4.14: Enriched GO biological process terms for each cluster (which has an enrichment score and corresponding functional enrichment term within the specific cutoff) in the combination of Sorafenib-Akti2 treated Huh7 network are demonstrated with a previously given threshold FDR ≤ 0.05. Thereafter, negative logarithm base 10 was applied to the p-values of the genes in all clusters. The color intensity, based on adjusted p-values, depicts the level of significancy of the corresponding functional enrichments. GeneCount refers to the number of genes involved in the associated biological process enrichment category.

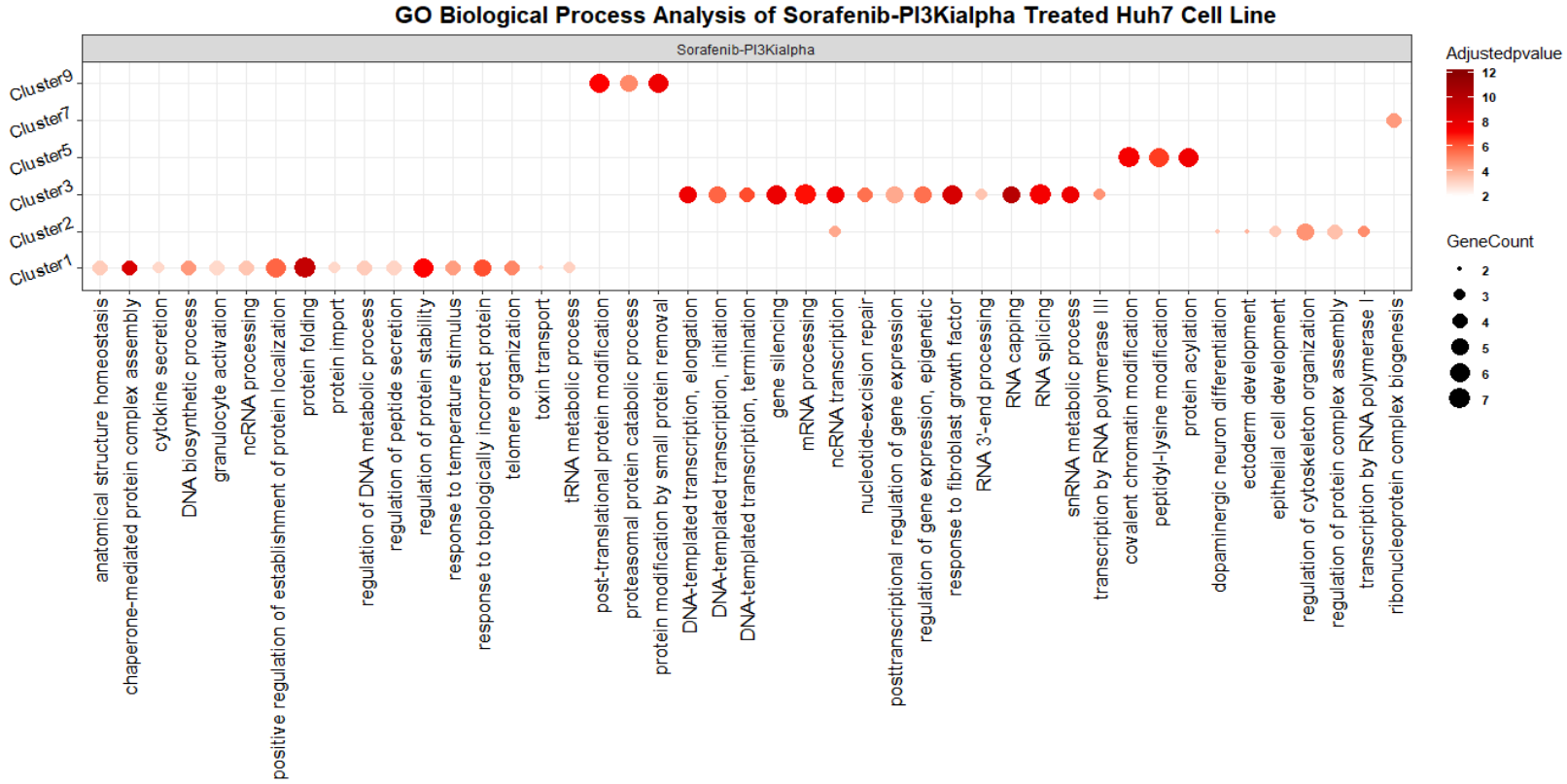

Figure 4.15: Enriched GO biological process terms for each cluster (which has an enrichment score and corresponding functional enrichment term within the specific cutoff) in the combination of Sorafenib-PI3Ki-α treated Huh7 network are demonstrated with a previously given threshold FDR ≤ 0.05. Subsequently, negative logarithm base 10 was applied to the p-values of the genes in all clusters. The color intensity, based on adjusted p-values, depicts the level of significancy of the corresponding functional enrichments. GeneCount refers to the number of genes involved in the associated biological process enrichment category.

Cluster 1 is solely composed of metabolic process events, including drug metabolic process, cofactor metabolic process, generation of precursor metabolites and energy, organic substance metabolic processes (nucleoside bisphosphate metabolism, ribonucleotide metabolic process), and so on. There are 15 functional enrichment terms for the category of GO biological process in the first cluster. Second cluster is enriched in several transport associated biological processes and process utilizing autophagic mechanism (parent term, cellular process). Third cluster is enriched in several cellular catabolic and metabolic processes, translation, signal transduction pathways, cellular protein modification processes (protein polyubiquitination, post-translational protein modification). Cluster 4 is enriched in several biological process terms. Cellular component organization, cellular development process (in particular, muscle cell differentiation), intracellular signal transduction (child term, signal transduction by p53 class mediator), cell-cell signalling by Wnt (parent term, cell communication) are a couple of the functional terms in a Mahlavu treatment with Sorafenib as a single agent (See Figure 4.16).

Second cluster consists of organelle organization-related terminologies (specifically, DNA conformation change, organelle fission), DNA metabolic process (child term, DNA recombination), cellular biosynthetic process (e.g. DNA replication), cellular protein catabolic process and cellular protein modification process. Third cluster comprises of several cellular metabolic processes. In cluster 4, several RNA metabolic process events (e.g.,RNA splicing) and macromolecule localization are significantly enriched. Transport is main functional enrichment term in Clusters 6 and 7. Cluster 5 includes the parent terms, namely localization, translation, nucleic acid metabolic process and cellular component biogenesis. One of the enriched terms in Cluster 8 is process utilizing autophagic mechanism (parent term, cellular process) in a combined treatment with Sorafenib and Akti-2 in Mahlavu cells (See Figure 4.17).

Second cluster comprises of several intracellular transport categorical functional terms and process utilizing autophagic mechanism. Multiple clusters have several enrichment terms in the category of negative regulation of cell cycle (e.g., negative regulations of both cell cycle progress, mitotic cell cycle, etc.), negative regulation of organelle organization and cellular protein localization in the combination of multiple agents, Sorafenib and PI3Ki-α in Mahlavu cells (See Figure 4.18).

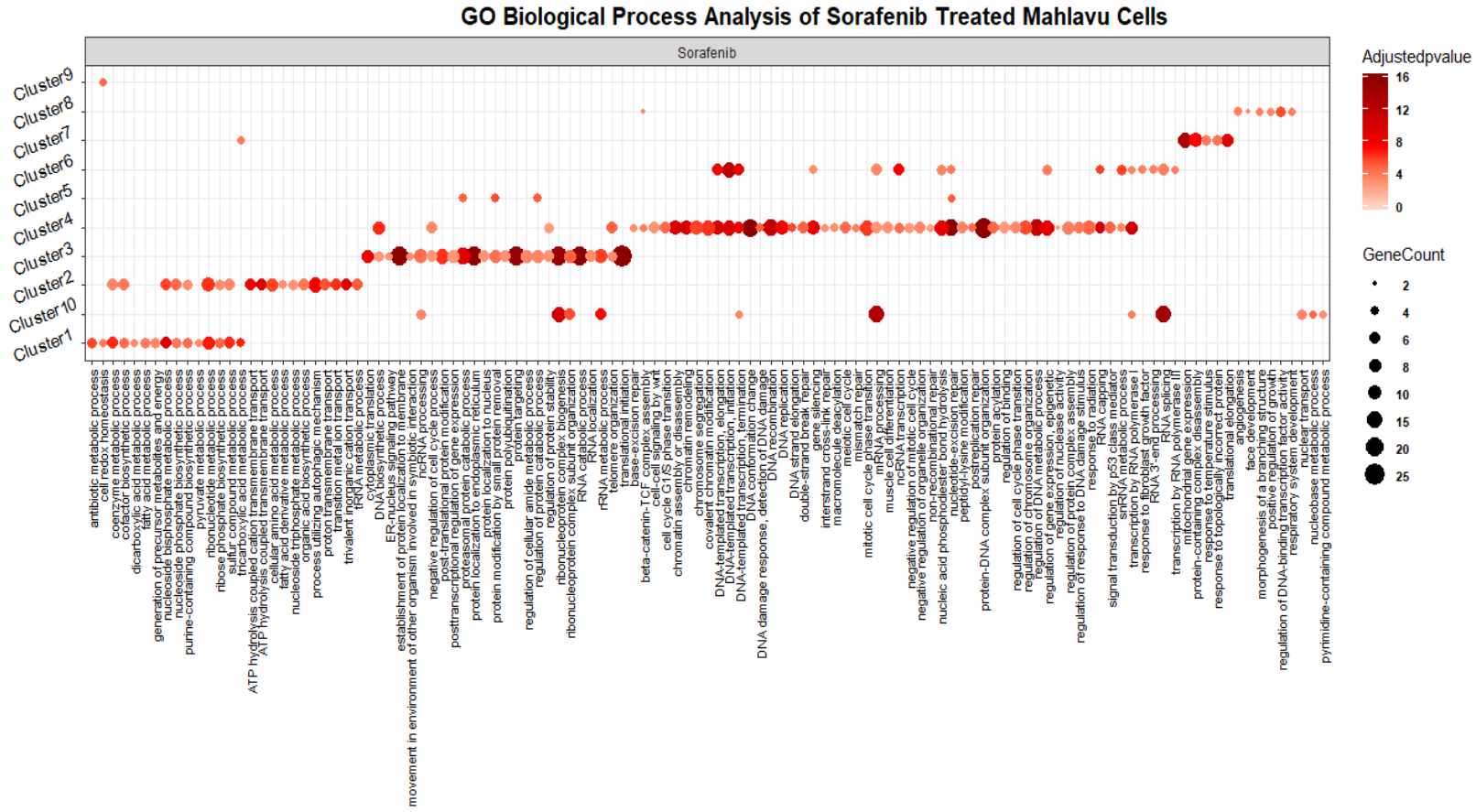

Figure 4.16: Enriched GO biological process terms for each cluster in Sorafenib-treated Mahlavu network are demonstrated with a previously given threshold FDR ≤ 0.05. After that, negative logarithm base 10 was applied to the p-values of the genes in all clusters. The color intensity, based on adjusted p-values, depicts the level of significancy of the corresponding functional enrichments. GeneCount refers to the number of genes involved in the associated biological process enrichment category.

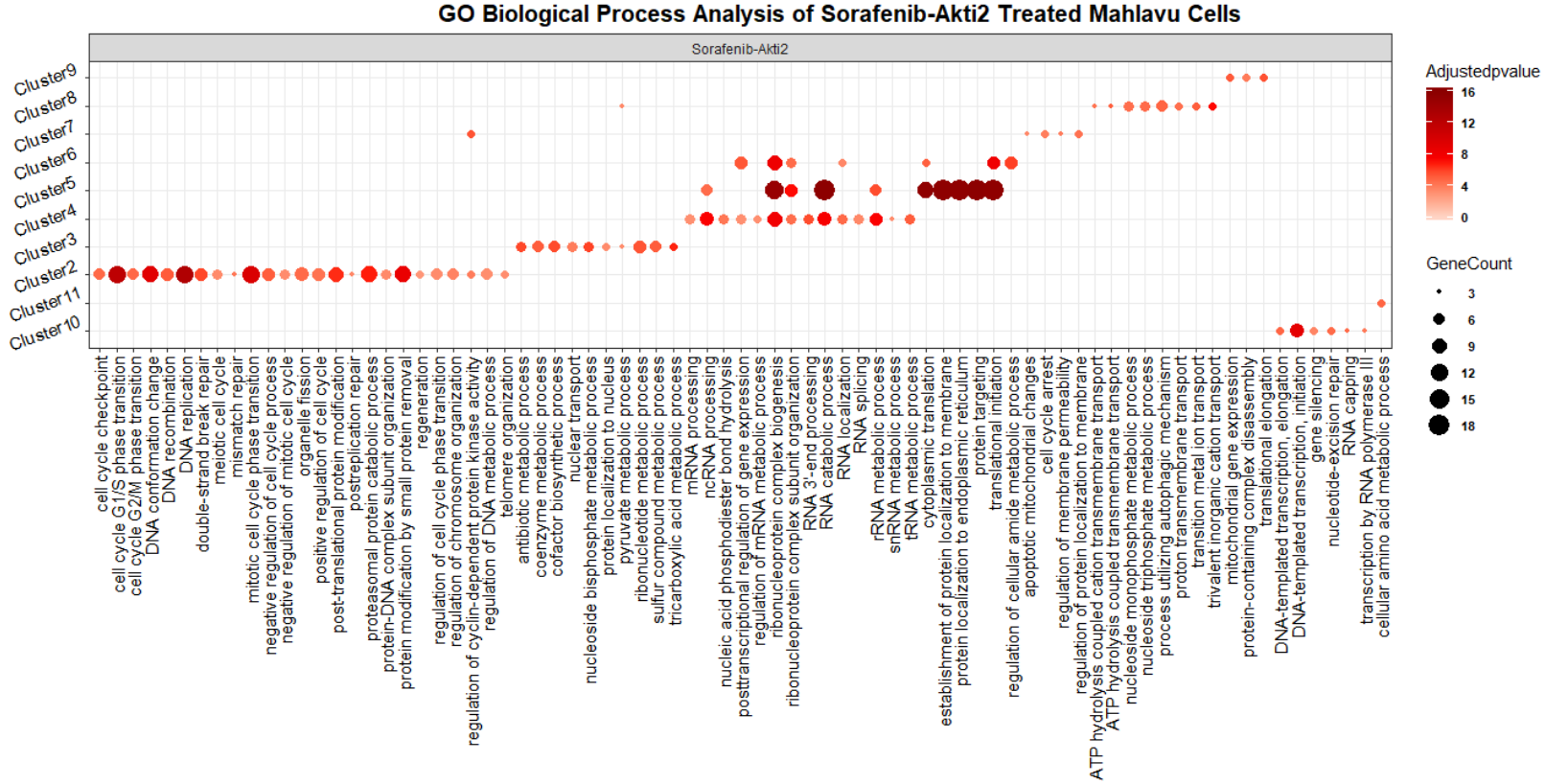

Figure 4.17: Enriched GO biological process terms for each cluster (which has an enrichment score and corresponding functional enrichment term within the specific cutoff) in the combination of Sorafenib-Akti2 treated Mahlavu network are demonstrated with a previously given threshold FDR ≤ 0.05. Then, negative logarithm base 10 was applied to the p-values of the genes in all clusters. The color intensity, based on adjusted p-values, depicts the level of significancy of the corresponding functional enrichments. GeneCount refers to the number of genes involved in the associated biological process enrichment category.

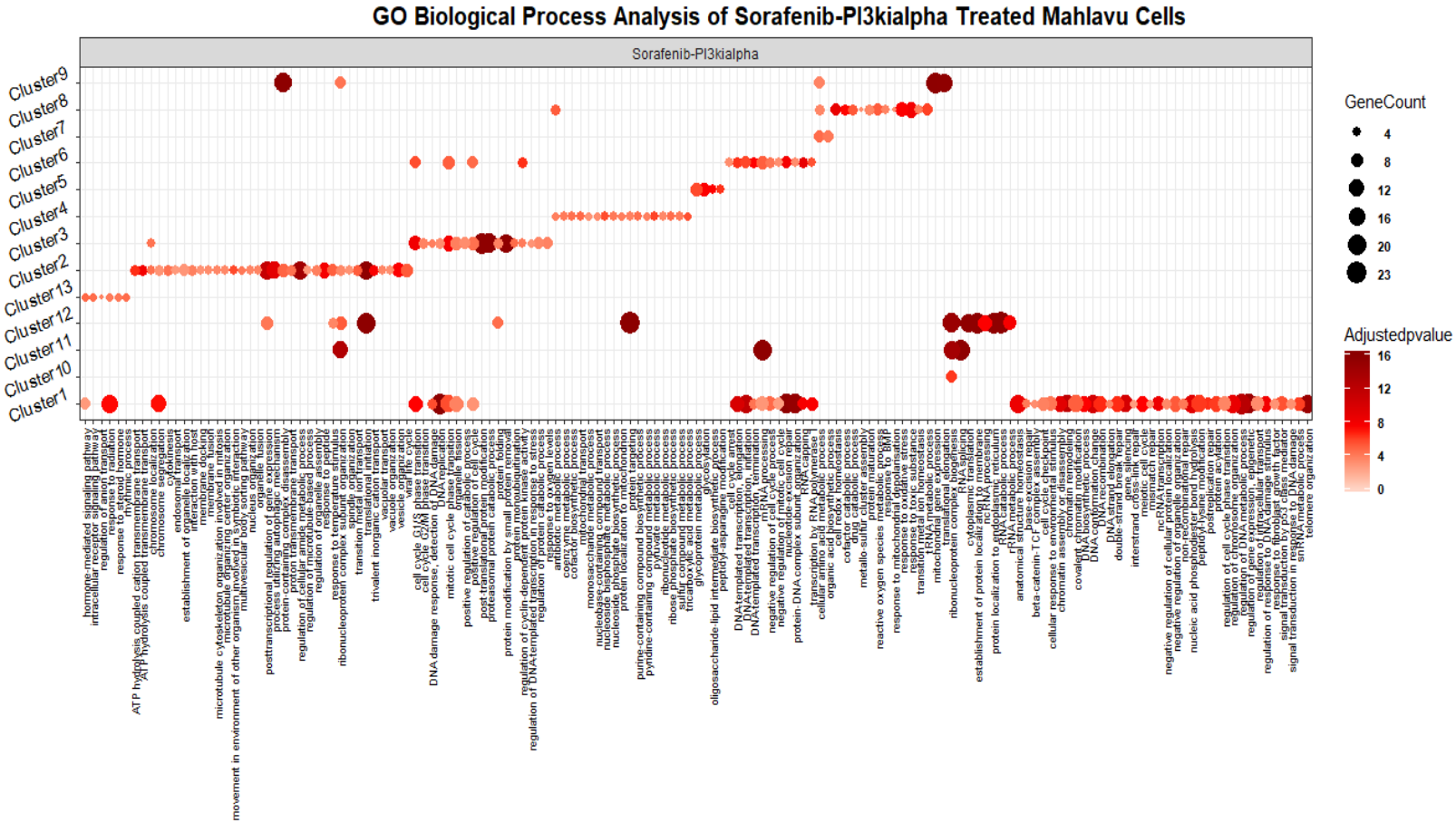

Figure 4.18: Enriched GO biological process terms for each cluster (which has an enrichment score and corresponding functional enrichment term within the specific cutoff) in the combination of Sorafenib-PI3Ki-α treated Mahlavu network are demonstrated with a previously given threshold FDR ≤ 0.05. Following that, negative logarithm base 10 was applied to the p-values of the genes in all clusters. The color intensity, based on adjusted p-values, depicts the level of significancy of the corresponding functional enrichments. GeneCount refers to the number of genes involved in the associated biological process enrichment category.

4.2 Literature and Obtained Targets of Drug Treatments and Small Molecule Inhibitors in HCC Networks

The literature and obtained (direct and indirect) targets of molecular targeted agents in our hepatocarcinoma networks are examined individually to find out whether our reconstructed networks are specific to the perturbations of drugs, inhibitors or their combination. Indirect targets are off-target effectors.

The target of Akti-2 inhibitor is AKT2 gene (Bhutani, Sheikh, & Niazi, 2013). When we added an extra filter to our method, no target was observed in the networks of both cell lines. In order to demonstrate a target, we selected the first neighbors of selected nodes in the network, and obtained AKT2 gene as a target for Akti-2. Akti1-2 inhibits both AKT1 and AKT2 genes (Bhutani et al., 2013). Again, no target was detected in the networks of Huh7 and Mahlavu cell lines. After the selection of the first degree neighbour of nodes, AKT2 gene was come up as our target. Before demonstrating the first degree neighbors of the nodes, RAC3 and PRKCB were two significant nodes in our network that might be related targets for both AKT inhibitors in two inhibitor treated Mahlavu cells (See Table 4.3).

The literature targets of LY294002 are PI3KCG and PIM1 (Jacobs et al., 2005; Semba, Itoh, Ito, Harada, & Yamakawa, 2002). These targets were not found in both networks. LY294002 is a PI3K inhibitor. PIK3R3, MCM2 and MCM8 were important nodes within the threshold of extra filtering in Huh7 cells. When we applied the first degree neighbor nodes to seek a literature target, mTOR and ATR were found. Liu, et al. suggested that both genes are distantly related to Class IV of (P. Liu, Cheng, Roberts, & Zhao, 2009). For Mahlavu cells, PIK3C3 and MCM2 were in significant nodes (within the cutoff of extra filter). When we picked the first degree neighbors of our nodes, mTOR, ATR, MCM2, MCM3, MCM4, MCM5, MCM6 and MCM7 were determined as indirect targets (See Table 4.3).

PI3Ki-α inhibits PI3K alpha isoforms. For Huh7 cells, PIK3C3 (VPS34) and MCM4 genes were detected in the network as potential significant targets of PI3Ki-α (Burke, 2018). When we applied the first degree neighbor nodes to find out more important genes, ATR, MCM2, MCM4, MCM5, MCM6, and MCM7 were found as off-target effectors. In the aspect of Mahlavu cells, PIK3C3, MCM2, MCM5, MCM6 and MCM7 genes were seen in the network. To seek more nodes, we picked first degree neighbors of nodes and obtained ATM, ATR, and MCM4 as indirect targets (See Table 4.3).

The literature targets of Rapamycin (trade name: Sirolimus), are mTOR, FKBP1A and FGF2 (Lau, So, & Leung, 2013; Lisi, Aceto, Navarra, & Dello Russo, 2015). Interestingly, mTOR was obtained as a target for Huh7 cell line. No other target was observed after searching for the selected degree node neighbors in Huh7 cells once more. Before carrying out our target mTOR in Mahlavu cells, we again applied the first degree neighbors of selected nodes within our network. As expected, Rapamycin is involved in mTOR signalling pathway and pathways in cancer (See Table 4.3).

The well-known literature targets of Sorafenib (trade name: Nexavar) is BRAF, RAF1, PDGFR, VEGFR, and FGFR (Morse et al., 2019). It is a multi-kinase inhibitor. Sorafenib is involved in several pathways, namely MAPK signalling pathway, ErbB signalling pathway, VEGF signalling pathway, pathways in cancer, renal cell carcinoma, thyroid cancer, and hepatocellular carcinoma (Katopodis et al., 2019; Smolle, Taucher, Petru, & Haybaeck, 2014). Before checking the first degree neighbors, we did not detect any target within the strict cutoff for both cell lines, unfortunately. In order to observe nodes, we picked the first degree neighbors of nodes and obtained RAF1 and FGFR2 in Huh7 cells. BRAF, RAF1, RET and FGFRL1 were determined as our new targets in Mahlavu cells (See Table 4.4).

Sorafenib-Akti2 network is a combination of Sorafenib and Akti-2 inhibitor. Before searching for the first degree neighbors, we did not detect any known target within the strict cutoff for both cells. To observe nodes, we picked the first degree neighbors of nodes and obtained PDGFRB, FGFRL1, AKT1, RAC1 and RAC3 in Huh7 cells. In the aspect of Mahlavu cells, RAF1, BRAF, PDGFRA, RET, AKT1 and RAC2 were detected as our targets (See Table 4.4).

Sorafenib-PI3Kialpha network is a combination of Sorafenib and PI3Kialpha. Before searching for the first degree neighbors, we did not detect any known target within the strict cutoff for both cell lines. In order to observe nodes, we picked the first degree neighbors of nodes and obtained PDGFRA, PDGFRB, RET, MCM2, MCM3, MCM4, MCM5, MCM6, MCM7, mTOR, and PLK1 in Huh7 cells. In the aspect of Mahlavu cells, FGFRL1, MCM4, MCM5, MCM6, MCM7, MCM8, mTOR, and PLK1 were detected as our new targets (See Table 4.4).

The literature targets of Wortmannin are PIK3CG, PLK1, PIK3CA, and PIK3R1. It is a PI3K inhibitor. It is more potentially effective than LY294002 (Mcnamara & Degterev, 2011). PIK3R1, MCM4 and MCM8 were obtained as targets for Huh7 cells. Before carrying out mTOR in Huh7 cells, we again applied the first degree neighbors of selected nodes within our network. In the aspect of Mahlavu cells, PIK3C3, PIK3R1 and MCM3 genes were detected in the network. In order to seek more nodes, we picked first degree neighbors of nodes and obtained PLK1, mTOR, MCM4 and MCM7 (See Table 4.3).

Table 4.3: Obtained targets of Rapamycin and several inhibitors including their involvement in various regulated pathways are listed. *sign indicates the previously mentioned multiple description of the genes in the network.

Network	Cell Line	Obtained Targets	Gene Description	Regulated Processes/Pathways
Akti-2 **Akti-1-2**	Huh7, Mahlavu	AKT2	RAC-Beta Serine/Threonine (S/T) Specific Protein Kinase including SH2-like domains	PI3K/AKT/mTOR Insuling receptor signaling pathway MAPK pathway Ras pathway Cell survival, cell cycle progression, angiogenesis, metabolism, apoptosis
LY294002	Huh7	PIK3R3, mTOR, ATR, MCM2	Phosphatidylinositol 3-kinase (PIK3) regulatory subunit gamma Metabolic homeostasis DNA damage sensor DNA replication licensing factor	EGFR tyrosine kinase inhibitor resistance ErbB signaling pathway Endocrine resistance HIF-1 signaling pathway Cell cycle p53 signalling pathway DNA replication
LY294002	Mahlavu	PIK3C3,mTOR, ATR,MCM2,MCM3, MCM4, MCM5, MCM6, MCM7	PIK3 catalytic subunit type 3 (S/T) Protein Kinase mTOR and ATR Mini-chromosome maintenance proteins (MCM)	Inositol phosphate metabolism Metabolic pathways Phospholipase D pathway Fanconi anemia pathway Human papillomavirus infection Cell cycle
PI3Ki-α	Huh7	PIK3C3, ATR, MCM2, MCM4, MCM5, MCM6, MCM7	PIK3 catalytic subunit class III Ataxia telangiectasia and RAD3-related Mini-chromosome maintenance complex components	Apelin signaling pathway Phagosome Cellular senescence Initial phase of eukaryotic DNA replication
PI3Ki-α	Mahlavu	PIK3C3, ATM, ATR, MCM2, MCM4, MCM5, MCM6, MCM7	PIK3 catalytic subunit type III Ataxia Telangiectasia Mutated DNA replication licensing factors	Tuberculosis Apoptosis p53 signaling pathway Human immunodeficiency virus 1 infection Cell cycle
Rapamycin	Huh7, Mahlavu	mTOR	Mechanistic (mammalian) target of rapamycin	AMPK signaling pathway
Wortmannin	Huh7	PIK3R1, MCM4*,MCM8*, mTOR*	PIK3 regulatory subunit gamma	Natural killer cell mediated cytotoxicity GnRH Secretion Insulin Resistance
Wortmannin	Mahlavu	PIK3C3, PIK3R1*, MCM3*, PLK1*, mTOR*, MCM4*, MCM7*	PIK3 catalytic subunit type III	Phagosome Axon guidance Progesterone-mediated oocyte maturation Insulin signaling pathway

Table 4.4: Obtained targets of Sorafenib and several agents including their involvement in various regulated pathways are listed. *sign indicates the previously mentioned multiple description of the genes in the network.

Network	Cell Line	Obtained Targets	Gene Description	Regulated Processes/Pathways
Sorafenib	Huh7	RAF1, FGFR2	RAF-1 proto-oncogene Fibroblast growth factor receptor II	MAPK pathway Ras pathway Regulation of actin cytoskeleton
Sorafenib	Mahlavu	BRAF, RAF1, RET, FGFRL1	B-RAF proto-oncogene S/T protein kinase RAF proto-oncogene S/T protein kinase Proto-oncogene Tyrosine (Y) protein kinase RET Fibroblast growth factor (FGF) receptor-like1	Hepatocellular carcinoma Hepatitis C and Hepatitis B MAPK signaling pathway Central carbon metabolism in cancer FGF receptor signaling pathway
Sorafenib-Akti2	Huh7	PDGFRB,AKT1,FGFRL1, RAC1,RAC3	Platelet-derived growth factor receptor beta RAC S/T protein kinase Fibroblast growth factor receptor-like I Rac family small GTPaseI	MAPK signaling pathway PI3K/Akt pathway Signaling pathways regulating pluripotency of stem cells FGF receptor signaling pathway Ras signaling pathway
Sorafenib-Akti2	Mahlavu	PDGFRA,BRAF,AKT1,RET, RAF1,RAC2	platelet derived growth factor receptor alpha S/T protein kinase AKT S/T kinase1 RET proto-oncogene RAF-1 proto-oncogene RAS-related C3 botulinum toxin substrate2	Chemokine pathway cAMP signalling pathway Platelet activation Thyroid cancer Gap junction Focal adhesion
Sorafenib-PI3Kialpha	Huh7	PDGFRA*, PDGFRB*, RET*, MCM2, MCM3, MCM4, MCM5, MCM6, MCM7, mTOR* and PLK1	MCM proteins Polo-like kinase 1	Calcium signaling pathway JAK-STAT pathway ERK signaling DNA replication Longevity regulating pathway Oocyte meiosis
Sorafenib-PI3Kialpha	Mahlavu	FGFRL1*, MCM4*, MCM5*, MCM6*, MCM7*, MCM8*, mTOR, PLK1*	Mechanistic target of Rapamycin	Thermogenesis FoxO signaling pathway

4.3 Common Characteristics of Sorafenib-Related Multiple Network Comparisons

In order to detect common patterns and traits between Sorafenib-related multiple agents treated networks and to identify potential similarities, overlapping genes are analyzed through the following steps.

4.3.1 DeMAND Reveals That Sorafenib Interferes with Protein Folding Through Chaperone Activity in Huh7 Cell Line

To find out the overlapping part of multiple Huh7 networks and perform more analysis on these important genes, Venn Diagrams are initially depicted.

For a triple comparison of Huh7 cells, Sorafenib treated network includes 104 nodes. The combination of Sorafenib treated with PI3Kialpha inhibitor network has 107 nodes. Another pairwise combination of Sorafenib and Akti2 treated network contains 139 nodes. The number of intersection of three networks which corresponds to the overlapping genes is 15 (See Figure 4.19).

For a pairwise diagram instance, Akti2 treated Huh7 network includes 342 nodes. The pairwise combination of Sorafenib and Akti2 treated Huh7 network has 139 nodes. The number of overlapping proteins of both Huh7 networks shown in the intersection part which corresponds to 58 (See Figure 4.19).

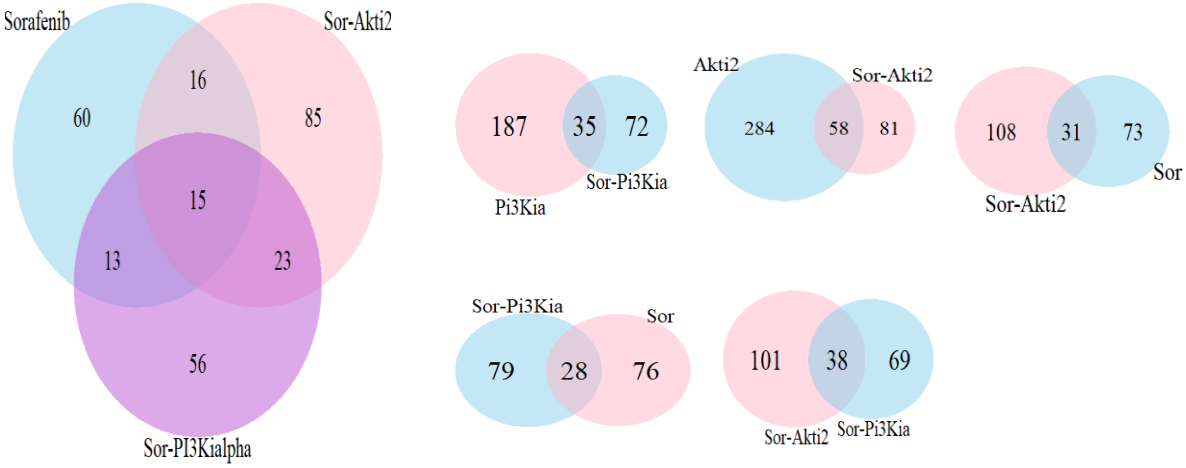

Figure 4.19: Demonstration of Venn diagrams of Huh7 cell lines. To find out the number of overlapping genes in Sorafenib treated network, the combination of Sorafenib-Akti2 treated network and the combination of Sorafenib-PI3Kialpha treated Huh7 network, Venn Diagrams are depicted. Pairwise Venn diagrams are also drawn to observe and compare Sorafenib-treated network versus inhibitors (Akti-2 and Pi3kialpha). Sor is the abbreviation of Sorafenib and PI3kia is the abbreviation of PI3kialpha in the diagrams.

Table 4.5: The overlapping genes in Sorafenib-related multiple Huh7 networks that are Sorafenib treated network, the combination of Sorafenib-Akti2 treated network and the combination of Sorafenib-PI3Kialpha treated Huh7 network are demonstrated.

Overlapping Genes in Huh7 Networks				
ATP6V1A	BUD31	CCT2	CCT3	DARS
DHX15	GNL2	HSP90AA1	HSP90AB1	KARS
KRR1	PFDN2	RPF2	RPS14	SUMO1

Gene Ontology (GO) Biological Process enrichment analysis was performed in order to have a general idea about the larger processes in which overlapping genes in Sorafenib-related multiple Huh7 networks were involved. These overlapping genes mostly took part in the protein assembly, organization, transport, cellular component biogenesis, chromosome organization, localization, cellular process, homeostatic process, regulation of biological quality, metabolic processes and RNA processing (Figure 4.20). The genes were resulted in the following enrichment terms such as chaperone-mediated protein complex assembly, ribonucleoprotein complex subunit organization, toxin transport, ribonucleoprotein complex biogenesis, telomere organization, protein localization to nucleus, protein folding, anatomical structure homeostasis, DNA biosynthetic process, DNA metabolic process, ncRNA processing (See Figure 4.20).

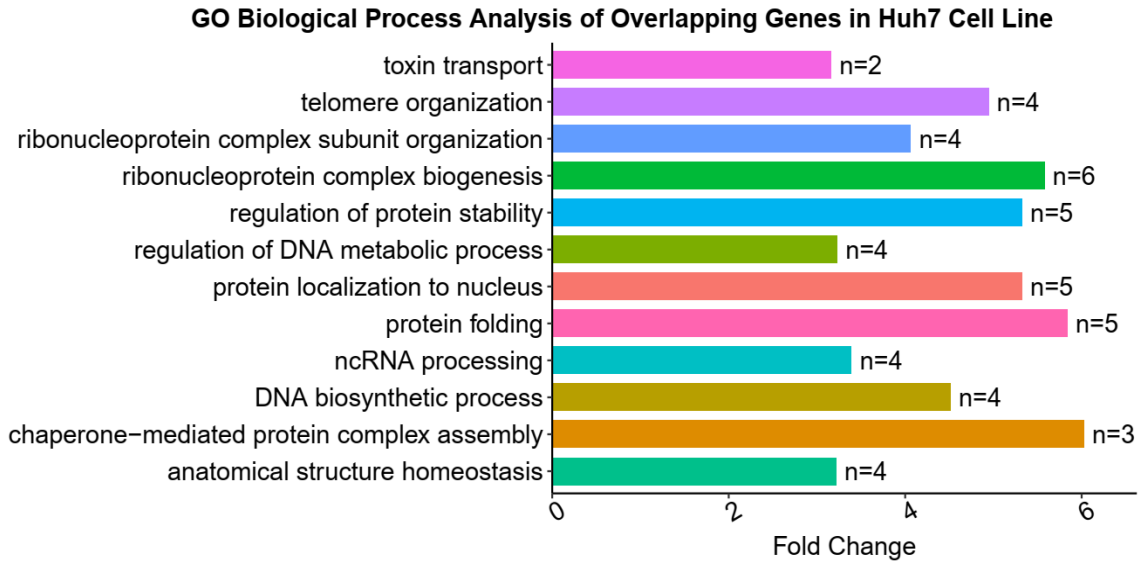

Figure 4.20: GO biological process no redundant overrepresentation enrichment analysis (ORA) of overlapping Huh7 genes was conducted by WebGestaltR package. Functional enrichment biological process terms were resulted with a previously given threshold FDR ≤ 0.05. n was the total number of overlapping genes for each specific biological process enrichment terms category in the bar chart. Negative logarithm base 10 was applied to the p-values of overlapping genes in Huh7 network. Fold change represented these adjusted p-values.

GO Molecular Function enrichment analysis was performed in order to have an idea about molecular-level activities of overlapping genes in Huh7 network. These overlapping genes were mostly involved in enzyme binding and protein binding (Figure 4.21). The genes were resulted in functional enrichment terms, including unfolded protein binding, protein binding involved in protein folding, ubiquitin-like protein ligase binding, and disordered domain specific binding (See Figure 4.21).

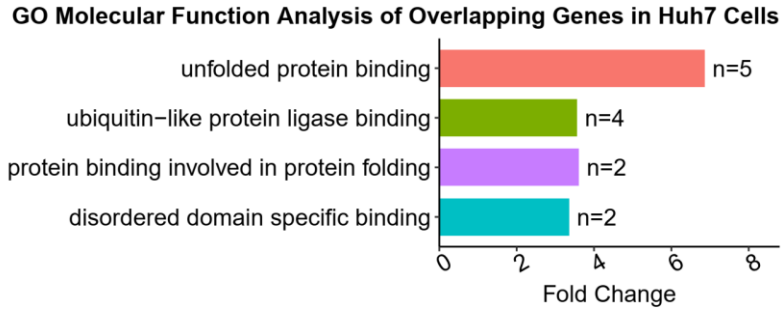

Figure 4.21: GO molecular function no redundant ORA of overlapping Huh7 genes was performed by WebGestaltR. Enriched molecular functional terms were resulted with a previously given threshold FDR ≤ 0.05. n was the number of overlapping genes for each specific molecular function enrichment terms category in the bar chart. Negative logarithm base 10 was applied to the p-values of overlapping genes in Huh7 network. Fold change represented these adjusted p-values.

GO Cellular Component enrichment analysis was performed in order to have an idea about the locations where overlapping genes in Huh7 network were carried out their functions. Cellular component enrichment outcomes of these overlapping genes were localized in chaperone complex and myelin sheath (See Figure 4.22).

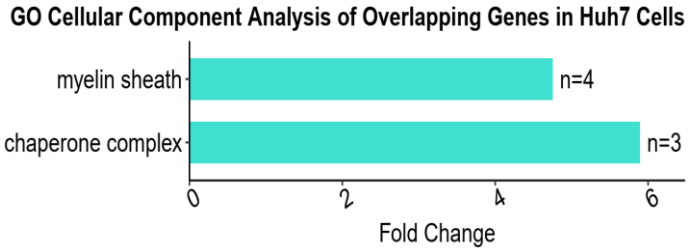

Figure 4.22: GO cellular component no redundant enrichment analysis of overlapping Huh7 genes was done by WebGestaltR package. Enriched cellular component terms are resulted with a previously given threshold FDR ≤ 0.05. n was the total number of overlapping genes for each specific cellular component enrichment terms category in the bar chart. Negative logarithm base 10 was applied to the p-values of overlapping genes in Huh7 network. Fold change represented these adjusted p-values.

To have an idea about pathways that overlapping genes in Huh7 network were involved in, we conducted a **KEGG pathway** enrichment analysis. Unfortunately, the overlapping genes did not have any functional enrichment KEGG pathway terms within FDR threshold 0.05.

Reactome pathway enrichment analysis was performed to have a general idea about pathways in which overlapping genes in Huh7 network were taken part in. These overlapping genes were mostly included in protein folding, cellular response to heat stress, metabolism of amino acids and derivatives, axon guidance, translation, and cilium assembly (Figure 4.23). The genes were resulted in the following enrichment terms, namely chaperonin-mediated protein folding, HSF1 activation, selenoamino acid metabolism, Sema3A PAK dependent axon repulsion, cytosolic tRNA aminoacylation, and BBSome-mediated cargo-targeting to cilium (See Figure 4.23).

Three aspects of gene ontology and Reactome pathway induce correlated enriched resulting outcomes with each other. One of the enriched consequences of cellular localization, chaperone complex, is significantly related to protein binding involved in protein folding and unfolded protein binding which refer to chaperone activity as a molecular functional term. Of the biological process enrichments associated with overlapping Huh7 genes, chaperone-mediated protein complex assembly and protein folding are essential terms consistent with the previous results. Given the enriched terms of Reactome pathway, protein folding and its child terms, including chaperonin-mediated protein folding and cooperation of Prefoldin and TriC/CCT in actin and tubulin folding etc. indicate that protein folding is the most significant category of overlapping Huh7 genes in Reactome pathway. Collectively, these findings suggest that overlapping genes in Sorafenib-related multiple Huh7 networks potentially interfere with protein folding through chaperone activity.
In this context, Sauzay et al. highlighted that Sorafenib can get involved in the processes of chaperoning and protein folding in Huh7 cell line (Sauzay et al., 2018).

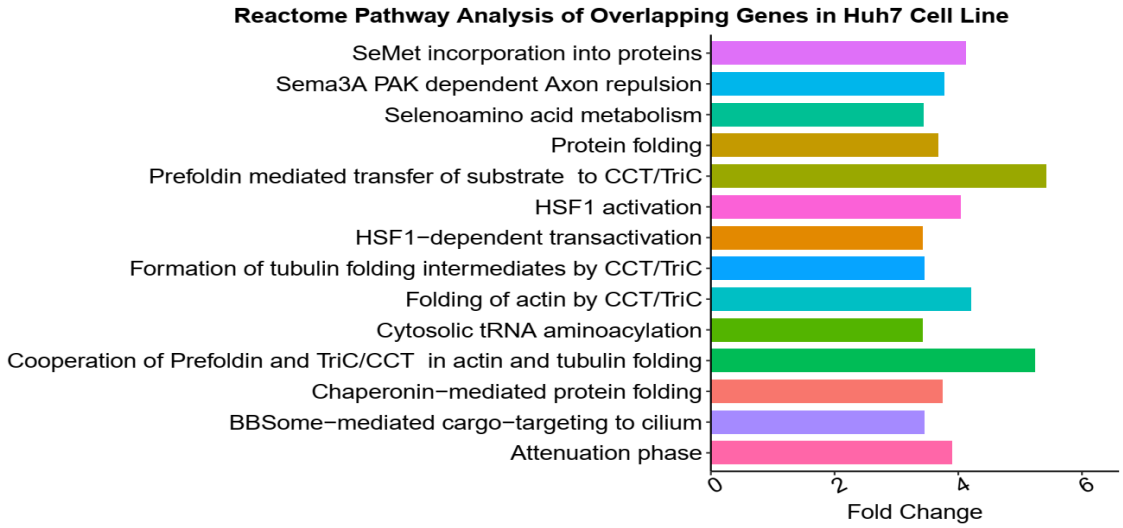

Figure 4.23: Reactome pathway enrichment analysis of overlapping Huh7 genes was conducted by WebGestaltR package. Enriched terms are resulted with a previously given threshold FDR $\leq$ 0.05. Negative logarithm base 10 was applied to the p-values of overlapping genes in Huh7 network. Fold change represented these adjusted p-values.

4.3.2 *DeMAND Indicates That Sorafenib Modulates Regulation of Autophagy in Mahlavu Cell Line*

To find out the overlapping part of multiple Mahlavu networks and perform more analysis on these important genes, Venn Diagrams are initially depicted.

For a triple comparison of Mahlavu cell line, Sorafenib treated network has 304 nodes. An example of drug and drug inhibitor together network, combination of Sorafenib treated with PI3Kialpha inhibitor, includes 428 nodes. Another example of drug and drug inhibitor combination network, Sorafenib and Akti2 network contains 229 nodes. The number of intersection of three networks which corresponds to the overlapping genes is 51 (See Figure 4.24).

For a pairwise Venn diagram instance, Akti2 treated Mahlavu network has 390 nodes. The combination of Sorafenib and Akti2 treated Mahlavu network has 229 nodes. The number of overlapping proteins of both Mahlavu networks is 72 (See Figure 4.24).

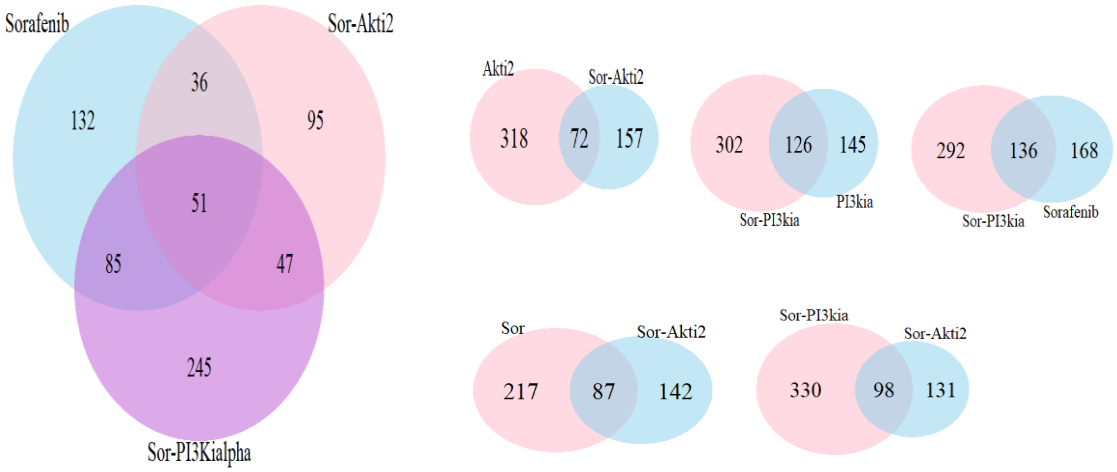

Figure 4.24: Demonstration of Venn diagrams of Mahlavu cells. In order to find out the number of overlapping genes in Sorafenib treated network, the combination of Sorafenib-Akti2 treated network and the combination of Sorafenib-PI3Kialpha treated Mahlavu network, Venn Diagrams are depicted. Pairwise Venn diagrams are also drawn to observe and compare Sorafenib-treated network versus inhibitors (Akti-2 and Pi3kialpha). Sor is the abbreviation of Sorafenib and PI3kia is the abbreviation of PI3kialpha in the diagrams.

GO Biological Process enrichment analysis was conducted to have a general idea about the larger processes where overlapping genes in Mahlavu network were involved in. These overlapping genes mostly took part in DNA repair, response to stimulus, localization, transport, cellular component organization or biogenesis, translation, homeostatic process, chromosomal organization, several cellular processes, including drug metabolic process (See Figure 4.25). The genes were resulted in the large variety of functional enrichment terms, namely interstrand cross-link repair, DNA damage response detection of DNA

damage, ribonucleoprotein complex localization, trivalent inorganic cation transport, protein-DNA complex subunit organization, translational initiation, cell redox homeostasis, telomere organization, and antibiotic metabolic process (See Figure 4.25).

Since the number of overlapping genes in Mahlavu networks was more than Huh7 networks, more enriched functional term outcomes in various categories were obtained in Mahlavu cells. For instance, interstrand cross-link repair, postreplication repair, and nucleotide-excision repair are child terms of DNA repair observed in only Mahlavu networks.

Given the numbers and categories of GO biological process terms, parent terminology is similar for both cell lines; however, child terms belonging to a particular parent term are more various in Mahlavu cells. For example, parent term transport has only a child term toxin transport in Huh7 network. The same parent term has 3 child terms, including ATP hydrolysis coupled transmembrane transport, ATP hydrolysis coupled cation transmembrane transport, and trivalent inorganic cation transport.

Common GO biological process enrichment terms between Mahlavu and Huh7 cell lines are ribonucleoprotein complex biogenesis (parent term: cellular component biogenesis) and telomere organization (parent term: chromosome organization).

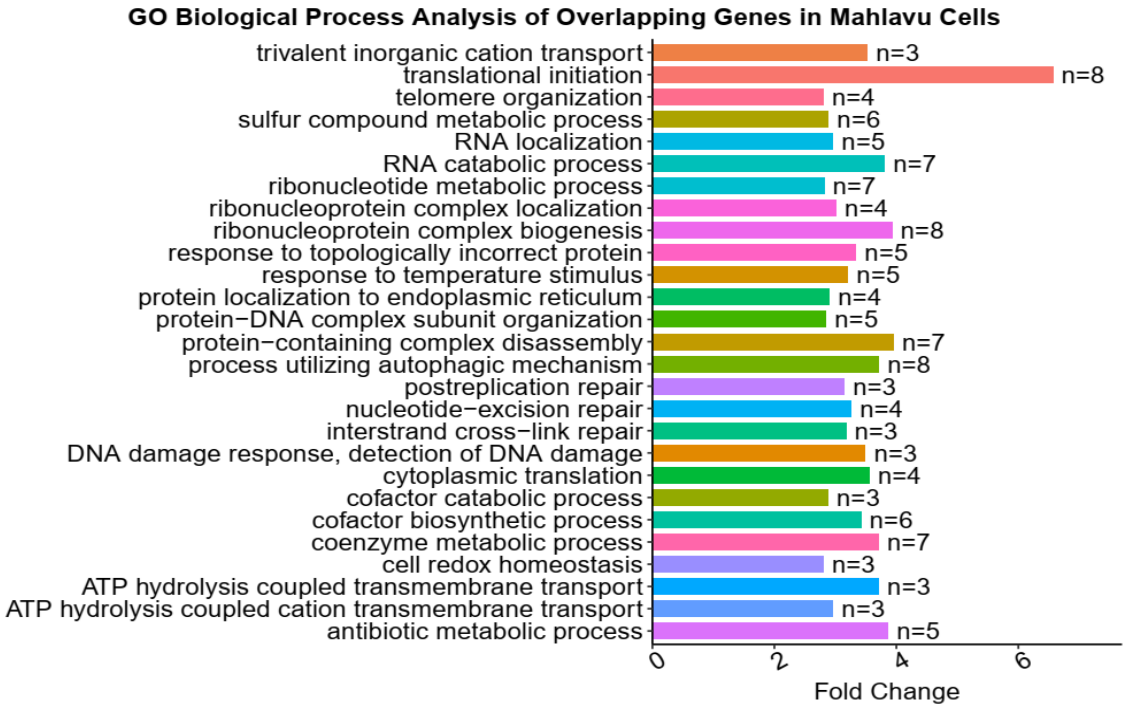

Figure 4.25: GO biological process no redundant ORA of overlapping Mahlavu genes was done by WebGestaltR. Functional enrichment biological process terms were resulted with a given threshold FDR ≤ 0.05. n was the total number of overlapping genes for each specific biological process enrichment terms category in the bar chart. Negative logarithm base 10 was applied to the p-values of overlapping genes in Mahlavu network. Fold change represented the adjusted p-values.

GO Molecular Function enrichment analysis was conducted to have an idea about molecular-level activities of overlapping genes in Mahlavu network. These overlapping genes were involved in fundamental key concepts, including structural constituent of ribosome, ATPase activity, and heat shock protein binding (See Figure 4.26). Common GO molecular function enrichment term between Mahlavu and Huh7 cell lines is protein binding (at the parent name level).

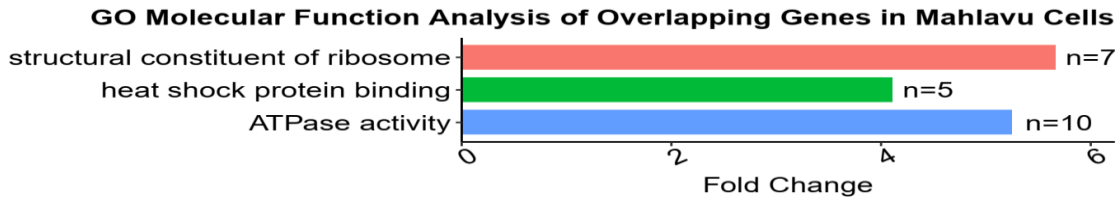

Figure 4.26: GO molecular function no redundant ORA of overlapping Mahlavu genes was done by WebGestaltR package. Enriched molecular functional terms were resulted with a given threshold FDR ≤ 0.05. n was the number of overlapping genes for each specific molecular function enrichment terms category in the bar chart. Negative logarithm base 10 was applied to the p-values of overlapping genes in Mahlavu network. Fold change represented the adjusted p-values.

GO Cellular Component enrichment analysis was performed to have an idea about the locations where overlapping genes in Mahlavu network were carried out their functions. Cellular Component enrichment outcomes of these overlapping genes were localized in several different locations, namely myelin sheath, ribosome, cytosolic part, pigment granule, chaperone complex, vesicle lumen, and proton-transporting two-sector ATPase complex (See Figure 4.27). Common GO cellular component enriched terms between Mahlavu and Huh7 cell lines are chaperone complex and myelin sheath, respectively.

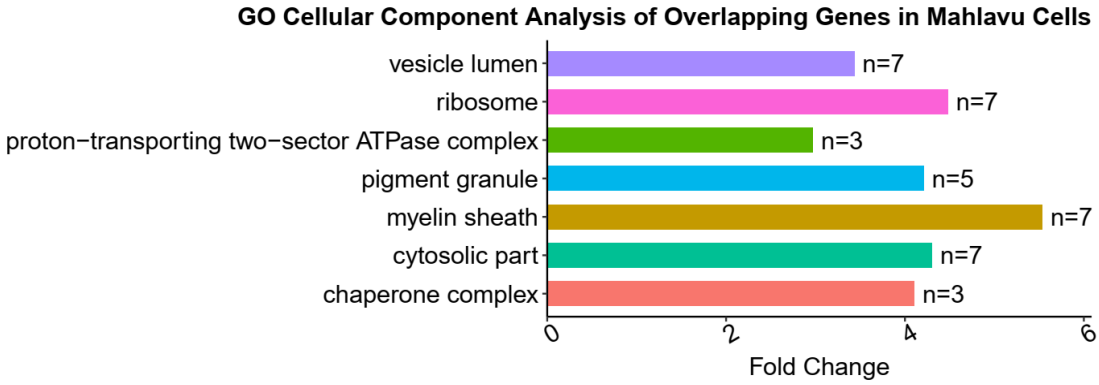

Figure 4.27: GO cellular component no redundant ORA of overlapping Mahlavu genes was done by WebGestaltR package. Enriched cellular component terms were resulted with a given threshold FDR ≤ 0.05. n was again the number of overlapping genes for each specific cellular component enrichment terms category in the bar chart. Negative logarithm base 10 was applied to the p-values of overlapping genes in Mahlavu network. Fold change represented the adjusted p-values.

KEGG pathway enrichment analysis was performed in order to have a general idea about pathways in which overlapping genes in Mahlavu network were taken part in. These overlapping genes were included in ribosome.

Reactome Pathway enrichment analysis was conducted to have an idea about pathways in which overlapping genes in Mahlavu network were taken part in. The number of enriched Reactome pathway terms is obtained as 177 (Figure 4.28). These overlapping genes were included in various different categories. The most enriched term groups in Reactome pathways are belonging to cell cycle, cellular responses to external stimuli, disease, signal transduction, DNA repair, translation, DNA replication, programmed cell death, transport of small molecules, axon guidance, immune system, transcription, and several metabolism categories, including the metabolism of amino acids and derivatives and metabolism of RNA. The genes were resulted in the following enrichment terms, namely S phase, cellular responses to stress, infectious disease, degradation of DVL, translesion synthesis by POLK, eukaryotic translation initiation, DNA replication pre-initiation, regulation of apoptosis, iron uptake and transport, regulation of expression of SLITs and ROBOs, Dectin-1 mediated noncanonical NF-kB signalling, regulation of RUNX3 expression and activity, selenoamino acid metabolism, AUF1 (hnRNP D0) binds and destabilizes mRNA (See Figure 4.28).

Due to the number of overlapping genes in Mahlavu networks was more than Huh7 networks, more enriched term results in various categories were obtained in Mahlavu cells. For instance, cell cycle related terms, including mitotic G1-G1/S phases, S phase, mitotic G2-G2/M phases, regulation of mitotic cell cycle, p53-Independent G1/S DNA damage checkpoint, and many other child sub-pathways observed in only Mahlavu networks.
Common Reactome pathway enrichment terms between Mahlavu and Huh7 cell lines are HSF1-dependent transactivation, HSF1 activation, attenuation phase (parent term of the previous 3 terms: cellular response to heat stress (child sub-pathway of cellular responses to external stimuli)), and selenoamino acid metabolism (parent term: metabolism of amino acids and derivatives).

Three aspects of gene ontology, KEGG and Reactome pathways induce various enriched resulting outcomes. One of the enriched consequences of cellular compartment, pigment granule, which is derived from lysosome, is related to 2 molecular functional terms, namely heat-shock protein binding-through chaperone-mediated autophagy- and ATPase activity-through autophagy-. Of the biological process enrichments associated with overlapping Mahlavu genes, process utilizing autophagic mechanism, response to topologically incorrect protein and protein-containing complex disassembly are essential terms. In addition to the biological terms, by incidence, cellular process, response to stimulus and cellular component organization are parent terms of the biological enrichments. From the perspective of Reactome pathway level enrichment, cellular responses to stress, HSF1-dependent transactivation, cellular responses to heat stress and attenuation phase refer that cellular response to stress (parent term: cellular response to external stimuli) is a remarkable category of overlapping Mahlavu genes in Reactome

pathway. Taken together, these findings observed from distinct ontologies and pathway suggest that overlapping genes in Sorafenib-related multiple Mahlavu networks might potentially interfere with autophagy through cellular responses to external stimuli (in our case, Sorafenib and co-treatments of Sorafenib with inhibitors).
In the light of previous analysis context, Yazdani, et al. and Dominguez et al. highlighted that Sorafenib can get involved in the regulation of autophagy and its subtypes in hepatoma cells (Prieto-Domínguez et al., 2016; Yazdani, Huang, & Tsung, 2019).

Another enriched consequences of cellular compartment, proton-transporting two-sector ATPase complex, is significantly related to ATPase activity as a molecular functional term. Of the biological process enrichments associated with overlapping Mahlavu genes, ATP hydrolysis coupled transmembrane transport, trivalent inorganic cation transport, and ATP hydrolysis coupled cation transmembrane transport are essential terms with the previous results. In addition to the biological terms, by incidence, transport is a parent name terminology of the enrichments. Given the enriched terms of Reactome pathway, iron uptake and transport and its child term transferrin endocytosis and recycling which incorporate the event of ATP hydrolysis remark that transport of small molecules is a significant category of overlapping Mahlavu genes in Reactome pathway. Collectively, these findings suggest that overlapping genes in Sorafenib-related multiple Mahlavu networks Sorafenib can potentially get involved in the processes of ATPase associated events which might be involved in transport activity.
In this context, Jiang et al., emphasized that sodium-potassium pump inclusion is constitutively increasing in many cancers. Further, ATPase complex might be involved in demonstrating several distinct functions (Jiang et al., 2018).

Another enriched results of cellular compartment, ribosome, is significantly correlated with structural constituent of ribosome as a molecular functional term. Given the enriched terms of biological process, protein localization to endoplasmic reticulum, cytoplasmic translation, translational initiation, and RNA catabolic process are vital category of overlapping Mahlavu genes. Subsequently, translation, cellular protein localization, and macromolecule catabolic process are parent name terminologies of the biological enrichments. From the perspective of KEGG pathway level enrichment, ribosome is a crucial functionally enriched term consistent with the previous results. Of the Reactome pathway enrichments associated with overlapping Mahlavu genes, translation, metabolism of amino acids and derivatives, GTP hydrolysis and joining of the 60S ribosomal subunit, eukaryotic translation initiation, peptide chain elongation, and formation of a pool of free 40S subunits remark that translation is a crucial category. Altogether, these findings observed from distinct ontologies and pathways indicate overlapping genes in Sorafenib-related multiple Mahlavu networks potentially interfere with translation events.

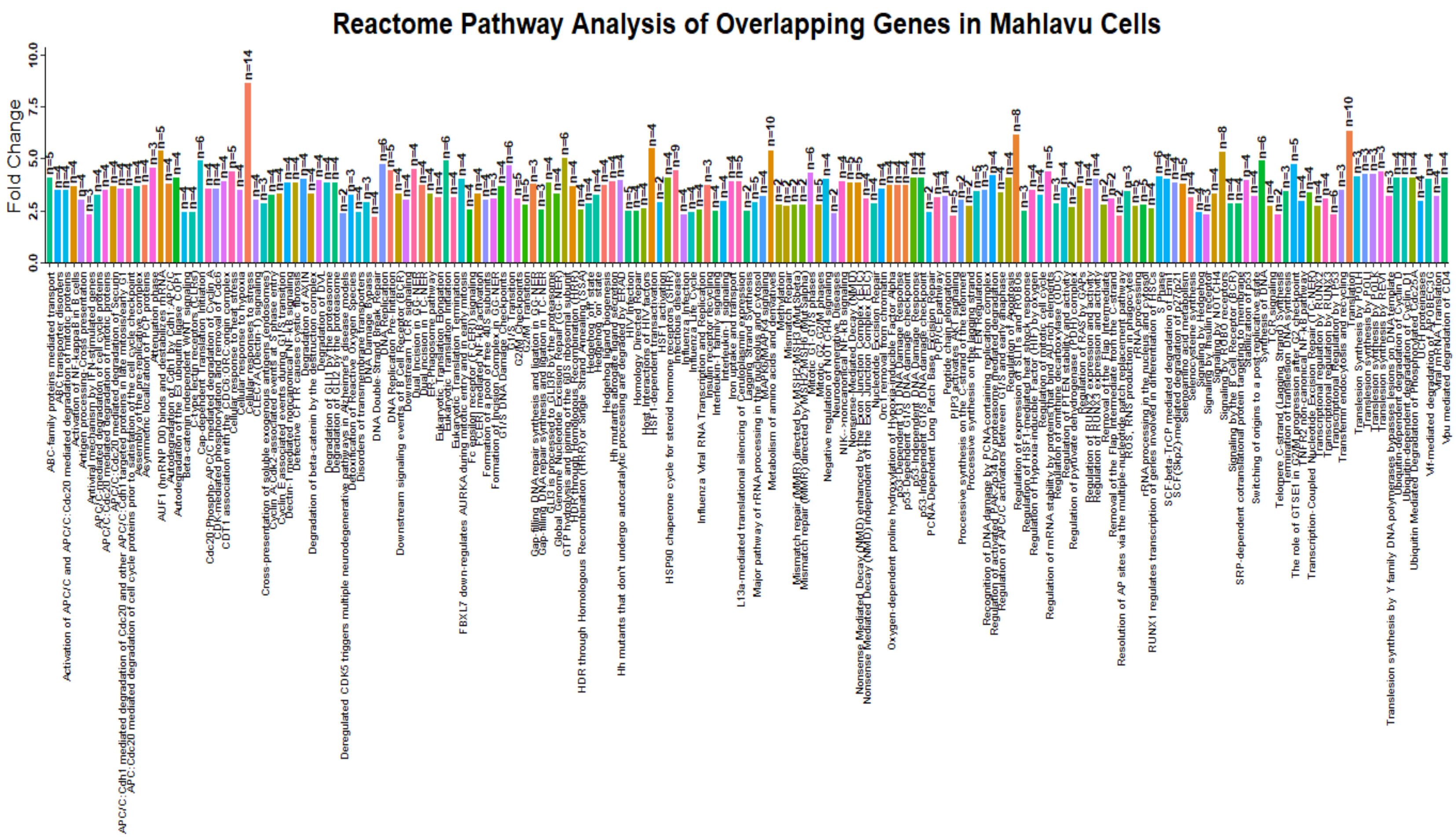

Figure 4.28: Reactome pathway enrichment analysis of overlapping Mahlavu genes was done by WebGestaltR package. Enriched terms are resulted with a previously given threshold FDR ≤ 0.05. n was the total number of overlapping genes for each specific Reactome pathway enrichment terms category in the bar chart. Negative logarithm base 10 was applied to the p-values of overlapping genes in Mahlavu network. Fold change represented these adjusted p-values.

Table 4.6: The overlapping genes in Sorafenib-related multiple Mahlavu networks that are Sorafenib treated network, the combination of Sorafenib-Akti2 treated network and the combination of Sorafenib-PI3Kialpha treated Mahlavu network are indicated.

Overlapping Genes in Mahlavu Networks																
ABCE1	ASF1A	ATP6V1A	ATP6V1B2	ATP6V1E2	CDC40	CHMP2A	COQ6	DLAT	EIF2S2	EIF4A3	EIF5	ELP3	ERCC5	ERN1	FBL	HSP90AB1
HSP90B1	HSPA2	HSPA8	ISCU	IST1	MAT1A	MAT2A	MRPL27	MRPS12	MTIF2	NARS	NMD3	NSA2	OXSM	PCNA	PDHB	POLR3A
PRDX1	PRDX2	PRDX6	PSMB2	PSMD6	PSMD7	RAD51	RBKS	RPA1	RPL12	RPL19	RPL30	RPTOR	STIP1	TSPO	UBA52	RPL17-C18orf32

4.4 Functional Enrichment Analyses of the Reconstructed Networks

In order to retrieve biological information about our reconstructed networks of both hepatocarcinoma cell lines and identify involved larger biological processes, molecular-level activities, cellular localizations, and their inclusion in pathways (namely, KEGG and Reactome), we performed overrepresentation enrichment analysis for each network. For this purpose, WebGestaltR package was used to reveal fundamental biological insights. Following that, we drew several heatmaps to visualize network similarity and difference and had a prior knowledge on the tendency of enriched terms in the reconstructed networks before clustering our dataset.

4.4.1 GO Biological Process Analyses of Huh7 and Mahlavu Cell Lines

As shown in heatmap figure in Appendix, columns indicate 9 reconstructed **Huh7** networks, and rows are the union of corresponding functional enriched GO biological process terms in the heatmap. The enriched Huh7 terms were listed by a given threshold, FDR ≤ 0.01. To visualize all 9 Huh7 networks together in a single heatmap, this threshold was chosen. Thereafter, the negative logarithm base 10 of FDR results of significantly enriched terms were applied. We further found that cellular component biogenesis, intracellular protein transport, translation, protein localization and folding, cellular catabolic process and metabolic process are highly enriched in Sorafenib-treated Huh7 network. As clearly observed from the enrichment terms, for Huh7 cell line, Sauzay and her colleagues have highlighted that Sorafenib intrude on several protein mechanisms, namely folding, chaperoning, turnover and production of proteins which correlate with our resulted network treated with single agent, Sorafenib (Sauzay et al., 2018). In the concept of the most significant enriched terms, Huh7 cells treated with Sorafenib and co-treatment of Sorafenib and Akti-2 demonstrate similar characteristic pattern. Co-treatment of Sorafenib and Akti-2 is resulted in downregulation of enrichment terms, including regulation of cell cycle, nucleic acid metabolic process, and cellular component organization compared to single treatment of Akti-2. Single treatment with Akti-2 agent and Akti-1-2 agent shows nearly the same characteristics.

Contrary to the network similarity, combined treatment of Sorafenib and PI3ki-α indicates a different behavioral pattern. Of the GO biological process enrichments associated with co-treatment of Sorafenib and PI3ki-α, RNA metabolic process, transcription and RNA processing are significant category of the genes in this network. Co-treatment of Sorafenib and PI3ki-α negatively regulates cell cycle process and DNA repair compared to single treatment of Sorafenib. Singh and her colleagues have highlighted that the alpha isoform of PI3K is involved in cell cycle process, DNA repair mechanisms and replication (Singh, Dar, & Dar, 2016). Single treatment with PI3ki-α also results in negative regulation of cell cycle process. Although PI3Ki-α is used at very low doses, it demonstrates an effective behavior, as our conclusion. In the aspect of single agent treatment with PI3ki-α, several catabolic processes are enriched, including protein catabolic processes (child term, regulation of protein catabolic process and proteasomal protein catabolic process) and nucleic acid catabolic process (specifically, RNA catabolic process). Intriguingly, single

treatment of PI3ki-α cause several immune responses in Huh7 cells within FDR ≤ 0.01. Production of molecular mediator of immune response and somatic diversification of immune responses are the child terms of immune system process. Heatmap figure is in the section of Appendix B.

We analyze that the total number of enriched GO biological process terms in Sorafenib-treated network is 73 for **Mahlavu** cell line (within FDR ≤ 0.01); whereas, this number equals to 24 for Sorafenib-treated Huh7 cells (This is an expected result of overall nodes in both networks, 304 nodes vs 104 nodes (See Table 4.2), and Mahlavu cell line is more aggressive type due to PTEN deficiency which acts as a tumor suppressor for the downstream of the PI3K/AKT signaling cascade (Chamcheu et al., 2019). All of the most significant terms in Huh7 cells also appear as much significant as in Mahlavu cells. Here, the critical point is that since the number of the enrichment terms in Mahlavu cells is higher, the number of highly-enriched terms appear as significant is also higher in Mahlavu cells. In addition to the most significant enriched terms in Huh7 cells, we found several categories of process, namely cellular metabolic process, transcription, organic acid metabolic process, cellular component organization, and RNA metabolic process. Further, given the numbers and categories of GO biological process terms, RNA metabolic and catabolic processes, negative regulation of cell cycle (child term, cell cycle arrest), cellular protein localization, translation, intracellular transport, drug metabolic process, cellular component biogenesis and chromosome organization. Co-treatment of Sorafenib and Akti-2 is resulted in reduction of enrichment terms such as macromolecule localization, response to chemical and stimuli compared to single treatment of Akti-2. In the concept of the most significant enriched terms, Mahlavu cells treated with Sorafenib and co-treatment of Sorafenib and PI3ki-α demonstrate similar characteristic pattern. Of the GO biological process enrichments associated with co-treatment of Sorafenib and PI3ki-α, translation, intracellular transport, cell cycle phase transition (G1/S phase transition, mitotic cell cycle phase transition), transcription, organelle organization, response to stimulus, several catabolic processes (proteasomal protein catabolic process, regulation of protein catabolic process, RNA catabolic process) are significant enriched terminologies. Co-treatment of Sorafenib and PI3ki-α is resulted in inhibition of enrichment terms, namely negative regulation of DNA repair and RNA metabolic process compared to single treatment of PI3ki-α. Although cell cycle arrest is enriched in Mahlavu cells upon treatment with Sorafenib as a single agent, combination of Sorafenib and PI3ki-α demonstrates a different characteristic, and enriched in cell cycle phase transition-related terminologies, same as the trend in treatment with PI3ki-α. Again, PI3Ki-α is used at very low doses, yet it demonstrates an effective behavior in Mahlavu cells. Heatmap figure is in Appendix B section.

4.4.2 GO Molecular Function Analyses of Huh7 and Mahlavu Cell Lines

Protein binding, transferase activity, catalytic activity, nucleic acid binding, and protein folding chaperone are the main enriched GO molecular function terms in combined treatment of Sorafenib and PI3kiα. Combined treatment of Sorafenib and PI3kiα is resulted in inhibition of enrichment terms binding (bindings of protein-containing

complex, chromatin, nucleic acid, and protein) and catalytic activity. As clearly observed from the enrichment terms, for **Huh7** cell line, Sauzay et al. emphasized that Sorafenib intrude on several protein mechanisms, namely folding, chaperoning, turnover and production of proteins (Sauzay, et al., 2018). The enriched Huh7 terms were listed by a given threshold, FDR ≤ 0.05. Further, single treatment of Sorafenib is resulted in enzyme binding (i.e., histone deacetylase binding), transferase activity, pyrophosphatase activity, catalytic activity and nucleic acid binding. Freese and her colleagues mentioned that histone deacetylase is an enzyme which majorly acts in carcinogenesis and further stages of hepatoma. Such that, epigenetics is a newly emerging field in the perspective of targeted therapy and if the level of high expression of histone deacetylases is observed, it can be it can be concluded that they may contribute to promote hepatocarcinoma by mis-acetylation of histone proteins (Freese et al., 2019; Y. Li et al., 2019). Huh7 cells co-treated with Sorafenib and Akti-2 demonstrates similar enrichment characteristic trend with the previous networks. Additionally, transcription factor binding (parent term: protein binding) is only enriched in this network. In the concept of the significant GO molecular function terms, single treatment with both inhibitors (Akti-2 and PI3ki-α) behaves differently in Huh7 cells (See Figure 4.15). Co-treatment of Sorafenib and Akti-2 is resulted in inhibition of enrichment terms, namely catalytic activity and binding (in particular protein binding, nucleic acid binding, chromatin binding). (See Figure Appendix B.5)

For **Mahlavu** cells, combined treatment of Sorafenib and Akti-2 resulted in several GO molecular function enrichment terms, including binding, kinase activity, nucleotide binding, protein binding, enzyme regulator activity, hydrolyase activity and nucleic acid binding. Co-treatment of Sorafenib and Akti-2 is resulted in reduction of enrichment terms protein folding chaperone, ubiquitin-like protein ligase binding (parent term enzyme binding), damaged DNA binding (parent term nucleic acid binding), protein binding (child terms, including SMAD binding, phosphoprotein binding, protein N-terminus binding), catalytic activity (child term electron transfer activity), enzyme regulator activity, and enzyme binding (histone deacetylase and phosphatase bindings. The enriched Mahlavu terms were listed by a given threshold, FDR ≤ 0.05. In addition to Sor-Akti-2 treatment, single treatment of Sorafenib is resulted in enzyme binding, transferase activity, pyrophosphatase activity, catalytic activity, ATPase activity, and bindings of chromatin, enzyme, nucleic acid and proteins. In the context of the significant GO molecular function terms, single treatment with both inhibitors (Akti-2 and PI3ki-α) behaves distinctively in Mahlavu cells (See Figure 4.16). Combined treatment of Sorafenib and PI3kiα is resulted in transferase activity, peptidase activity, nucleic acid binding, enzyme binding, transcription factor binding, and protein binding (chaperone binding, misfolded protein binding, etc.). Interestingly, kinase regulator activity is significantly enriched in combination of Sorafenib and PI3kiα network in Mahlavu cells; however, treatments with both single agents, (Sorafenib, PI3kiα) are not enriched with the specific, kinase regulator activity. Co-treatment of Sorafenib and PI3kiα is resulted in inducing enrichment terms such as translation initiation factor binding, chaperone binding (parent terms: protein binding), tRNA binding (nucleic acid binding), metal cluster binding (parent terminology

binding), ubiquitin-like protein ligase binding (parent term enzyme binding), ligase activity (parent term catalytic activity) (See Figure Appendix B.6).

4.4.3 GO Cellular Component Analyses of Huh7 and Mahlavu Cell Lines

Single treatment of Sorafenib is enriched in GO cellular compartment enrichments, namely replication fork and nuclear chromatin (parent term: chromosome) related to the DNA replication. Histone deacetylase-associated genes (first class of HDACs, i.e., HDAC2) are observed in nuclear chromatin functional cellular localization term. Although Sorafenib suppresses the activity of histone deacetylases, we have observed their corresponded enrichment term in tumorigenic cells (T. P. Liu, Hong, & Yang, 2017). Also, euchromatin, another enriched term, is related to mRNA synthesis. In addition to transcription, translation related terms are observed. The enriched **Huh7** terms were listed by a given threshold, FDR ≤ 0.05. Huh7 cells co-treated with Sorafenib and Akti-2 demonstrates the enrichment terms in translation, nucleic acid metabolic process (child term methyltranseferase complex required for mRNA cap), and protein-containing complex (child terms Sm-like protein family complex, sno-RNA, spliceosomal complex). Cervello et al. highlighted that significantly enriched genes are belonging to transcription, protein biosynthesis and protein modification following Sorafenib treated hepatoma cells (Cervello et al., 2012), in the sense of correlating with our outcomes. Combined treatment of Sorafenib and PI3kiα is resulted in similar enrichment terms transcription and translation except transferase complex (child terms complexes of acetyltransferase and transferase complex, transferring phosphorus-containing groups), secretory granule (child term ficolin-1-rich granule). Herein, co-treatment with Sorafenib and PI3kiα suppresses the activity of histone deacetylases in hepatoma cells (See Figure Appendix B.7).

Mahlavu cells co-treated with Sorafenib and Akti-2 is mainly enriched in localization of protein-containing complex (mediator complex, exoribonuclease complex, preribosome, peptidase and transferase complexes), chromosome (condensed chromosome, chromosomal region). Combination of Akti-2 and Sorafenib is resulted in reduced mitochondria related localizations such as mitochondrion and mitochondrial inner membrane and DNA replication related terminology compared to single treatment in Mahlavu cells. Single treatment of Sorafenib is enriched in nucleus-related GO cellular compartment enrichments, including DNA repair complex, nucleolus, chromosome, transcription factor complex, and chromatin. Sorafenib demonstrates a distinctive enrichment character than the co-treatment of Sorafenib with Akti-2 in the sense of protein-containing complexes. Sorafenib-treated Mahlavu cells are also enhanced the enrichments of cell junction and membrane protein complex. The network treated with only Sorafenib shows similar enrichment characteristic patterns with combined treatment of Sorafenib and PI3kiα. Co-treatment of Sorafenib and PI3kiα is enhanced in mitochondrion-related enriched terms compared to single treatment of PI3kiα. Whether Sorafenib and PI3kiα combination network is compared with the single treatments, more nucleus related terms are enriched in the combination drug treatment. The enrichment terms observed in the combination network is chromosome, DNA-packaging complex, nuclear body, and nucleus. The enriched Mahlavu terms were listed by a given threshold,

FDR ≤ 0.05. Interestingly, co-treatment with Sorafenib and PI3kiα suppresses the activity of histone deacetylases in Mahlavu cells, unlike single agent (Sorafenib) treatment. In Sorafenib treated Mahlavu cells, histone deacetylase molecules are detected in several localizations, including nuclear chromatin, ATPase complex, transcription factor complex (See Figure Appendix B.8).

4.4.4 KEGG Pathway Analyses of Huh7 and Mahlavu Cell Lines

Nucleotide metabolism, transcription, folding, sorting and degradation are the main enriched KEGG pathway terms in combined treatment of Sorafenib and PI3ki-α **Huh7** network. Interestingly, co-treatment of Sorafenib and PI3ki-α resulted in inhibition of enrichment terms, namely cell growth and death, DNA replication, translation, folding, sorting and degradation, proliferation, DNA repair, and transcription. Additionally, single agent treatment of Sorafenib is resulted in several KEGG enriched terminologies, including translation, transcription, replication and repair. Huh7 cells co-treated with Sorafenib and Akti-2 do not provoke any KEGG pathway enrichment terms, except translation related terms. Co-treatment of Sorafenib and Akti-2 resulted in inhibition of enrichment terms, including carbohydrate metabolism, folding, sorting and degradation, cell growth and death, and aging. As an observation, single treatment with both inhibitors (Akti-2 and PI3ki-α) behaves dissimilarly in Huh7 cells. In the concept of the significant KEGG pathway enriched terms, both Sorafenib and Sorafenib-Akti-2 networks contain more common patterns for Huh7 cell line; conversely, Sorafenib-PI3ki-α network acts differently (See Appendix B.3). The enriched Huh7 terms were listed by a given threshold, FDR ≤ 0.05. Single treatment with Akti-2 agent and Akti-1-2 agent shows nearly the same functional term with their similar expression level.

Combined treatment of Sorafenib and PI3kiα is resulted in inhibition of enrichment terms, including folding, sorting and degradation, cell cycle, nucleotide metabolism, DNA replication, and infectious viral disease in **Mahlavu** cells. Co-treatment of Sorafenib with PI3ki-α exhibited enhanced enrichment terms in cell growth and death category (specifically, cellular senescence and necroptosis), and transport category (in particular, RNA transport). Mahlavu cells co-treated with Sorafenib and PI3ki-α inhibit carbohydrate metabolism enrichment terms. Furthermore, Mahlavu cells co-treated with Sorafenib and Akti-2 do not provoke any KEGG pathway enrichment terms in the category of replication and repair; whereas, the network is resulted in translation, aging and carbohydrate metabolism. Co-treatment of Sorafenib and Akti-2 resulted in inhibition of enrichment terms including several signal transduction terms, transport and catabolism (sub-pathway term autophagy). Moreover, single treatment of Sorafenib is enriched in several KEGG pathways such as lipid and carbohydrate metabolisms, translation, transcription, folding, sorting and degradation. Single treatment with Akti-2 and PI3ki-α acts differently in Mahlavu cells. Common KEGG pathway enrichment terminologies between Sorafenib-PI3ki-α treated Mahlavu and Huh7 cell lines are folding, sorting and degradation, transcription, and nucleotide metabolism. Translation and transcription are mutual KEGG pathway terms of co-treatment of Sorafenib and Akti-2 and single treatment of Sorafenib

in both hepatoma cell lines (See Appendix B.4). The enriched Mahlavu terms were listed by a given threshold, FDR ≤ 0.05.

4.4.5 Reactome Pathway Analyses of Huh7 and Mahlavu Cell Lines

Common Reactome pathway enrichment terms between Sorafenib-related three networks are translation, metabolism of amino acids, axon guidance, and disease (sub-pathway terms, including infectious disease, influenza infection, influenza life cycle, influenza viral RNA transcription and replication). Primarily, axon guidance is the off-target effect observed in Sorafenib-related three **Huh7** networks. Blackadar et al. and Plummer et al. stated that viruses and bacteria are some of the infectious carcinogens that may cause severe situations (Blackadar, 2016; Plummer et al., 2016). El Dika and her colleagues mentioned that HBV, liver inflammation, diabetes, non-alcoholic steatohepatitis to cirrhosis is promoted by HIV (El Dika, Harding, & Abou-Alfa, 2017). In addition to the mutual terminology, Huh7 cells treated with Sorafenib agent is also enriched in Reactome pathway events mostly related to translational process, and metabolism of RNA. Cervello and his co-workers highlighted that significantly enriched genes are belonging to transcription, and protein biosynthesis-related mechanisms following Sorafenib treated hepatoma cells (Cervello et al., 2012), in the concept of correlating with our resulting outcomes.

Combined treatment of Sorafenib and Akti-2 resulted in several Reactome pathway Huh7 enrichment terms that are mainly categorized in translation and rRNA processing. The network treated with only Sorafenib demonstrates similar Reactome enrichment characteristic patterns with combined treatment of Sorafenib and Akti-2; whereas, combined treatment of Sorafenib and PI3kiα indicates a distinctive trend. Combined treatment of Sorafenib and PI3kiα resulted in several pathways, including HIV infection and HIV-related pathways, RNA metabolic process, transcription, RNA splicing, programmed cell death (child terms, apoptosis and regulation of apoptosis), diseases of signal transduction, transcription, and so on. These results are validated through the similar conclusions with the previous different enrichment ontologies (See Appendix B). FGFR2, one of the significant targets of Sorafenib (Morse et al., 2019), related pathways are detected in the co-treatment of Sorafenib and PI3ki-α. The parent term name of all the sub-pathways is FGFR in disease.

Common Reactome pathway enrichment terms between Sorafenib-related three **Mahlavu** networks are translation, metabolism of amino acids, programmed cell death, disease (virus-related sub-events and infectious disease), cellular responses to external stimuli, transcription-related processes, metabolism of RNA, immune system, axon guidance (parent term, developmental biology), cellular response to stress (including hypoxia-related sub-events), transport, signal transduction (mainly, Notch and Wnt signaling), and so on. Several studies have shown HIF-related events and WNT pathways are associated with each other. Actually, HIF provokes abnormal signaling of WNT pathway, and that correlates a crosstalk between these cascades (Bogaerts et al., 2014; Khalaf et al., 2018). Additionally, immune system-related sub-pathway events and axon guidance are the off-

target effect observed in Sorafenib-related three Mahlavu networks. Mahlavu cells treated with single agent, Sorafenib is enriched in Reactome pathway events mostly related to infectious disease (HIV infection, influenza infection), RNA metabolic process (mRNA splicing, mRNA capping, nonsense-mediated decay), energy-related metabolism events, namely pyruvate metabolism and citric acid (TCA) cycle, apart from the common Reactome pathway terminologies. Although Reactome gives more functional enrichment terms, the parent terminology of this database is correlated with the results of KEGG pathway. These outcomes are validated through the similar conclusions with the previous different enrichment ontologies (See Appendix B).

Combined treatment of Sorafenib and Akti-2 resulted in several Reactome pathway enrichment terms that are mainly categorized in pyruvate metabolism and TCA cycle, immune system, transcription, Notch signaling, and programmed cell death (apoptosis) other than mutual enrichment terminologies. T cell receptor (TCR) signaling, B cell receptor (BCR) signaling, Interleukin-1 family signaling, CLEC7A (Dectin-1) signaling which might be associated with off-target effects in the co-treatment of Sorafenib with Akti-2. In the aspect of related signal transduction pathway, Huang et al. have emphasized the upregulation of Notch4 receptor in 68% of tumorigenic hepatoma cells (Huang, Li, Zheng, & Wei, 2019).

Combined treatment of Sorafenib and PI3kiα resulted in several functional pathways, namely Wnt signaling, Notch signaling, signaling by Hedgehog, BCR signaling, signaling by nuclear receptors, and telomere maintenance, microRNA biogenesis, programmed cell death (apoptosis). BCR signaling, signaling by nuclear receptors (also including sub-pathway term, Estrogen (ESR)-mediated signaling) are off-target effects upon treatments with both agents, Sorafenib and PI3kiα. For the context of related terminologies, Wnt signalling dysregulation activates several embryonic development pathways that lead to hepatic oncogenesis (Wands & Kim, 2014). The more Notch1 receptor is overexpressed, the more tumorigenic potential candidate hepatoma cells become (Ning, Wentworth, Chen, & Weber, 2009). Bogaerts et al. suggested that Notch signaling modulates several processes including apoptosis that is correlated with our results (Bogaerts et al., 2014). Corte and her colleagues mentioned that signaling by Hedgehog is crucial for both production of liver cancer cells and their progress by involving with its aberrantly activated form at the embryonic developmental stage of healthy liver cells which result in stem cell growth and promotion recruiting tumorigenic liver cells derivation (Della Corte et al., 2017). From the telomere perspective, Zeng et al. expressed that in order to retain the length of telomere, high levels of telomerase enzyme have been found in many cancers due to the short length form of telomere is detected in carcinogenesis (Nault, Ningarhari, Rebouissou, & Zucman-Rossi, 2019); as a result, both length is hazardous in the context of hepatocarcinoma (Zeng et al., 2017).

4.5 Most Significant Nodes in Sorafenib-Related Multiple Reconstructed Hepatocarcinoma Networks

To observe the importance of the nodes in Sorafenib-related multiple reconstructed networks, and compare similarities/differences between the networks, the most significant nodes based on the value of betweenness centrality are shown in Table 4.7. In Table 4.7, top 10 ranking genes are listed in descending order according to centrality value (betweenness centrality) with their correspondent known cellular compartments and functions in Sorafenib-related multiple reconstructed networks for both hepatoma cell lines. Some of the genes can be detected multiple times in the reconstructed networks.
As shown in Figure 4.29, top 10 Huh7 genes in a single treatment of Sorafenib are resulted in very essential parental term categories, namely metabolism of proteins and RNA, developmental biology, infectious disease, and metabolism events. Combined treatment of Sorafenib and Akti-2 displays a similar enrichment pattern with Sorafenib-treated reconstructed network. In addition to these enrichment terms, co-treatment of Sorafenib and Akti-2 network is resulted in signal transduction (specifically, mTOR signalling and mTORC1-mediated signalling), and specific stress-related processes, including cellular response to heat stress. Apart from the previous networks, the combination of Sorafenib and PI3kiα is enriched in metabolism of proteins (in particular, chaperonin-mediated protein folding). Huh7 cells treated with this combination demonstrate disparate biological characteristic signature than other Sorafenib-treated multiple Huh7 networks.

mTOR, a Ser/Thr kinase, regulates several crucial cellular aspects, namely metabolism, cell growth, and aging. The atypical kinase is a part of two complexes, mTORC1 and mTORC2, respectively (Saxton & Sabatini, 2017). In the light of RPS6 and mTOR interaction reflecting from our inferences of Reactome pathway analysis, Calvisi et al. emphasized that RPS6 is a target of mTORC1 and resulting signals of the targets induce lipogenesis in HCC cells. Subsequently, the proteins involved in lipogenesis promotes mTOR-mediated cell growth in hepatoma cells (Calvisi et al., 2011).

As shown in Figure 4.30, top 10 Mahlavu genes in a single treatment of Sorafenib are resulted in 164 Reactome pathway enrichment terms (within FDR ≤ 0.05). As its number implies, there are many enriched terms. Notch and Wnt signalling have more Reactome sub-pathway terminologies in this network. Apart from these crucial pathways, the top 10 genes provoke enrichment terms such as diseases of signal transduction, MAPK family signalling cascades, immune system responses (including cytokine signalings (several sub-pathways, IL-1 signaling), and signallings of BCR and TCR). The immune system associated signaling pathways are the off-target effects.

Wnt signalling, a well-known conserved cascade, regulates multiple fundamental processes, including cellular differentiation and proliferation, angiogenesis, and stages of human embryogenesis (Komiya & Habas, 2008). Further, Wands et al. suggested that Wnt signalling dysregulation activates several embryonic development pathways that lead to hepatic oncogenesis (Wands & Kim, 2014). Wnt/ß-catenin cascade is known for its role in liver cell function and development. Given the enriched terms of Reactome pathway in

Figure 4.30, Khalaf and his colleagues have hypothesized that hypoxia and its related term pathways (in particular, hypoxia-inducible factors) cause abnormal signalling of Wnt/ß-catenin (Khalaf et al., 2018). As Bogaerts and her colleagues emphasized that, there is a crosstalk between Wnt/ß-catenin and hypoxia that has been validated by the experimental results (Bogaerts et al., 2014).

Notch signalling, an evolutionary conserved cascade, modulates several essential processes, namely cellular differentiation and proliferation, morphogenesis, stem-cell maintenance, and apoptosis (Bogaerts et al., 2014). 4 distinct Notch receptors, specifically, Notch1, Notch2, Notch3 and Notch4, are involved in tumorigenesis in hepatoma cells (Huang et al., 2019). Of Reactome pathway enrichments associated with top ranking genes in a single treatment with Sorafenib, Notch1 and Notch4 involving signalling sub-pathways are obtained along with the parent pathway, Notch signalling. Huang and his colleagues have emphasized the upregulation of Notch4 receptor in 68% of tumorigenic hepatoma cells (Huang et al., 2019). Additionally, Ning and his co-workers suggested that the more Notch1 receptor is overexpressed, the more tumorigenic potential candidate hepatoma cells become (Ning et al., 2009).

As shown in Figure 4.31, top 10 Mahlavu genes in a combined treatment of Sorafenib and Akti-2 are resulted in 79 Reactome pathway enrichment terms (within FDR ≤ 0.05). The functional enrichment terms are surprisingly mainly categorized in VEGF signalling, one of the notable targets of Sorafenib, ErbB signalling pathway (via EGFR and ErbB-2) and immune response. To make it clear, VEGFR2-related term is a Reactome sub-pathway that belongs to VEGF signalling. As Gampel and her colleagues suggested that KDR/FLK-1 is a gene which encodes VEGFR2 protein (Gampel et al., 2006). At this point, the results of the overlapping id of proteins indicate that heatshock family proteins (in particular, HSP90 class) and mTOR is a member of the subterm which substantiate no targeted gene and VEGF related protein product is observed.

Vascular endothelial growth factor, VEGF, is a metabolically crucial protein that is indispensable for the processes of both vascularization and angiogenesis. Of note, Angiogenesis is one of the acquired characteristic abilities of the cancerous cells, briefly, a hallmark of cancer (Hanahan & Weinberg, 2011). There are 5 types of VEGF ligands, namely VEGFA-D and placental growth factor. VEGFR, a Tyrosine kinase receptor, is specific for its ligand and 3 major kinds of these receptors are VEGFR1-3 (C. K. Lin et al., 2019). In hepatoma cells, the upregulated levels of VEGF expression is detected and very high levels of VEGF is marked at metastatic stage (Matsui et al., 2015). Concisely, upon stimulation by ligand and its specific VEGF receptor, the process of phosphorylation is occurred. As a result, vascular endothelial survival, proliferation and migration are constitutively increased (Miettinen, Rikala, Rys, Lasota, & Wang, 2012). At this level, the role of Sorafenib is to block the potential activity of VEGFR2 autophosphorylation which is intervened by VEGF ligands (Wilhelm et al., 2008).
Interestingly, top 10 Mahlavu genes in a combined treatment of Sorafenib and PI3Ki-α are not resulted in any pathway enrichment terms within our determined FDR cutoff (FDR ≤ 0.05).

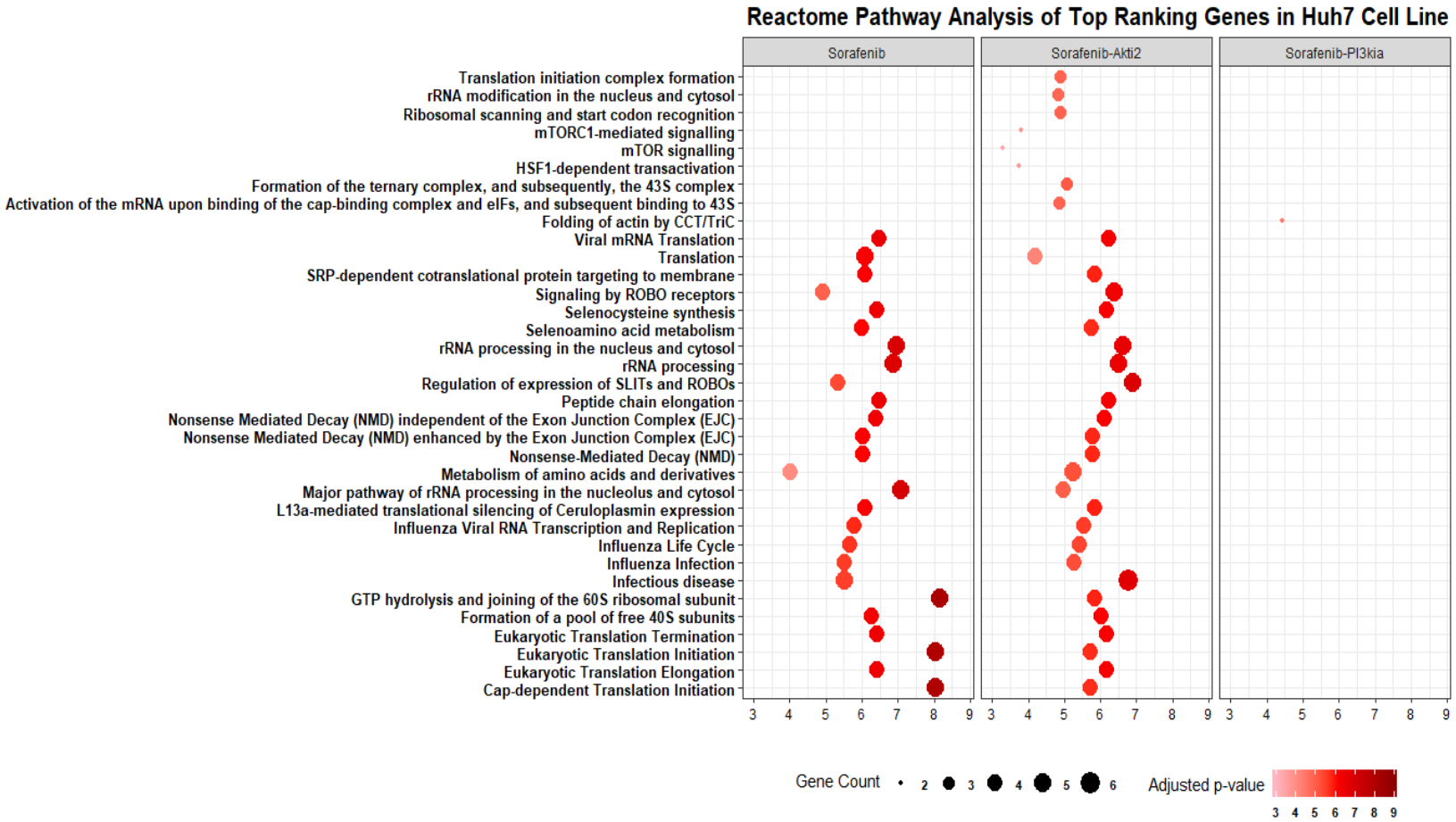

Figure 4.29: Enriched terms of top ranking genes in Sorafenib-related multiple Huh7 networks are listed with a previously given threshold FDR ≤ 0.05. Thereafter, negative logarithm base 10 was applied to the p-values of the top ranking genes in hepatoma cells. The x axis is assigned to the logarithmically adjusted p-values. The color intensity, based on adjusted p-values, shows the level of significancy of the corresponding functional enrichments. Gene count refers to the number of genes involved in the corresponding Reactome pathway enrichment category. The total number of enriched terms is 35.

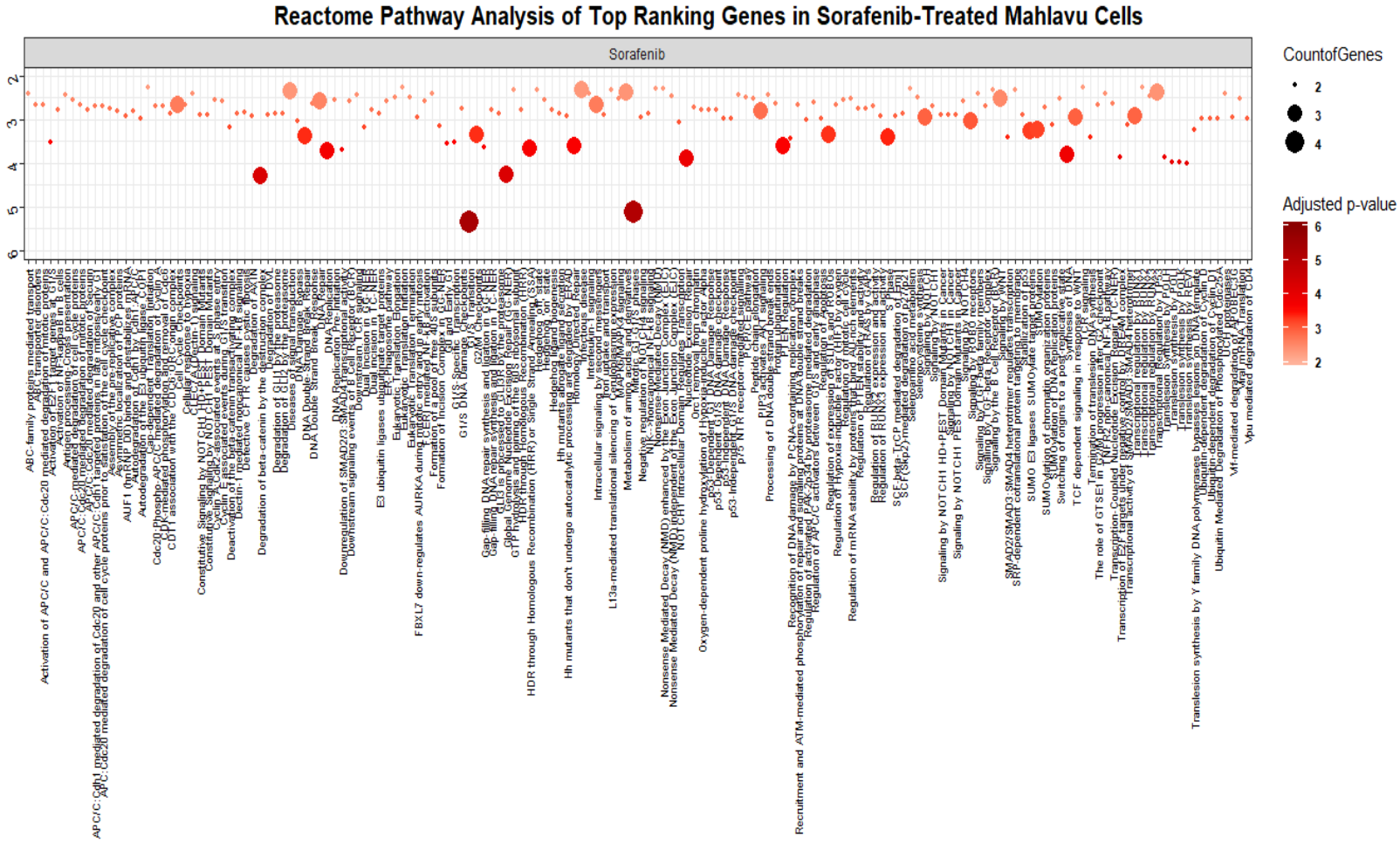

Figure 4.30: Enriched terms of top ranking genes in Sorafenib-treated Mahlavu network are listed with a previously given threshold FDR ≤ 0.05. Next, negative logarithm base 10 was applied to the p-values of the top ranking genes in hepatoma cells. The y axis is assigned to the logarithmically adjusted p-values. The color intensity, based on adjusted p-values, depicts the level of significancy of the corresponding functional enrichments. CountofGenes refers to the number of genes involved in the corresponding Reactome pathway enrichment category. The total number of enriched terms is 164.

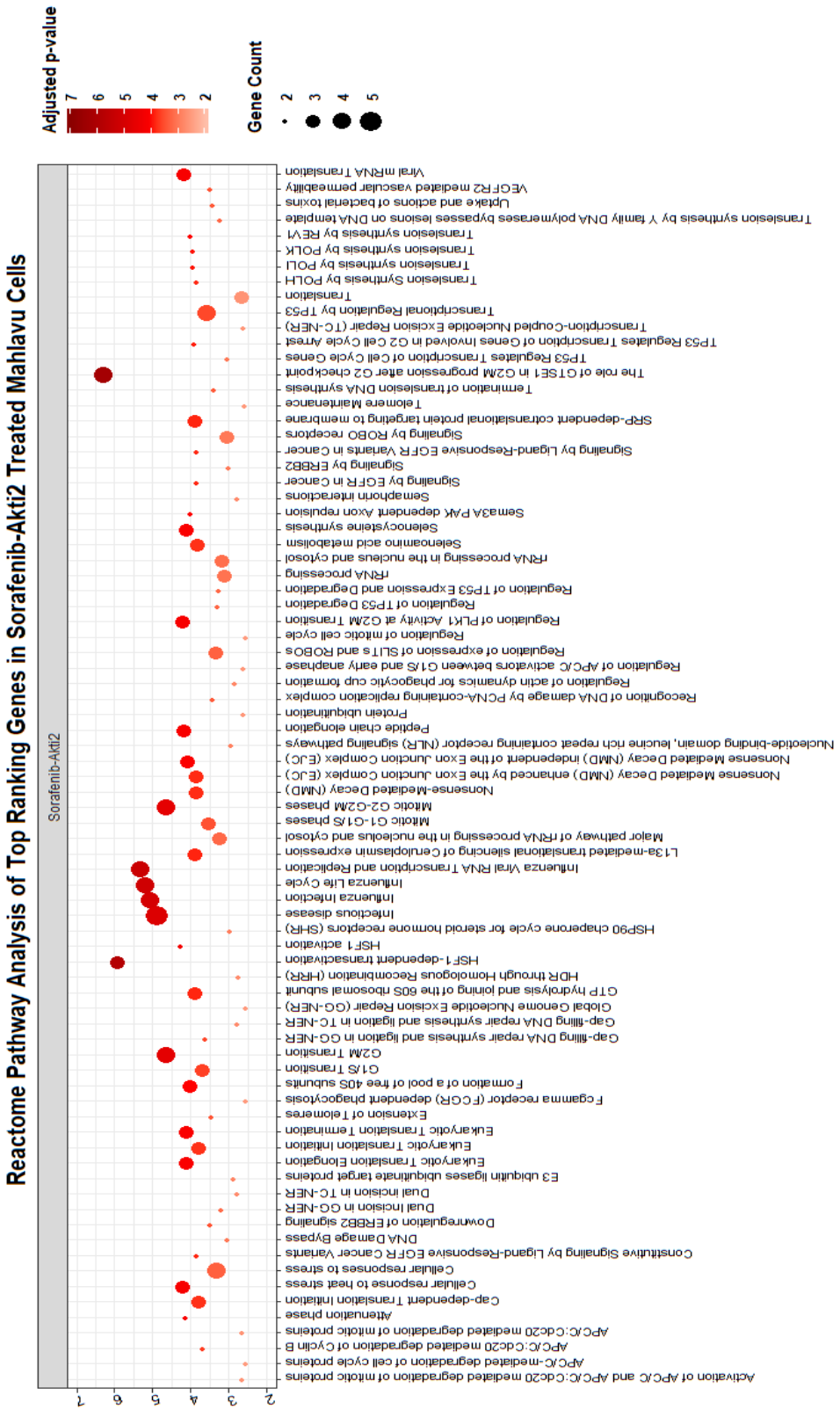

Figure 4.31: Enriched terms of top ranking genes in Sorafenib-Akti2 treated Mahlavu network are listed with a previously given threshold FDR ≤ 0.05. Afterwards, negative logarithm base 10 was applied to the p-values of the top ranking genes in hepatoma cells. The y axis is assigned to the logarithmically adjusted p-values. The color intensity, based on adjusted p-values, depicts the level of significancy of the corresponding functional enrichments. Gene count refers to the number of genes involved in the corresponding Reactome pathway enrichment category. The total number of enriched terms is 79.

Table 4.7: Top ranking genes in Sorafenib-related multiple networks of both cell line with their corresponding subcellular localizations, functions and centrality values. Centrality refers to the betweenness centrality.

	Name	Centrality	Location	Function
Sorafenib treated Huh7 network	RPL10A	0.453268	Unknown	Large ribosomal subunit (60S) component
	ASF1B	0.371925	Nucleus	Histone deposition, exchange, removal
	EIF5B	0.344495	Cytoplasm	Translation initiation
	FBL	0.329647	Nucleolus	rRNA processing through methylation
	RPL8	0.287876	Cytoplasm	Large ribosomal subunit (60S) component
	HSP90AB1	0.224688	Cytoplasm, Melanosome	Cell cycle control, signal transduction
	YEATS4	0.214638	Nucleus	Transcriptional activation by histone acetylation
	RPL37	0.198145	Unknown	Binding to 23S rRNA
	MCTS1	0.196373	Cytoplasm	Translation initiation
	RPS4X	0.165124	Cytoplasm	Small ribosomal subunit (40S) component
Sorafenib treated Mahlavu network	PCNA	0.149277	Nucleus	DNA replication
	MED31	0.100637	Nucleus	Mediator complex component
	PFDN5	0.093512	Nucleus, Cytoplasm	Chaperonin-mediated protein folding
	UBA52	0.076544	Ubiquitin: Cytoplasm, nucleus	Chromatin structure maintenance
	HDAC1	0.071903	Nucleus	Histone deacetylation
	SUMO1	0.069055	Nucleus, cell membrane	Nuclear transport, DNA replication and repair
	RPL3	0.060503	Nucleolus, cytoplasm	Large ribosomal subunit (60S) component
	PSMD2	0.060451	Unknown	Cell cycle progression, apoptosis, DNA repair
	HSP90B1	0.054777	ER lumen, melanosome	Processing and secreted proteins transportation
	ATP6V1B2	0.050986	Endomembrane system	Acidifying intracellular eukaryotic organelles
Sorafenib-Akti2 treated Huh7 network	RPS6	0.186896	Unknown	Cell growth control
	PSMD4	0.171179	Unknown	Maintenance of homeostasis
	HSP90AB1	0.152654	Cytoplasm, Melanosome	Cell cycle control, signal transduction
	NAT10	0.106472	Nucleolus, Midbody	Acetylation of histone and tRNA
	RPS24	0.103909	Unknown	pre-rRNA processing and 40S maturation
	PFDN2	0.093783	Cytoplasm, Mitochondrion	Chaperonin-mediated protein folding
	RPL13A	0.086199	Cytoplasm	Repression of inflammatory genes
	RPS14	0.084463	Unknown	Small ribosomal subunit (40S) component
	RPF2	0.083967	Nucleolus	Large ribosomal subunit (60S) assembly
	MTOR	0.080149	Lysosome, Cytoplasm	Cellular metabolism regulator, growth, survival
Sorafenib-Akti2 treated Mahlavu network	PCNA	0.115123	Nucleus	DNA replication
	RPLP0	0.099738	Nucleus, Cytoplasm	Large ribosomal subunit (60S) component
	HSP90AB1	0.097462	Cytoplasm, Melanosome	Cell cycle control, signal transduction
	MTOR	0.095784	Lysosome, Cytoplasm	Cellular metabolism regulator, growth, survival
	RPL8	0.086992	Cytoplasm	Large ribosomal subunit (60S) component
	HSP90AA1	0.081894	Cell Membrane, Melanosome	Cell cycle control, signal transduction
	CCNB1	0.079462	Nucleus,Cytoplasm,centrosome	Cell cycle control at G2/M transition
	MED31	0.077753	Nucleus	Mediator complex component
	RUVBL2	0.072295	Nucleoplasm, Cytoplasm	ATPase and DNA helicase activities
	UBA52	0.068779	Ubiquitin: Cytoplasm, nucleus	Chromatin structure maintenance
Sorafenib-PI3Kia treated Huh7 network	POLR2C	0.254899	Nucleus	Eukaryotic mRNA synthesis
	RUVBL2	0.252597	Nucleoplasm, Cytoplasm	ATPase and DNA helicase activities
	TUFM	0.237713	Mitochondrion	Protein translation in mitochondria
	CAD	0.231285	Nucleus, Cytoplasm	Nucleotide metabolism
	HSP90AB1	0.201812	Cytoplasm, cell membrane	Cell cycle control, signal transduction
	CCT6A	0.195366	Cytoplasm	Folding of Actin and Tubulin
	PSMD4	0.173453	Unknown	Maintenance of homeostasis
	SUMO1	0.159236	Nucleus, Cell Membrane	Nuclear transport, DNA replication and repair
	POLR1B	0.145165	Nucleolus	Transcription of rRNA
	CCT3	0.130216	Cytoplasm	Telomere maintenance
Sorafenib-PI3Kia treated Mahlavu network	PCNA	0.102494	Nucleus	DNA replication
	NARS	0.090176	Cytoplasm	tRNA aminoacylation
	ASF1A	0.085435	Nucleus	Histone deposition, exchange, removal
	POLR2B	0.071666	Nucleus	mRNA and many non-coding RNAs synthesis
	RPLP0	0.063374	Nucleus, Cytoplasm	Large ribosomal subunit (60S) component
	HSP90AB1	0.060987	Cytoplasm, Nucleus	Cell cycle control, signal transduction
	ABCE1	0.058507	Cytoplasm, Mitochondrion	Block activity of Ribonuclease L.
	USP14	0.048995	Cytoplasm, Cell membrane	Deubiquitination
	SUMO1	0.048832	Cell membrane, nucleus	Nuclear transport, DNA replication and repair
	TADA2A	0.046475	Nucleus, chromosome	Chromatin remodelling

CHAPTER 5

CONCLUSION

5.1 Concluding Remarks

In this thesis study, we focused on elucidating the hidden significant molecular targets or modulators in hepatocarcinoma networks which were treated with multiple molecular targeted agents by inferring the dysregulation of the Interactome. In other words, we revealed the mechanism of action of molecular targeted therapeutic agents in the context of multiple different hepatoma networks beyond the list of genes. Toward this purpose, we reconstructed 18 hepatocarcinoma networks treated with distinct molecular targeted agents to develop a further understanding of the gene perturbation level and compared the significantly enriched biological responses predominantly in the aspects of cellular state.

Acquired resistance to Sorafenib in hepatocarcinoma, the parallel alternative PI3K/AKT/mTOR signaling pathway, its high alteration rate (~51%), and the unchanged survival ratio of hepatoma leads to designing a molecular targeted therapy in which targeted therapeutic agents with the combination of well-known multi-kinase inhibitor Sorafenib are imperatively needed. For this purpose, small molecular agents which were targeting the cascade of PI3K/AKT/mTOR, namely pan-PI3K inhibitors, isoform-specific PI3K inhibitor, and isoform-specific or non-specific AKT inhibitors, and mTOR inhibitor were analyzed in two distinct hepatoma cell lines that have a differential PI3K/AKT cascade behavior. Huh7 cell line has normoactive pathway. On the other hand, due to tumor suppressor PTEN deletion, Mahlavu cell line has a hyperactive pathway. In addition to the small compound inhibitors, Sorafenib targets multiple kinases. In this study, Raf/MEK/ERK pathway was targeted by Sorafenib (primarily inhibiting Raf kinase), and VEGFR and PDGFR were also inhibited by Sorafenib that targeting cellular growth, proliferation and angiogenesis (Figure 3.2). From pharmacology-based targeted therapy perspective, it is indispensable to understand the underlying mechanism how Sorafenib and PI3K/AKT/mTOR pathway inhibitors act at signaling level, and further increasing the efficiency of Sorafenib by combined treatments and also to elucidate the off-target effects of multiple molecular targeted agents or combination of them.

We used DeMAND network modelling algorithm developed by Califano Lab to compare GEPs (from CanSyL dataset) and assesses the alteration in the individual interactions from STRING (Interactome). DeMAND searches for the mechanism of action of the agents in a network context as an alternative to differential gene expression analysis. It integrates

the possible interactions between each entity using a reference interactome to obtain an analysis beyond a gene list. The required steps to have a final optimized reconstructed network and the needed additional filtering were detailed in the pipeline (Figure 3.1). Experimentally validated PPI obtained from STRING v9.1, although it is a non-context specific network, are used to clearly observe the signaling pathways that are involved in HCC. By choosing STRING interactome, both direct and indirect targets in the signaling pathways can be easily detected. Thereafter, we reconstructed 18 molecular targeted specific networks from each GEP. Each gene and interaction within these networks have a significant value that corresponds how strongly these genes are affected from the chemical network perturbation. Each distinct reconstructed network had a different number of genes and interactions (Tables 4.1 and 4.2). In Table 4.1, first two columns (except the name of the targeted agents) that indicate the number of reconstructed nodes and edges are the solely results of DeMAND. The average number of nodes and edges are about 1300 and 1900. The vast amount of the calculated KLD.p values is equal to 1; hence, we set specific thresholds to eliminate the least significant and insignificant results in the reconstructed networks. In Table 4.2, undirected reconstructed networks with the corresponding filtered numbers of nodes and edges are specified. CTNNB1 and GSK3B which are famous hepatoma mutations are detected in some of the reconstructed HCC networks (e.g., Figures 4.6 and 4.7). CTNNB1 is detected in 26% HCC tumors and both mutations are associated with Wnt signalling cascade.

To find out whether our reconstructed networks are specific to the perturbations of drugs, small molecule inhibitors or their combination, the literature and obtained targets of molecular targeted therapeutic agents in our hepatocarcinoma networks are examined individually (Tables 4.3 and 4.4). Obtained targets validate on-target and off-target effects in the reconstructed networks. MCM proteins are determined as indirect targets. Off-target effects are obtained from ATM and ATR (regulators of damage of DNA) through MCM complex subunits which reveal the subunit-related mechanism of action, as well. Both ATM and ATR genes are associated with p53 signaling pathway.
Additionally, since our molecular targeted agents were inhibitors, we did not expect to detect their direct targets in the reconstructed networks. For this reason, we also checked the first degree neighbors of the nodes to check the presence of the targets. Most of the primary targets were not observed in the networks except only one target in LY294002 agent treated Mahlavu network, PI3Ki-α treated networks of both cell lines, Wortmannin agent treated Huh7 network, Rapamycin treated Huh7 network. Both PI3Ki-α and Rapamycin are used at very low doses; such that, whether the doses are increased (for instance, up to the dose of Sorafenib), we will probably not observe the direct targets in the reconstructed networks. Another perspective is that, although PI3Ki-α is used at very low doses (0.1 μM), it demonstrates an effective behavior as our conclusion. Its combination treatment with multikinase inhibitor Sorafenib works more effectively, suggesting that more potential promising targeted agent treatment in hepatocarcinoma. DeMAND reveals not only mechanism of action but drug similarity, as well. Co-treatment of Sorafenib and Akti-2 displays similar enrichment patterns with Sorafenib-treated reconstructed network for Huh7 cell line (e.g., Figure 4.29). RPS6 is a major downstream

target of mTORC1 in hepatoma. For the suggested mechanism of action, AKT-mTORC1-RPS6 is detected which promotes lipogenesis.

After performing overlapping genes analyses, to specifically determine common characteristics between Sorafenib-related multiple networks and to identify MoA of molecular targeted therapeutic agents in both HCC cells, we figured out that protein folding through chaperone-mediated activity is interfered with our well-known multikinase inhibitor, Sorafenib in Huh7 cell line (Figures 4.19 - 4.23). We listed the common genes in Sorafenib-related multiple reconstructed networks by DeMAND (Table 4.5). As a literature evidenced support of this association between Sorafenib and protein folding through chaperone-mediated activity revealed by DeMAND, Sauzay and her colleagues deduced a closer inference in our context (Sauzay et al., 2018).

In the aspect of overlapping genes analyses for Mahlavu cell line, we deciphered that the regulation of autophagy (through cellular responses to external stimuli) is potentially interfered with our molecular targeted agent, Sorafenib (Figures 4.24 - 4.28). It is based on DeMAND's elucidating discovery for the first time in Mahlavu cells. Yazdani et al. and Dominguez et al. suggested the connection between Sorafenib and regulation of autophagy with a similar resulting outcome in hepatocarcinoma cell lines (but not including Mahlavu cells) (Prieto-Domínguez et al., 2016; Yazdani et al., 2019). Mutual genes in Sorafenib-related multiple reconstructed networks by DeMAND are listed (Table 4.6).

Another overlapping genes analyses for Mahlavu cell line, we suggested that processes of ATPase associated events involved in transport activity are potentially intensified with our multikinase inhibitor agent, Sorafenib (Figures 4.24 - 4.28). As a literature support of this relation between Sorafenib and processes of ATPase associated events involved in transport activity revealed by DeMAND, Jiang et al., emphasized that this pump's aberrant activity in several cancers. Sodium-potassium pump inclusion is constitutively increasing in many cancers (Jiang et al., 2018). It is again based on the elucidating potential discovery of DeMAND for the first time in Mahlavu cells and needs more considerable supporting information from HCC clinical studies. HSP90AB1 (heat-shock protein) and ATP6V1A (V-type ATPase) are the common overlapping genes detected in both hepatoma cell lines. HSP90AB1 is a molecular chaperone protein.

5.2 Future Perspectives

For targeted therapy approach, we may combine multiple different agents together. In this study, we mostly analyzed PI3Ki-α and Akti-2 inhibitors, combination with Sorafenib. Whether we add one more agent, associated with mTOR; three agents in combined form will be together for more highly efficient molecular targeted therapy. From our inferences, mTOR or related TOR complex proteins, are involved in several different enrichment categorical terms more often than any other target. Therefore, new agent might be dual PI3K/mTOR inhibitors or mTOR inhibitor agent.

Recent studies have demonstrated that histone deacetylase promote hepatocarcinoma by mis-acetylation of histone proteins (Freese et al., 2019; Y. Li et al., 2019) in Huh7 cells. Such that, we may apply to use histone deacetylase inhibitors (HDACi) for our next step (based on our significant results of associated with histone deacetylases). In other words, epigenomics data may be integrated into our future network studies in HCC.

Additionally, microRNA biogenesis, our significantly found functional terminology in co-treatment of Sorafenib and PI3kiα network, Bai et al. have highlighted that microRNAs are included in hepatocarcinogenesis promotion in a very recent study (Bai, Gao, Du, Yang, & Zhang, 2019). We may consider about using microRNA inhibitors to obtain the outcomes of targeted therapy elaborately and comprehensive understanding.

For more extensive research, we may consider integrating the mutation data related to hepatocarcinoma associated with our work and subsequently reveal the mechanism of action via network-based molecular targeted therapeutic agent transcriptomics.

REFERENCES

Abdel Sammad, A. A., El-Bassuoni, M., & Talaat, R. M. (2013). An Implication of Epstein-Barr Virus in Hepatocellular Cancer Patient. *Egyptian Journal of Medical Microbiology*, *22*(1), 109–116. https://doi.org/10.12816/0004934

Abeyrathna, P., & Su, Y. (2015, November 1). The critical role of Akt in cardiovascular function. *Vascular Pharmacology*, Vol. 74, pp. 38–48. https://doi.org/10.1016/j.vph.2015.05.008

Adnane, L., Trail, P. A., Taylor, I., & Wilhelm, S. M. (2006). Sorafenib (BAY 43-9006, Nexavar®), a Dual-Action Inhibitor That Targets RAF/MEK/ERK Pathway in Tumor Cells and Tyrosine Kinases VEGFR/PDGFR in Tumor Vasculature. *Methods in Enzymology*. https://doi.org/10.1016/S0076-6879(05)07047-3

Aebersold, R., & Mann, M. (2003, March 13). Mass spectrometry-based proteomics. *Nature*, Vol. 422, pp. 198–207. https://doi.org/10.1038/nature01511

Bader, G. D., Betel, D., & Hogue, C. W. V. (2003). BIND: the Biomolecular Interaction Network Database. *Nucleic Acids Research*, *31*(1), 248–250. https://doi.org/10.1093/nar/gkg056

Bai, J., Gao, Y., Du, Y., Yang, X., & Zhang, X. (2019). MicroRNA-300 inhibits the growth of hepatocellular carcinoma cells by downregulating CREPT/Wnt/β-catenin signaling. *Oncology Letters*, *18*(4), 3743–3753. https://doi.org/10.3892/ol.2019.10712

Balogh, J., Iii, D. V., Asham, E. H., Burroughs, S. G., Boktour, M., Saharia, A., … Monsour, H. P. (2016). Hepatocellular carcinoma: a review. *Journal of Hepatocellular Carcinoma*, 3–41. https://doi.org/10.2147/JHC.S61146

Bansal, M., Gatta, G. D., & di Bernardo, D. (2006). Inference of gene regulatory networks and compound mode of action from time course gene expression profiles. *Bioinformatics*, *22*(7), 815–822. https://doi.org/10.1093/bioinformatics/btl003

Bernardo, D. Di, Thompson, M. J., Gardner, T. S., Chobot, S. E., Eastwood, E. L., Wojtovich, A. P., … Collins, J. J. (2005). Chemogenomic profiling on a genome-wide scale using reverse-engineered gene networks. *Nature Biotechnology*, *23*(3), 377–383. https://doi.org/10.1038/nbt1075

Bhutani, J., Sheikh, A., & Niazi, A. K. (2013). Akt inhibitors: Mechanism of action and implications for anticancer therapeutics. *Infectious Agents and Cancer*, *8*(1). https://doi.org/10.1186/1750-9378-8-49

Blackadar, C. B. (2016, February 10). Historical review of the causes of cancer. *World Journal of Clinical Oncology*, Vol. 7, pp. 54–86. https://doi.org/10.5306/wjco.v7.i1.54

Bogaerts, E., Heindryckx, F., Vandewynckel, Y. P., Van Grunsven, L. A., & Van Vlierberghe, H. (2014). The roles of transforming growth factor-β, Wnt, Notch and hypoxia on liver progenitor cells in primary liver tumours (review). *International Journal of Oncology*, *44*(4), 1015–1022. https://doi.org/10.3892/ijo.2014.2286

Brito, A. F., Abrantes, A. M., Pinto-Costa, C., Gomes, A. R., Mamede, A. C., Casalta-Lopes, J., … Botelho, M. F. (2012). Hepatocellular Carcinoma and Chemotherapy: The Role of p53. *Chemotherapy*, *58*(5), 381–386. https://doi.org/10.1159/000343656

Buontempo, F., Ersahin, T., Missiroli, S., Senturk, S., Etro, D., Ozturk, M., … Neri, M. L. (2011). Inhibition of Akt signaling in hepatoma cells induces apoptotic cell death independent of Akt activation status. *Investigational New Drugs*, *29*(6), 1303–1313. https://doi.org/10.1007/s10637-010-9486-3

Burke, J. E. (2018). Molecular Cell Review Structural Basis for Regulation of Phosphoinositide Kinases and Their Involvement in Human Disease. *Molecular Cell*, *71*, 653–673. https://doi.org/10.1016/j.molcel.2018.08.005

Calvisi, D. F., Wang, C., Ho, C., Ladu, S., Lee, S. A., Mattu, S., … Evert, M. (2011). Increased lipogenesis, induced by AKT-mTORC1-RPS6 signaling, promotes development of human hepatocellular carcinoma. *Gastroenterology*, *140*(3), 1071-1083.e5. https://doi.org/10.1053/j.gastro.2010.12.006

Carbon, S., Douglass, E., Dunn, N., Good, B., Harris, N. L., Lewis, S. E., & Mungall, C. J. (2019). The Gene Ontology Resource: 20 years and still GOing strong. *Nucleic Acids Research*, *47*(D1), D330–D338. https://doi.org/10.1093/nar/gky1055

Castelli, G., Pelosi, E., & Testa, U. (2017, September 20). Liver cancer: Molecular characterization, clonal evolution and cancer stem cells. *Cancers*, Vol. 9. https://doi.org/10.3390/cancers9090127

Cervello, M., McCubrey, J. A., Cusimano, A., Lampiasi, N., Azzolina, A., & Montalto, G. (2012). Targeted therapy for hepatocellular carcinoma: Novel agents on the horizon. *Oncotarget*, Vol. 3, pp. 236–260. https://doi.org/10.18632/oncotarget.466

Chamcheu, Roy, Uddin, Banang-Mbeumi, Chamcheu, Walker, … Huang. (2019). Role and Therapeutic Targeting of the PI3K/Akt/mTOR Signaling Pathway in Skin Cancer: A Review of Current Status and Future Trends on Natural and Synthetic

Agents Therapy. *Cells*, *8*(8), 803. https://doi.org/10.3390/cells8080803

Cheng, A.-L., Hsu, C.-H., Shen, Y.-C., Shao, Y.-Y., & Hsu, C. (2014). Sorafenib in advanced hepatocellular carcinoma: current status and future perspectives. *Journal of Hepatocellular Carcinoma*, 85. https://doi.org/10.2147/jhc.s45040

D'Alessandro, L. A., Meyer, R., & Klingmüller, U. (2013). Hepatocellular carcinoma: A systems biology perspective. *Frontiers in Physiology*, *4 FEB*(February), 1–6. https://doi.org/10.3389/fphys.2013.00028

Davis, W. J., Lehmann, P. Z., & Li, W. (2015, April 13). Nuclear PI3K signaling in cell growth and tumorigenesis. *Frontiers in Cell and Developmental Biology*, Vol. 3. https://doi.org/10.3389/fcell.2015.00024

Deane, J. A., & Fruman, D. A. (2004). P hosphoinositide 3-K inase : Diverse Roles in Immune Cell Activation . *Annual Review of Immunology*, *22*(1), 563–598. https://doi.org/10.1146/annurev.immunol.22.012703.104721

Della Corte, C. M., Viscardi, G., Papaccio, F., Esposito, G., Martini, G., Ciardiello, D., … Morgillo, F. (2017, June 28). Implication of the Hedgehog pathway in hepatocellular Carcinoma. *World Journal of Gastroenterology*, Vol. 23, pp. 4330–4340. https://doi.org/10.3748/wjg.v23.i24.4330

Dittmann, A., Werner, T., Chung, C. W., Savitski, M. M., Fälth Savitski, M., Grandi, P., … Drewes, G. (2014). The commonly used PI3-kinase probe LY294002 is an inhibitor of BET bromodomains. *ACS Chemical Biology*, *9*(2), 495–502. https://doi.org/10.1021/cb400789e

El-Serag, H. B. (2011). Hepatocellular carcinoma. *The New England Journal of Medicine*, *365*(12), 1118–1127.

El Dika, I., Harding, J. J., & Abou-Alfa, G. K. (2017). Hepatocellular carcinoma in patients with HIV. *Current Opinion in HIV and AIDS*, Vol. 12, pp. 20–25. https://doi.org/10.1097/COH.0000000000000335

Fabregat, A., Jupe, S., Matthews, L., Sidiropoulos, K., Gillespie, M., Garapati, P., … D'eustachio, P. (2018). The Reactome Pathway Knowledgebase. *Nucleic Acids Research*, *46*, 649–655. https://doi.org/10.1093/nar/gkx1132

Franceschini, A., Szklarczyk, D., Frankild, S., Kuhn, M., Simonovic, M., Roth, A., … Jensen, L. J. (2013). STRING v9.1: Protein-protein interaction networks, with increased coverage and integration. *Nucleic Acids Research*, *41*(D1). https://doi.org/10.1093/nar/gks1094

Freese, K., Seitz, T., Dietrich, P., Lee, S. M. L., Thasler, W. E., Bosserhoff, A., & Hellerbrand, C. (2019). Histone deacetylase expressions in hepatocellular carcinoma

and functional effects of histone deacetylase inhibitors on liver cancer cells in vitro. *Cancers*, *11*(10). https://doi.org/10.3390/cancers11101587

Gampel, A., Moss, L., Jones, M. C., Brunton, V., Norman, J. C., & Mellor, H. (2006). VEGF regulates the mobilization of VEGFR2/KDR from an intracellular endothelial storage compartment. *Blood*, *108*(8), 2624–2631. https://doi.org/10.1182/blood-2005-12-007484

Gedaly, R., Angulo, P., Chen, C., Creasy, K. T., Spear, B. T., Hundley, J., … Evers, B. M. (2012). The role of PI3K/mTOR inhibition in combination with sorafenib in hepatocellular carcinoma treatment. *Anticancer Research*, *32*(7), 2531–2536. Retrieved from http://www.ncbi.nlm.nih.gov/pubmed/22753710

Gerson, S. L., Caimi, P. F., William, B. M., & Creger, R. J. (2018). Pharmacology and Molecular Mechanisms of Antineoplastic Agents for Hematologic Malignancies. In *Hematology: Basic Principles and Practice* (pp. 849–912). https://doi.org/10.1016/B978-0-323-35762-3.00057-3

Gilot, D., Giudicelli, F., Lagadic-Gossmann, D., & Fardel, O. (2010). Akti-1/2, an allosteric inhibitor of Akt 1 and 2, efficiently inhibits CaMKIα activity and aryl hydrocarbon receptor pathway. *Chemico-Biological Interactions*, *188*(3), 546–552. https://doi.org/10.1016/j.cbi.2010.08.011

Gross, S., Rahal, R., Stransky, N., Lengauer, C., & Hoeflich, K. P. (2015, May 1). Targeting cancer with kinase inhibitors. *Journal of Clinical Investigation*, Vol. 125, pp. 1780–1789. https://doi.org/10.1172/JCI76094

Hanahan, D., & Weinberg, R. A. (2011). Hallmarks of cancer: The next generation. *Cell*. https://doi.org/10.1016/j.cell.2011.02.013

Huang, Q., Li, J., Zheng, J., & Wei, A. (2019). The carcinogenic role of the notch signaling pathway in the development of hepatocellular carcinoma. *Journal of Cancer*, Vol. 10, pp. 1570–1579. https://doi.org/10.7150/jca.26847

Iavarone, M., Cabibbo, G., Piscaglia, F., Zavaglia, C., Grieco, A., Villa, E., … Colombo, M. (2011). Field-practice study of sorafenib therapy for hepatocellular carcinoma: A prospective multicenter study in Italy. *Hepatology*, *54*(6), 2055–2063. https://doi.org/10.1002/hep.24644

Ito, T., Ando, H., Suzuki, T., Ogura, T., Hotta, K., Imamura, Y., … Handa, H. (2010). Identification of a primary target of thalidomide teratogenicity. *Science*, *327*(5971), 1345–1350. https://doi.org/10.1126/science.1177319

Iwao, C., & Shidoji, Y. (2014). Induction of nuclear translocation of mutant cytoplasmic p53 by geranylgeranoic acid in a human hepatoma cell line. *Scientific Reports*, *4*. https://doi.org/10.1038/srep04419

Jacobs, M. D., Black, J., Futer, O., Swenson, L., Hare, B., Fleming, M., & Saxena, K. (2005). Pim-1 ligand-bound structures reveal the mechanism of serine/threonine kinase inhibition by LY294002. *Journal of Biological Chemistry*, *280*(14), 13728–13734. https://doi.org/10.1074/jbc.M413155200

Jean, S., & Kiger, A. A. (2014). Classes of phosphoinositide 3-kinases at a glance. *Journal of Cell Science*, *127*(5), 923–928. https://doi.org/10.1242/jcs.093773

Jiang, W., Li, G., Li, W., Wang, P., Xiu, P., Jiang, X., … Jiang, H. (2018). Sodium orthovanadate overcomes sorafenib resistance of hepatocellular carcinoma cells by inhibiting Na+/K+-ATPase activity and hypoxia-inducible pathways. *Scientific Reports*, *8*(1). https://doi.org/10.1038/s41598-018-28010-y

Kanehisa, M., Sato, Y., Furumichi, M., Morishima, K., & Tanabe, M. (2019). New approach for understanding genome variations in KEGG. *Nucleic Acids Research*, *47*, 590–595. https://doi.org/10.1093/nar/gky962

Karovic, S., Shiuan, E. F., Zhang, S. Q., Cao, H., & Maitland, M. L. (2016). Patient-Level Adverse Event Patterns in a Single-Institution Study of the Multi-Kinase Inhibitor Sorafenib. *Clinical and Translational Science*, *9*(5), 260–266. https://doi.org/10.1111/cts.12408

Karp, P. D., Billington, R., Caspi, R., Fulcher, C. A., Latendresse, M., Kothari, A., … Subhraveti, P. (2018). The BioCyc collection of microbial genomes and metabolic pathways. *Briefings in Bioinformatics*, *20*(4), 1085–1093. https://doi.org/10.1093/bib/bbx085

Katopodis, P., Chudasama, D., Wander, G., Sales, L., Kumar, J., Pandhal, M., … Karteris, E. (2019, September 1). Kinase inhibitors and ovarian cancer. *Cancers*, Vol. 11. https://doi.org/10.3390/cancers11091357

Kerrien, S., Aranda, B., Breuza, L., Bridge, A., Broackes-Carter, F., Chen, C., … Hermjakob, H. (2012). The IntAct molecular interaction database in 2012. *Nucleic Acids Research*, *40*, 841–846. https://doi.org/10.1093/nar/gkr1088

Keshava Prasad, T. S., Goel, R., Kandasamy, K., Keerthikumar, S., Kumar, S., Mathivanan, S., … Pandey, A. (2009). Human Protein Reference Database-2009 update. *Nucleic Acids Research*, *37*, 767–772. https://doi.org/10.1093/nar/gkn892

Keskin, F., Suhre, A., Kose, K., Ersahin, T., Cetin, A. E., & Cetin-Atalay, R. (2013). Image Classification of Human Carcinoma Cells Using Complex Wavelet-Based Covariance Descriptors. *PLoS ONE*, *8*(1), 1–10. https://doi.org/10.1371/journal.pone.0052807

Khalaf, A. M., Fuentes, D., Morshid, A. I., Burke, M. R., Kaseb, A. O., Hassan, M., … Elsayes, K. M. (2018). Role of Wnt/β-catenin signaling in hepatocellular

carcinoma, pathogenesis, and clinical significance. *Journal of Hepatocellular Carcinoma*, *Volume 5*, 61–73. https://doi.org/10.2147/jhc.s156701

Knight, T., & Irving, J. A. E. (2014). Ras/Raf/MEK/ERK pathway activation in childhood acute lymphoblastic leukemia and its therapeutic targeting. *Frontiers in Oncology*. https://doi.org/10.3389/fonc.2014.00160

Komiya, Y., & Habas, R. (2008). Wnt signal transduction pathways. *Organogenesis*, Vol. 4, pp. 68–75. https://doi.org/10.4161/org.4.2.5851

Koul, P. A., & Mehfooz, N. (2019). Sirolimus in lymphangioleiomyomatosis. *Indian Chest Society*. https://doi.org/10.4103/lungindia.lungindia_280_19

Kudo, M. (2019). Targeted and immune therapies for hepatocellular carcinoma: Predictions for 2019 and beyond Conflict-of-interest statement. *World Journal of Gastroenterology*, *25*(7), 789–807. https://doi.org/10.3748/wjg.v25.i7.789

Kudo, M., Ikeda, M., Takayama, T., Numata, K., Izumi, N., Furuse, J., … Kokudo, N. (2016). Safety and efficacy of sorafenib in Japanese patients with hepatocellular carcinoma in clinical practice: a subgroup analysis of GIDEON. *Journal of Gastroenterology*, *51*(12), 1150–1160. https://doi.org/10.1007/s00535-016-1204-2

Lai, Y., Zhao, Z., Zeng, T., Liang, X., Chen, D., Duan, X., … Wu, W. (2018). Crosstalk between VEGFR and other receptor tyrosine kinases for TKI therapy of metastatic renal cell carcinoma. *Cancer Cell International*, *18*, 31. https://doi.org/10.1186/s12935-018-0530-2

Lamb, J., Crawford, E. D., Peck, D., Modell, J. W., Blat, I. C., Wrobel, M. J., … Golub, T. R. (2006). The connectivity map: Using gene-expression signatures to connect small molecules, genes, and disease. *Science*, *313*(5795), 1929–1935. https://doi.org/10.1126/science.1132939

Lau, M. T., So, W. K., & Leung, P. C. K. (2013). Fibroblast Growth Factor 2 Induces E-Cadherin Down-Regulation via PI3K/Akt/mTOR and MAPK/ERK Signaling in Ovarian Cancer Cells. *PLoS ONE*, *8*(3). https://doi.org/10.1371/journal.pone.0059083

Lencioni, R., Kudo, M., Ye, S.-L., Bronowicki, J.-P., Chen, X.-P., Dagher, L., … Sanyal, A. J. (2014). GIDEON (Global Investigation of therapeutic DEcisions in hepatocellular carcinoma and Of its treatment with sorafeNib): second interim analysis. *International Journal of Clinical Practice*, *68*(5), 609–617. https://doi.org/10.1111/ijcp.12352

Li, W., Wu, B. A., Zeng, Y. M., Chen, G. C., Li, X. X., Chen, J. T., … Zeng, Y. (2004). Epstein-Barr virus in hepatocellular carcinogenesis. *World Journal of Gastroenterology*, *10*(23), 3409–3413. https://doi.org/10.3748/wjg.v10.i23.3409

Li, Y., Rao, M., Zhang, N., Wu, L., Lin, N., & Zhang, C. (2019). BAY 87-2243 sensitizes hepatocellular carcinoma Hep3B cells to histone deacetylase inhibitors treatment via GSK-3β activation. *Experimental and Therapeutic Medicine*. https://doi.org/10.3892/etm.2019.7500

Liao, Y., Wang, J., Jaehnig, E. J., Shi, Z., & Zhang, B. (2019). WebGestalt 2019: gene set analysis toolkit with revamped UIs and APIs. *Nucleic Acids Research*, *47*(W1), W199–W205. https://doi.org/10.1093/nar/gkz401

Licata, L., Briganti, L., Peluso, D., Perfetto, L., Iannuccelli, M., Galeota, E., … Cesareni, G. (2012). MINT, the molecular interaction database: 2012 update. *Nucleic Acids Research*, *40*, 857–861. https://doi.org/10.1093/nar/gkr930

Lin, C. K., Lin, Y. H., Huang, T. C., Shi, C. S., Yang, C. T., & Yang, Y. L. (2019). VEGF mediates fat embolism-induced acute lung injury via VEGF receptor 2 and the MAPK cascade. *Scientific Reports*, *9*(1). https://doi.org/10.1038/s41598-019-47276-4

Lin, L., Yan, L., Liu, Y., Yuan, F., Li, H., & Ni, J. (2019). Incidence and death in 29 cancer groups in 2017 and trend analysis from 1990 to 2017 from the Global Burden of Disease Study. *Journal of Hematology & Oncology*, *12*(1), 96. https://doi.org/10.1186/s13045-019-0783-9

Lin, S., Hoffmann, K., & Schemmer, P. (2012). Treatment of Hepatocellular Carcinoma: A Systematic Review. *Liver Cancer*, *1*(3–4), 144–158. https://doi.org/10.1159/000343828

Lisi, L., Aceto, P., Navarra, P., & Dello Russo, C. (2015). MTOR kinase: A possible pharmacological target in the management of chronic pain. *BioMed Research International*, *2015*. https://doi.org/10.1155/2015/394257

Liu, H. Q., An, Y. W., Hu, A. Z., Li, M. H., Wu, J. L., Liu, L., … Chen, Y. (2019). Critical roles of the PI3K-Akt-mTOR signaling pathway in apoptosis and autophagy of astrocytes induced by methamphetamine. *Open Chemistry*, *17*(1), 96–104. https://doi.org/10.1515/chem-2019-0015

Liu, L., Cao, Y., Chen, C., Zhang, X., McNabola, A., Wilkie, D., … Carter, C. (2006). Sorafenib blocks the RAF/MEK/ERK pathway, inhibits tumor angiogenesis, and induces tumor cell apoptosis in hepatocellular carcinoma model PLC/PRF/5. *Cancer Research*, *66*(24), 11851–11858. https://doi.org/10.1158/0008-5472.CAN-06-1377

Liu, P., Cheng, H., Roberts, T. M., & Zhao, J. J. (2009). Targeting the phosphoinositide 3-kinase (PI3K) pathway in cancer. *Nature Reviews Drug Discovery*, *8*(8), 627–644. https://doi.org/10.1038/nrd2926

Liu, T. P., Hong, Y. H., & Yang, P. M. (2017). In silico and in vitro identification of

inhibitory activities of sorafenib on histone deacetylases in hepatocellular carcinoma cells. *Oncotarget*, *8*(49), 86168–86180. https://doi.org/10.18632/oncotarget.21030

Lounkine, E., Keiser, M. J., Whitebread, S., Mikhailov, D., Hamon, J., Jenkins, J., … Urban, L. (2012). Large Scale Prediction and Testing of Drug Activity on Side-Effect Targets. *Nature*, *486*(7403), 361–367. https://doi.org/10.1038/nature11159

Mani, K. M., Lefebvre, C., Wang, K., Lim, W. K., Basso, K., Dalla-Favera, R., & Califano, A. (2008). A systems biology approach to prediction of oncogenes and molecular perturbation targets in B-cell lymphomas. *Molecular Systems Biology*, *4*. https://doi.org/10.1038/msb.2008.2

Matsui, Y., Amano, H., Ito, Y., Eshima, K., Tamaki, H., Ogawa, F., … Majima, M. (2015). The role of vascular endothelial growth factor receptor-1 signaling in compensatory contralateral lung growth following unilateral pneumonectomy. *Laboratory Investigation*, *95*(5), 456–468. https://doi.org/10.1038/labinvest.2014.159

Maurer, G., Tarkowski, B., & Baccarini, M. (2011, August 11). Raf kinases in cancer-roles and therapeutic opportunities. *Oncogene*, Vol. 30, pp. 3477–3488. https://doi.org/10.1038/onc.2011.160

Mcnamara, C. R., & Degterev, A. (2011). *Small-molecule inhibitors of the PI3K signaling network Overview of phosphinositide-3-kinase signaling*. https://doi.org/10.4155/fmc.11.12

Miettinen, M., Rikala, M. S., Rys, J., Lasota, J., & Wang, Z. F. (2012). Vascular endothelial growth factor receptor 2 as a marker for malignant vascular tumors and mesothelioma: An immunohistochemical study of 262 vascular endothelial and 1640 nonvascular tumors. *American Journal of Surgical Pathology*, *36*(4), 629–639. https://doi.org/10.1097/PAS.0b013e318243555b

Miller, M. A. (2002, March). Chemical database techniques in drug discovery. *Nature Reviews Drug Discovery*, Vol. 1, pp. 220–227. https://doi.org/10.1038/nrd745

Morse, M. A., Sun, W., Kim, R., He, A. R., Abada, P. B., Mynderse, M., & Finn, R. S. (2019). The role of angiogenesis in hepatocellular carcinoma. *Clinical Cancer Research*, *25*(3), 912–920. https://doi.org/10.1158/1078-0432.CCR-18-1254

Nault, J. C., Ningarhari, M., Rebouissou, S., & Zucman-Rossi, J. (2019, September 1). The role of telomeres and telomerase in cirrhosis and liver cancer. *Nature Reviews Gastroenterology and Hepatology*, Vol. 16, pp. 544–558. https://doi.org/10.1038/s41575-019-0165-3

Ning, L., Wentworth, L., Chen, H., & Weber, S. M. (2009). Down-regulation of Notch1 signaling inhibits tumor growth in human hepatocellular carcinoma. *American Journal of Translational Research*, *1*(4), 358–366. Retrieved from

http://www.ncbi.nlm.nih.gov/pubmed/19956448

Nitulescu, G. M., Margina, D., Juzenas, P., Peng, Q., Olaru, O. T., Saloustros, E., … Tsatsakis, A. M. (2016). Akt inhibitors in cancer treatment: The long journey from drug discovery to clinical use (Review). *International Journal of Oncology*, *48*(3), 869–885. https://doi.org/10.3892/ijo.2015.3306

Park, S. H., Lee, Y., Han, S. H., Kwon, S. Y., Kwon, O. S., Kim, S. S., … Lee, J. H. (2006). Systemic chemotherapy with doxorubicin, cisplatin and capecitabine for metastatic hepatocellular carcinoma. *BMC Cancer*, *6*. https://doi.org/10.1186/1471-2407-6-3

Pellicoro, A., Ramachandran, P., Iredale, J. P., & Fallowfield, J. A. (2014). Liver fibrosis and repair: Immune regulation of wound healing in a solid organ. *Nature Reviews Immunology*, *14*(3), 181–194. https://doi.org/10.1038/nri3623

Plummer, M., de Martel, C., Vignat, J., Ferlay, J., Bray, F., & Franceschi, S. (2016). Global burden of cancers attributable to infections in 2012: a synthetic analysis. *The Lancet Global Health*, *4*(9), e609–e616. https://doi.org/10.1016/S2214-109X(16)30143-7

Pridgeon, C. S., Zhang, F., Heslop, J. A., Nugues, C. M. L., Neil, R., Park, B. K., & Goldring, C. E. P. (2016). DRUG DISCOVERY TOXICOLOGY. In J. Will Yvonne, McDuffie J. Eric, Olaharski Andrew J. & D. Brandon (Eds.), *Drug Discovery Toxicology: From Target Assessment to Translational Biomarkers* (First, pp. 333–345). https://doi.org/10.1002/9781119053248.ch21

Prieto-Domínguez, N., Ordóñez, R., Fernández, A., García-Palomo, A., Muntané, J., González-Gallego, J., & Mauriz, J. L. (2016, June 8). Modulation of autophagy by sorafenib: Effects on treatment response. *Frontiers in Pharmacology*, Vol. 7. https://doi.org/10.3389/fphar.2016.00151

Rodríguez, A., & DAndrea, A. (2017). *Fanconi anemia pathway*. https://doi.org/10.1016/j.cub.2017.07.043

Rollinger, J. M., Stuppner, H., & Langer, T. (2008). Virtual screening for the discovery of bioactive natural products. *Progress in Drug Research*, Vol. 65, pp. 212–249. https://doi.org/10.1007/978-3-7643-8117-2_6

Sauzay, C., Louandre, C., Bodeau, S., Anglade, F., Godin, C., Saidak, Z., … Galmiche, A. (2018). Protein biosynthesis, a target of sorafenib, interferes with the unfolded protein response (UPR) and ferroptosis in hepatocellular carcinoma cells. *Oncotarget*, *9*(9), 8400–8414. https://doi.org/10.18632/oncotarget.23843

Saxton, R. A., & Sabatini, D. M. (2017, March 9). mTOR Signaling in Growth, Metabolism, and Disease. *Cell*, Vol. 168, pp. 960–976.

https://doi.org/10.1016/j.cell.2017.02.004

Scannell, J. W., Blanckley, A., Boldon, H., & Warrington, B. (2012). Diagnosing the decline in pharmaceutical R&D efficiency. *Nature Reviews Drug Discovery*, *11*(3), 191–200. https://doi.org/10.1038/nrd3681

Schaefer, C. F., Anthony, K., Krupa, S., Buchoff, J., Day, M., Hannay, T., & Buetow, K. H. (2009). PID: the Pathway Interaction Database. *Nucleic Acids Research*, *37*(2). https://doi.org/10.1093/nar/gkn653

Sehgal, S. N. (2003). Sirolimus: Its discovery, biological properties, and mechanism of action. *Transplantation Proceedings*, *35*(3 SUPPL.), S7–S14. https://doi.org/10.1016/S0041-1345(03)00211-2

Semba, S., Itoh, N., Ito, M., Harada, M., & Yamakawa, M. (2002). The in vitro and in vivo effects of 2-(4-morpholinyl)-8-phenylchromone (LY294002), a specific inhibitor of phosphatidylinositol 3′-kinase, in human colon cancer cells. *Clinical Cancer Research*, *8*(6), 1957–1963.

Siegel, R. L., Miller, K. D., & Jemal, A. (2018). Cancer statistics, 2018. *CA: A Cancer Journal for Clinicians*, *68*(1), 7–30. https://doi.org/10.3322/caac.21442

Siegel, R. L., Miller, K. D., & Jemal, A. (2019). Cancer statistics, 2019. *CA: A Cancer Journal for Clinicians*, *69*(1), 7–34. https://doi.org/10.3322/caac.21551

Singh, P., Dar, M. S., & Dar, M. J. (2016). p110α and p110β isoforms of PI3K signaling: are they two sides of the same coin? *FEBS Letters*, *590*(18), 3071–3082. https://doi.org/10.1002/1873-3468.12377

Smolle, E., Taucher, V., Petru, E., & Haybaeck, J. (2014). Targeted treatment of ovarian cancer - The multiple-kinase - Inhibitor sorafenib as a potential option. *Anticancer Research*, *34*(4), 1519–1530.

Stark, C., Breitkreutz, B.-J., Reguly, T., Boucher, L., Breitkreutz, A., & Tyers, M. (2006). BioGRID: a general repository for interaction datasets. *Nucleic Acids Research*, *34*, 535–539. https://doi.org/10.1093/nar/gkj109

Szklarczyk, D., Gable, A. L., Lyon, D., Junge, A., Wyder, S., Huerta-Cepas, J., … Von Mering, C. (2018). STRING v11: protein-protein association networks with increased coverage, supporting functional discovery in genome-wide experimental datasets. *Nucleic Acids Research*, *47*, 607–613. https://doi.org/10.1093/nar/gky1131

Szymonowicz, K., Oeck, S., Malewicz, N. M., & Jendrossek, V. (2018, March 18). New insights into protein kinase B/Akt signaling: Role of localized akt activation and compartment-specific target proteins for the cellular radiation response. *Cancers*, Vol. 10. https://doi.org/10.3390/cancers10030078

Taghizadeh, M., Safari-Alighiarloo, N., & Tavirani, M. R. (2015). PROTEIN-PROTEIN INTERACTION DATABASES : AN OVERALL VIEW ON INTERACTOME ORGANIZATION THE NATURE OF PROTEIN-PROTEIN Proteomics Research Center , Faculty of Paramedical Sciences , Shahid Beheshti University of Medical. *International Journal of Analytical, Pharmaceutical and Biomedical Sciences*, *4*(1), 15–23.

Tong, Z., Zhou, Y., & Wang, J. (2019). Identifying potential drug targets in hepatocellular carcinoma based on network analysis and one-class support vector machine. *Scientific Reports*, *9*(10442). https://doi.org/10.1038/s41598-019-46540-x

Wands, J. R., & Kim, M. (2014). WNT/β-catenin signaling and hepatocellular carcinoma. *Hepatology*, *60*(2), 452–454. https://doi.org/10.1002/hep.27081

Wehling, M. (2009). Assessing the translatability of drug projects: What needs to be scored to predict success? *Nature Reviews Drug Discovery*, *8*(7), 541–546. https://doi.org/10.1038/nrd2898

Wen, Z., Jiang, R., Huang, Y., Wen, Z., Rui, D., Liao, X., & Ling, Z. (2019). Inhibition of lung cancer cells and Ras/Raf/MEK/ERK signal transduction by ectonucleoside triphosphate phosphohydrolase-7 (ENTPD7). *Respiratory Research*, *20*(1), 194. https://doi.org/10.1186/s12931-019-1165-0

Whittaker, S., Marais, R., & Zhu, A. X. (2010). The role of signaling pathways in the development and treatment of hepatocellular carcinoma. *Oncogene*, *29*(36), 4989–5005. https://doi.org/10.1038/onc.2010.236

Wilhelm, S. M., Adnane, L., Newell, P., Villanueva, A., Llovet, J. M., & Lynch, M. (2008, October 1). Preclinical overview of sorafenib, a multikinase inhibitor that targets both Raf and VEGF and PDGF receptor tyrosine kinase signaling. *Molecular Cancer Therapeutics*, Vol. 7, pp. 3129–3140. https://doi.org/10.1158/1535-7163.MCT-08-0013

Wilhelm, S. M., Carter, C., Tang, L., Wilkie, D., Mcnabola, A., Rong, H., … Trail, P. A. (2004). BAY 43-9006 Exhibits Broad Spectrum Oral Antitumor Activity and Targets the RAF/MEK/ERK Pathway and Receptor Tyrosine Kinases Involved in Tumor Progression and Angiogenesis. In *CANCER RESEARCH* (Vol. 64).

Woo, J. H., Shimoni, Y., Yang, W. S., Subramaniam, P., Iyer, A., Nicoletti, P., … Califano, A. (2015). Elucidating Compound Mechanism of Action by Network Perturbation Analysis HHS Public Access. *Cell*, *162*(2), 441–451. https://doi.org/10.1016/j.cell.2015.05.056

Xenarios, I., Rice, D. W., Salwinski, L., Baron, M. K., Marcotte, E. M., & Eisenberg, D. (2000). DIP: the Database of Interacting Proteins. In *Nucleic Acids Research* (Vol. 28). Retrieved from http://dip.doe-mbi.ucla.edu/

Xie, Y., Shi, X., Sheng, K., Han, G., Li, W., Zhao, Q., … Gu, Y. (2019). PI3K/Akt signaling transduction pathway, erythropoiesis and glycolysis in hypoxia (Review). *Molecular Medicine Reports*, *19*(2), 783–791. https://doi.org/10.3892/mmr.2018.9713

Yadav, R. R., Guru, S. K., Joshi, P., Mahajan, G., Mintoo, M. J., Kumar, V., … Bharate, S. B. (2016). 6-Aryl substituted 4-(4-cyanomethyl) phenylamino quinazolines as a new class of isoform-selective PI3K-alpha inhibitors. *European Journal of Medicinal Chemistry*, *122*, 731–743. https://doi.org/10.1016/j.ejmech.2016.07.006

Yang, S., & Liu, G. (2017, March 1). Targeting the RAS/RAF/MEK/ERK pathway in hepatocellular carcinoma. *Oncology Letters*, Vol. 13, pp. 1041–1047. https://doi.org/10.3892/ol.2017.5557

Yazdani, H., Huang, H., & Tsung, A. (2019). Autophagy: Dual Response in the Development of Hepatocellular Carcinoma. *Cells*, *8*(2), 91. https://doi.org/10.3390/cells8020091

Yuzugullu, H., Benhaj, K., Ozturk, N., Senturk, S., Celik, E., Toylu, A., … Ozturk, M. (2009). Canonical Wnt signaling is antagonized by noncanonical Wnt5a in hepatocellular carcinoma cells. *Molecular Cancer*, *8*, 90. https://doi.org/10.1186/1476-4598-8-90

Zeng, H., Wu, H. C., Wang, Q., Yang, H. I., Chen, C. J., Santella, R. M., & Shen, J. (2017). Telomere length and risk of hepatocellular carcinoma: A nested case-control study in Taiwan cancer screening program cohort. *Anticancer Research*, *37*(2), 637–644. https://doi.org/10.21873/anticanres.11358

Zhan, Y., Shen, L., Xu, W., Wu, X., Zhang, W., Wang, J., … Xu, K. F. (2018). Functional improvements in patients with lymphangioleiomyomatosis after sirolimus: An observational study. *Orphanet Journal of Rare Diseases*, *13*(1). https://doi.org/10.1186/s13023-018-0775-9

Zhang, Q., Yang, M., Qu, Z., Zhou, J., & Jiang, Q. (2016). Autophagy prevention sensitizes AKTi-1/2-induced anti-hepatocellular carcinoma cell activity in vitro and in vivo. *Biochemical and Biophysical Research Communications*, *480*(3), 334–340. https://doi.org/10.1016/j.bbrc.2016.10.043

Zhu, J., Ke, K., Xu, L., & Jin, J. (2019). Discovery of a novel phosphoinositide 3-kinase gamma (PI3Kγ) inhibitor against hematologic malignancies and theoretical studies on its PI3Kγ-specific binding mechanisms. *RSC Advances*, *9*(35), 20207–20215. https://doi.org/10.1039/c9ra02649e

APPENDIX A

Visual Illustrations of the Clustered Versions of the Reconstructed HCC Networks (PI3K Inhibitors and Akti-1-2) Representative Images

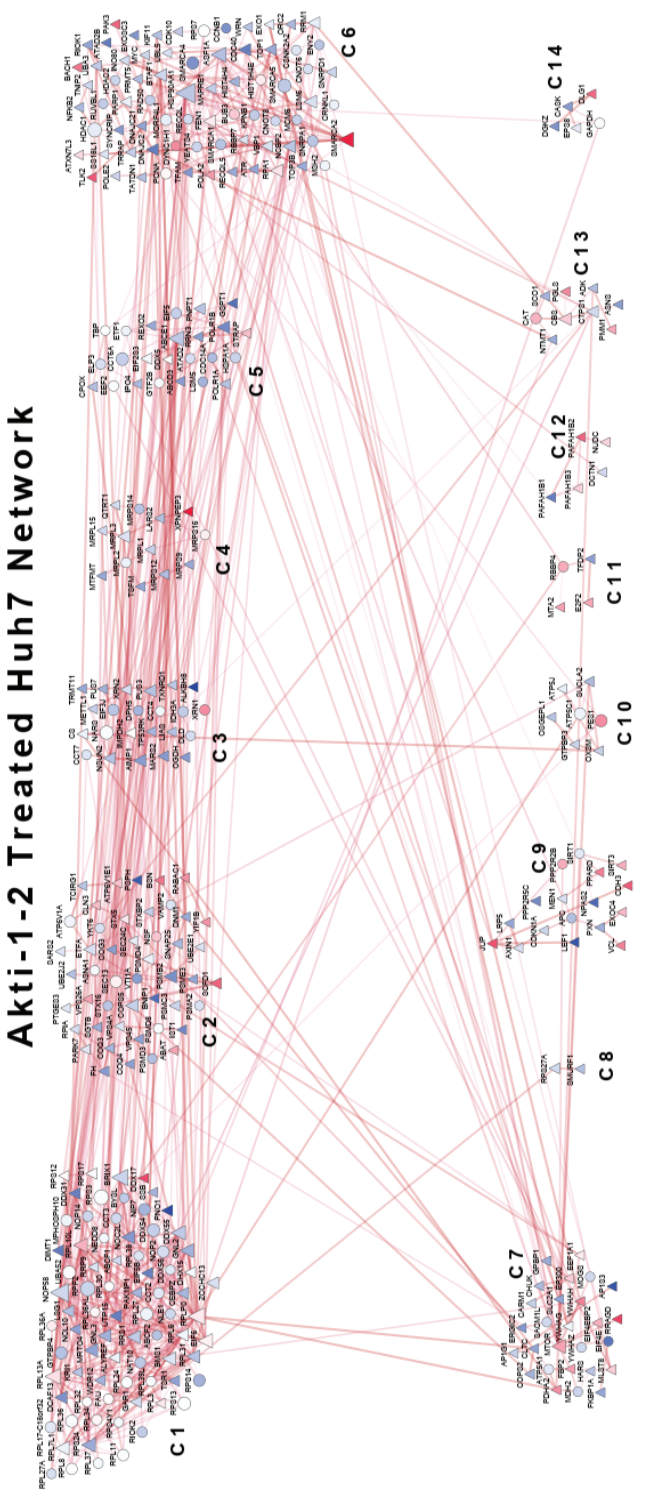

Figure A.1: Visual network image of the clustered version of Akti-1-2 treated Huh7 network. Total number of nodes in this network is 334, also the number of edges is 778. The network is divided into 14 distinct clusters.

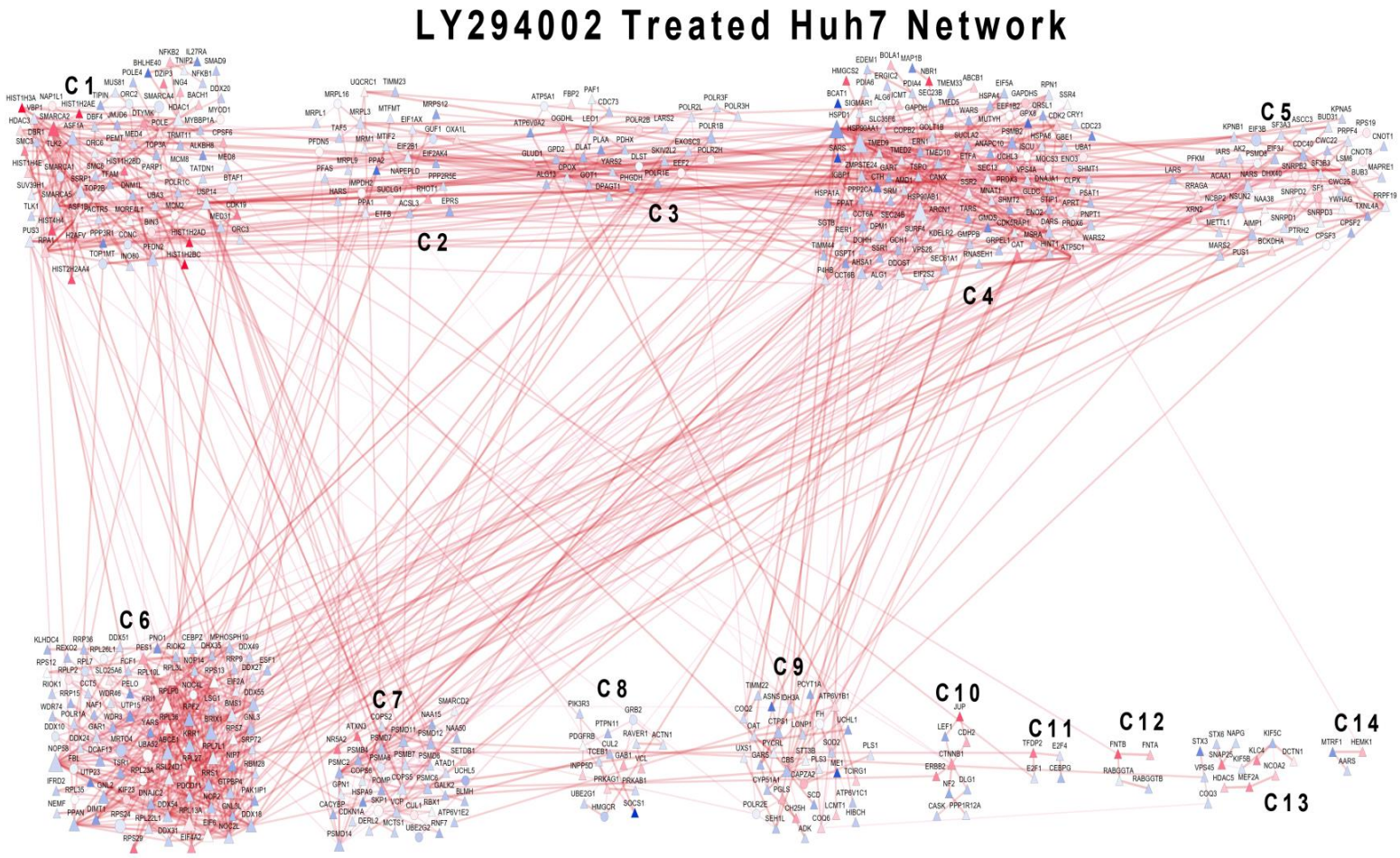

Figure A.2: Visual illustration of the clustered version of LY294002 treated Huh7 network. The network is separated into 14 distinct clusters. Total number of nodes in this network is 505, also the number of edges is 1298.

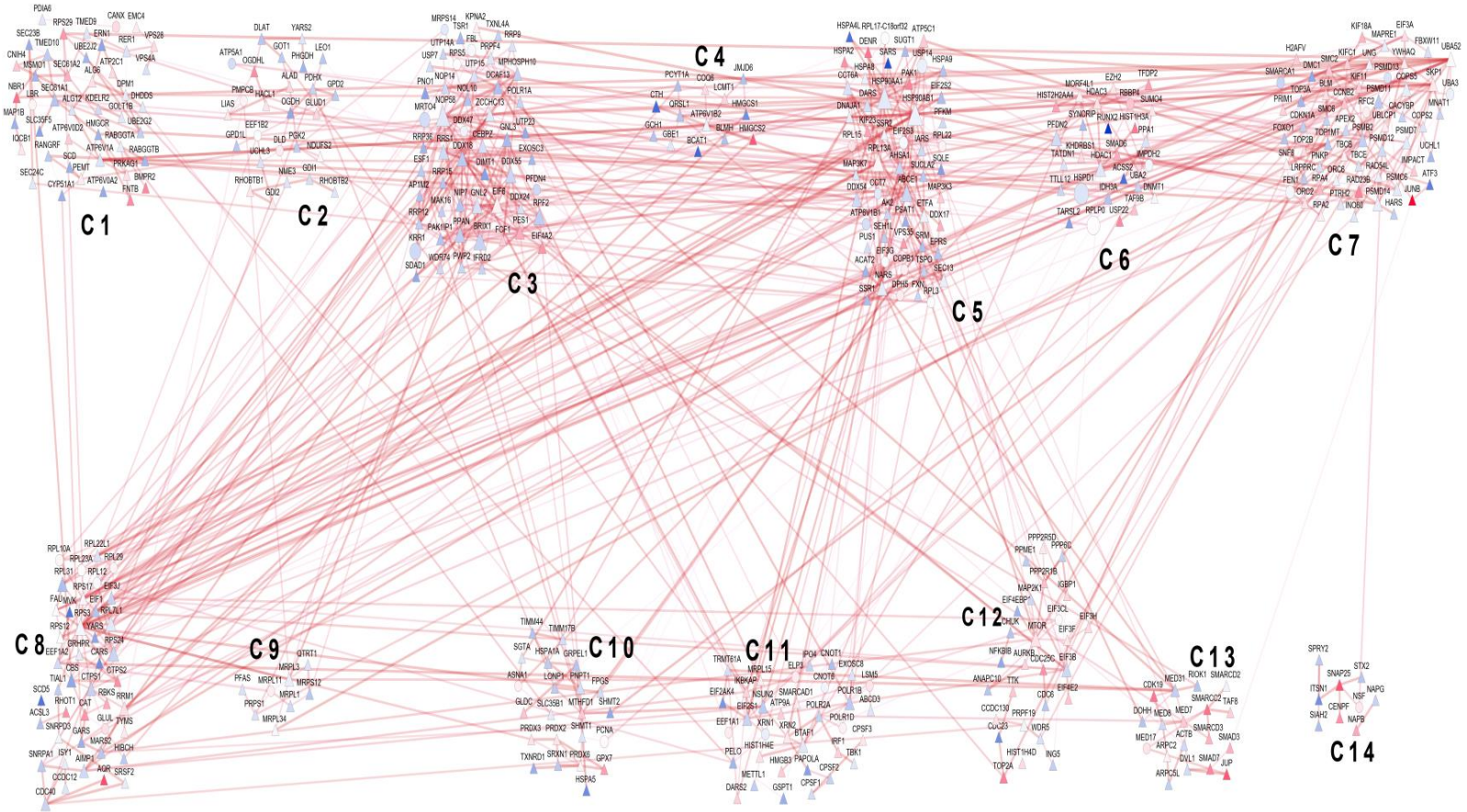

Figure A.3: Visual depicted network illustration of the clustered version of Rapamycin treated Huh7 network. Total number of nodes in this network is 431, also the number of edges is 904. The network is separated into 14 distinct clusters.

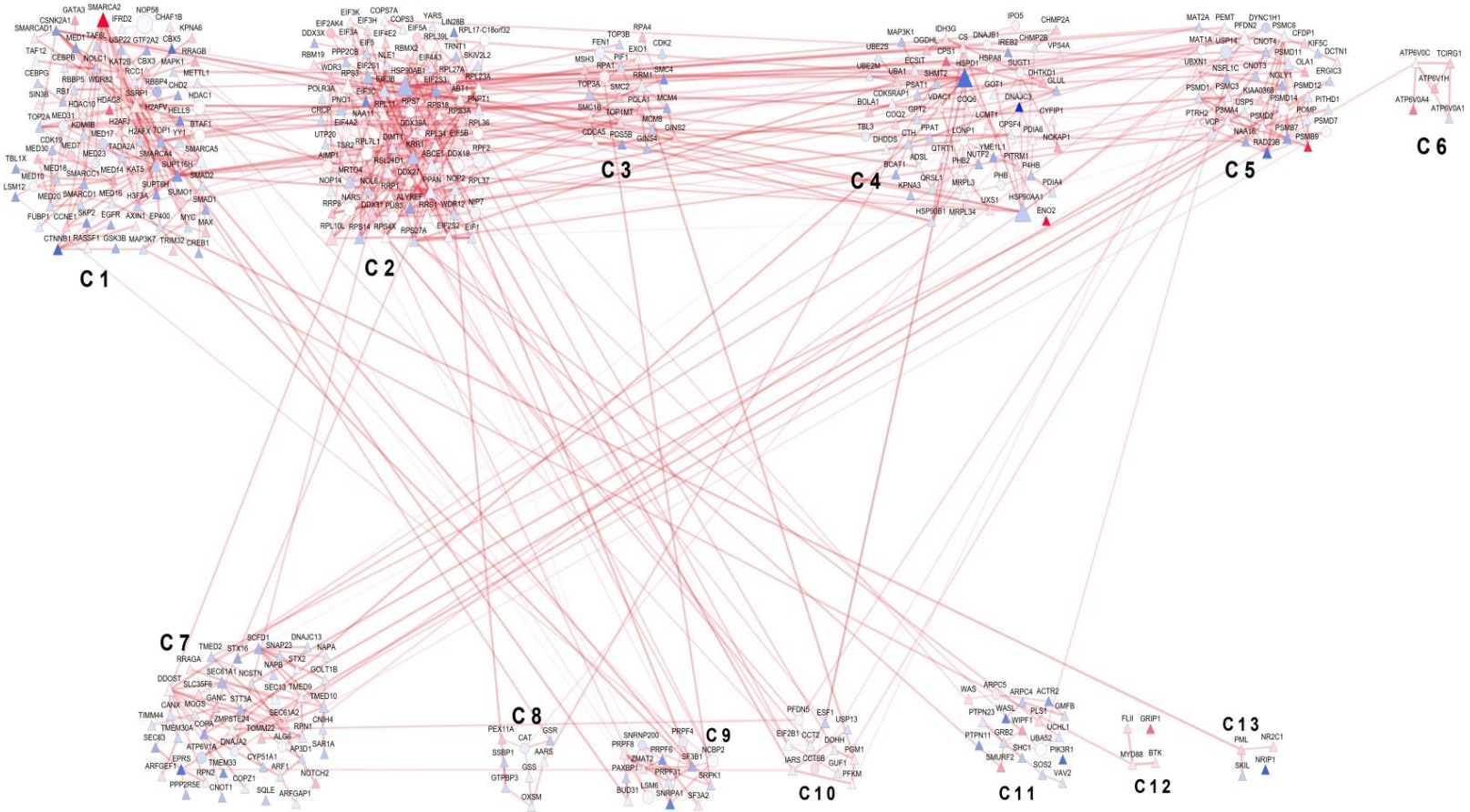

Figure A.4: Visual depicted representation of the clustered version of Wortmannin treated Huh7 network. Total number of nodes in this network is 383, also the number of edges is 797. The network is separated into 13 distinct clusters.

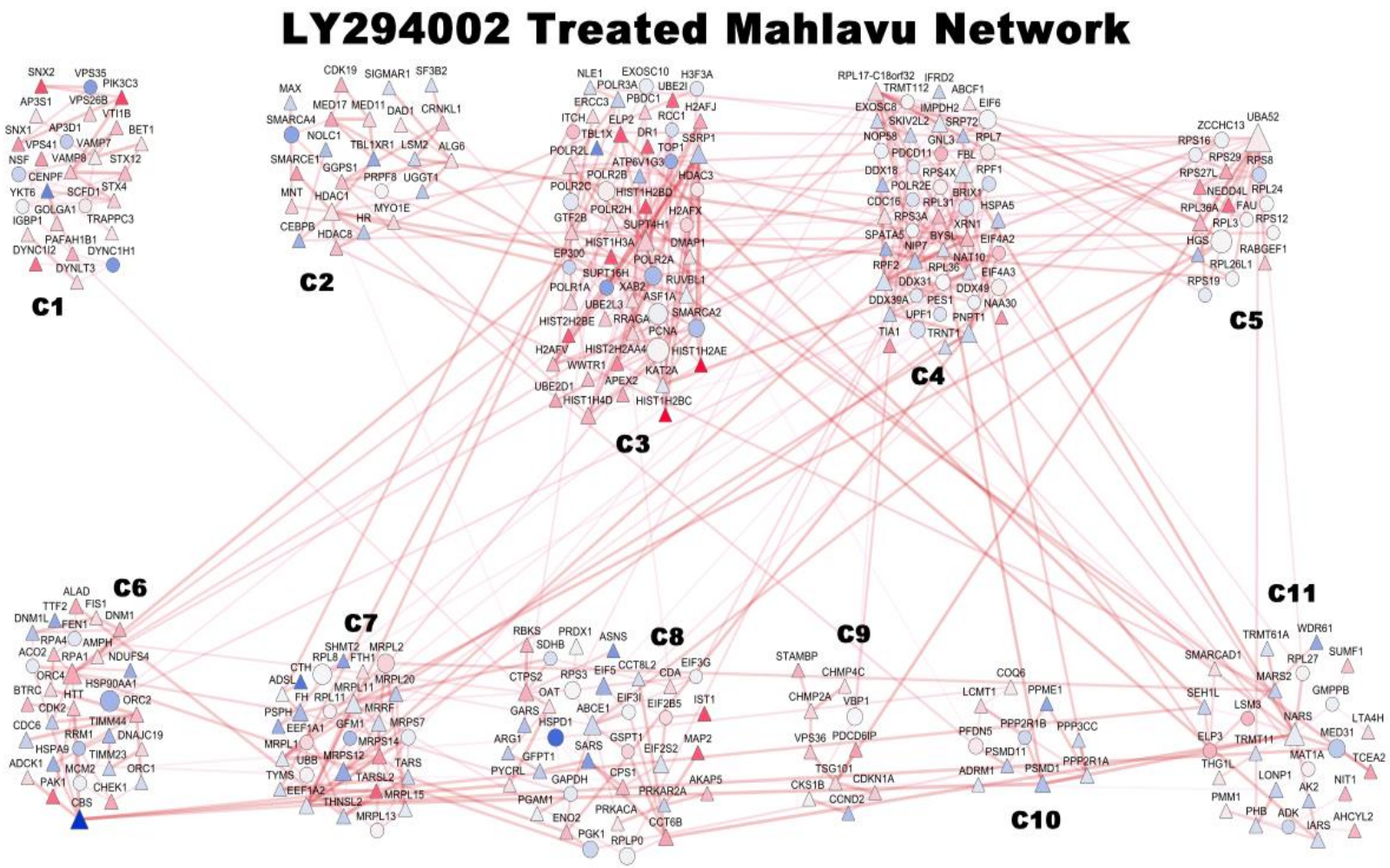

Figure A.5: Visual representational image of the clustered version of LY294002 treated Mahlavu network. Total number of nodes in this network is 287, and the number of edges is 539, as well. The network is grouped into 11 different clusters.

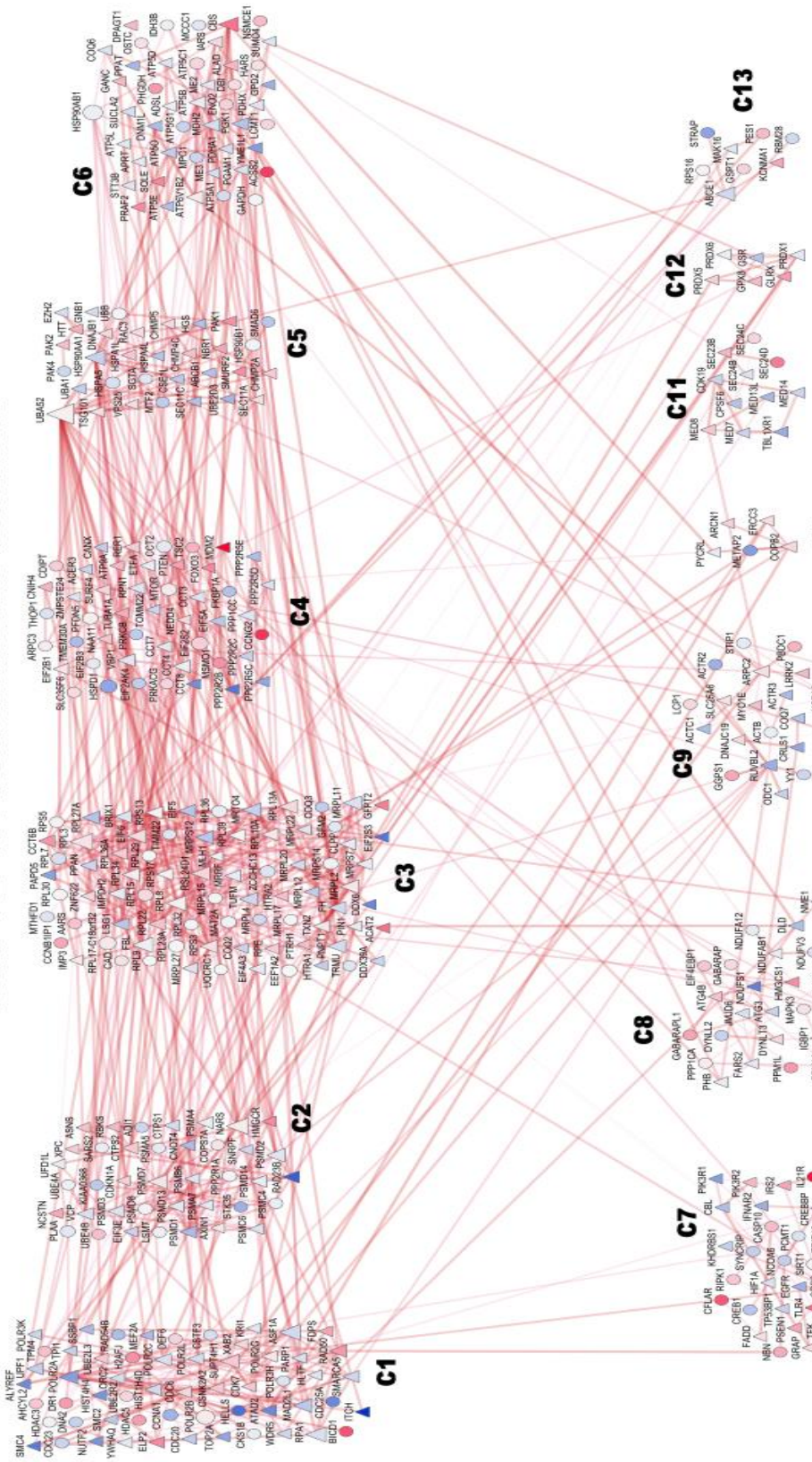

Figure A.6: Visual representational figure of the clustered version of Akti-1-2 treated Mahlavu network. The network is separated into 13 different clusters. Total number of nodes in this network is 402, and the number of edges is 943.

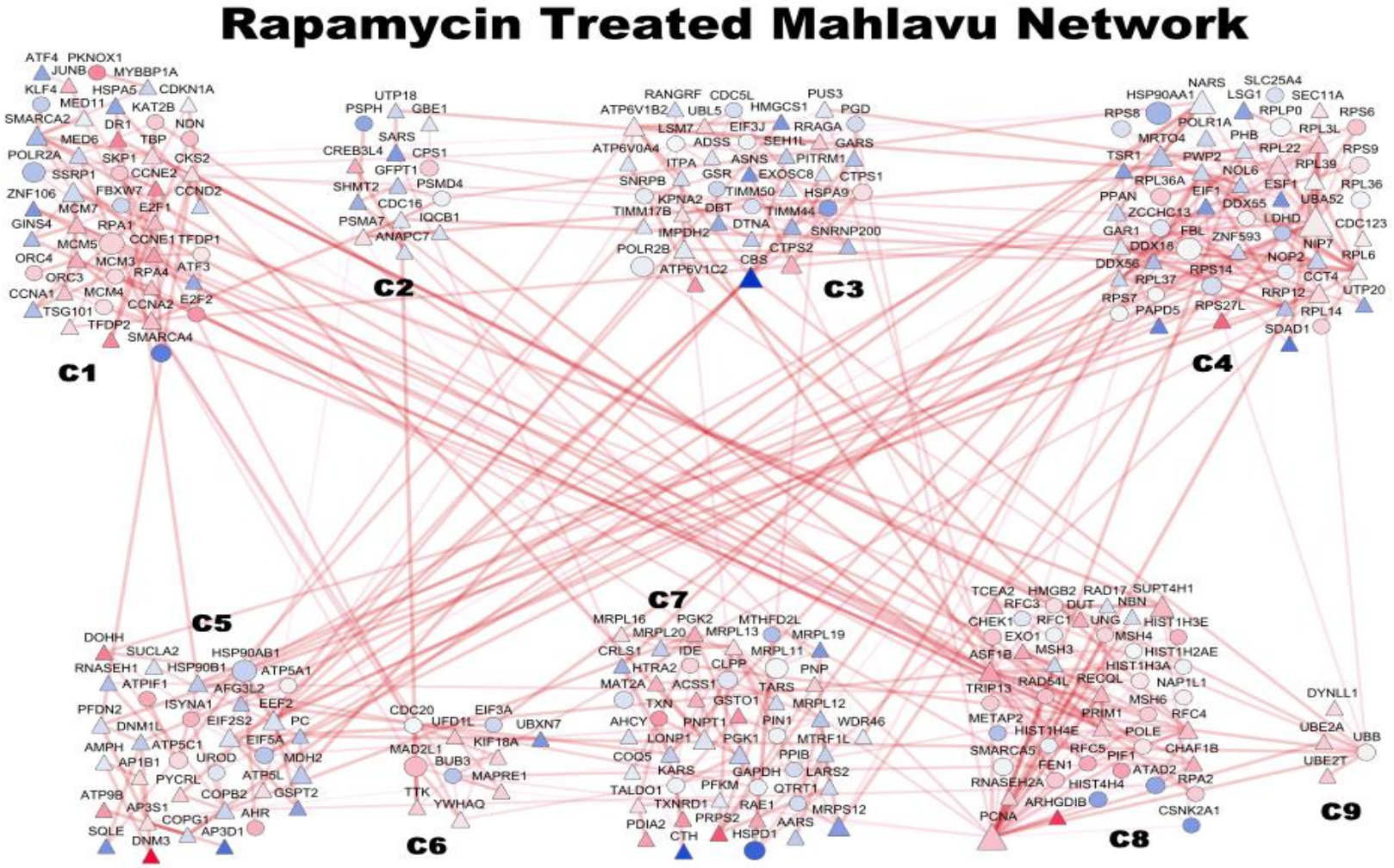

Figure A.7: Visual representation of the clustered version of Rapamycin treated Mahlavu network. Total number of nodes in this network is 259, and the number of edges is 532, as well. The network is divided into 9 different clusters.

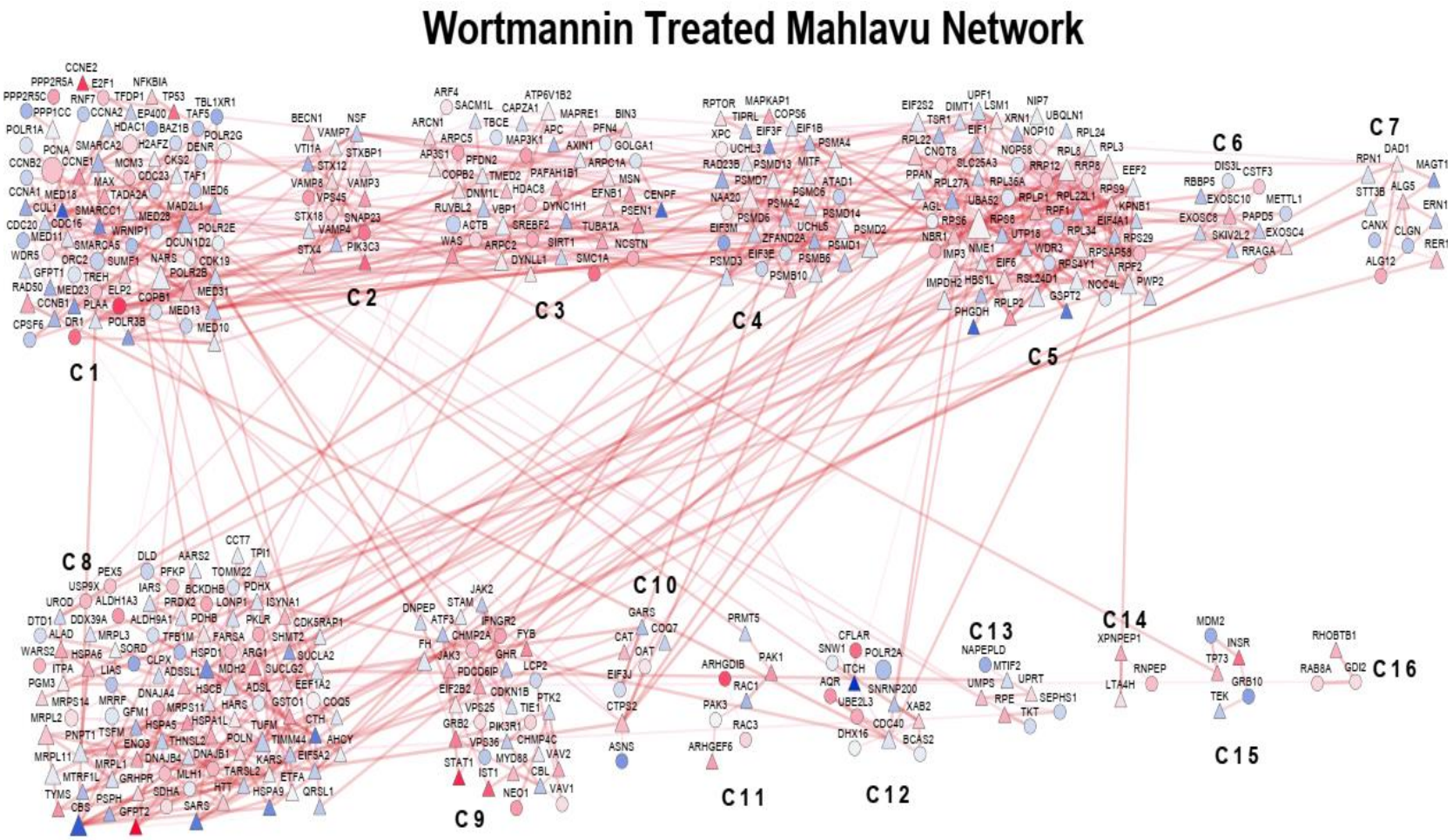

Figure A.8: Visual depicted representation of the clustered version of Wortmannin treated Mahlavu network. The network is divided into 16 different clusters. Total number of nodes in this network is 369, and the number of edges is 809.

APPENDIX B

Functional Enrichment Analyses of the Networks

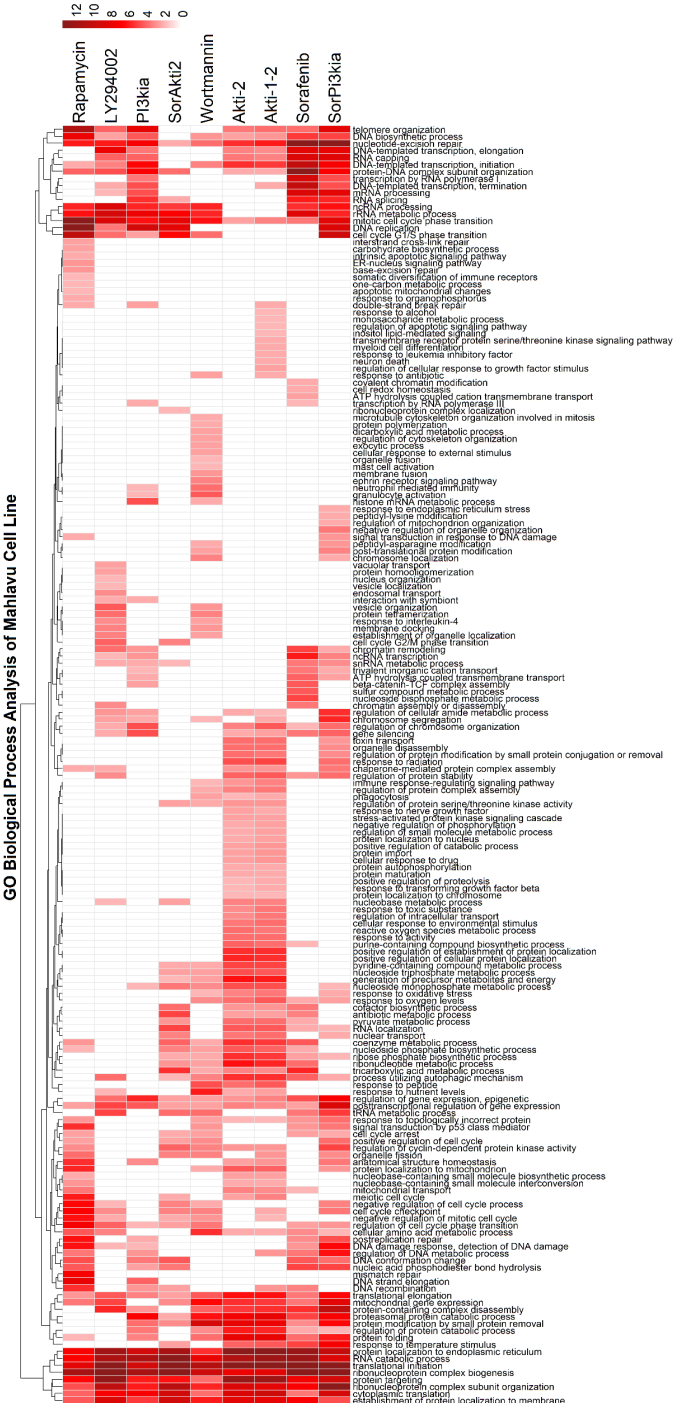

Figure B.1: GO biological process no redundant overrepresentation enrichment analysis of Mahlavu cell line was performed by WebGestaltR package. Heatmap demonstrates enriched biological process terms for each specific reconstructed Mahlavu network. Functional enrichment terms were listed by a given threshold, FDR ≤ 0.01. Subsequently, we took the negative logarithm base 10 of FDR values of significantly enriched terms. The total number of enriched terms in the heatmap is 182.

Figure B.2: GO biological process no redundant overrepresentation enrichment analysis of Huh7 cell line was performed by WebGestaltR package. Heatmap demonstrates enriched biological process terms for each specific reconstructed Huh7 network. Functional enrichment terms were listed by a given threshold, FDR ≤ 0.01. Next, we took the negative logarithm base 10 of FDR values of significantly enriched terms. The total number of enriched terms in this heatmap is 146.

Figure B.3: KEGG pathway enrichment analysis of Huh7 cells was performed by WebGestaltR. Heatmap demonstrates enriched KEGG pathway terms for each specific reconstructed Huh7 network. Functional enrichment terms were listed by a given threshold, FDR ≤ 0.05. The total number of enriched terms in this heatmap is 41. Additionally, we took the negative logarithm base 10 of FDR values of significantly enriched terms. The color intensity, based on adjusted logarithmic scale of FDR values, shows the level of significancy of the corresponding functional enrichments. Unless there is any enrichment score for the corresponding specific category of KEGG pathway enrichment terms in the network, white color is depicted for this purpose in the heatmap.

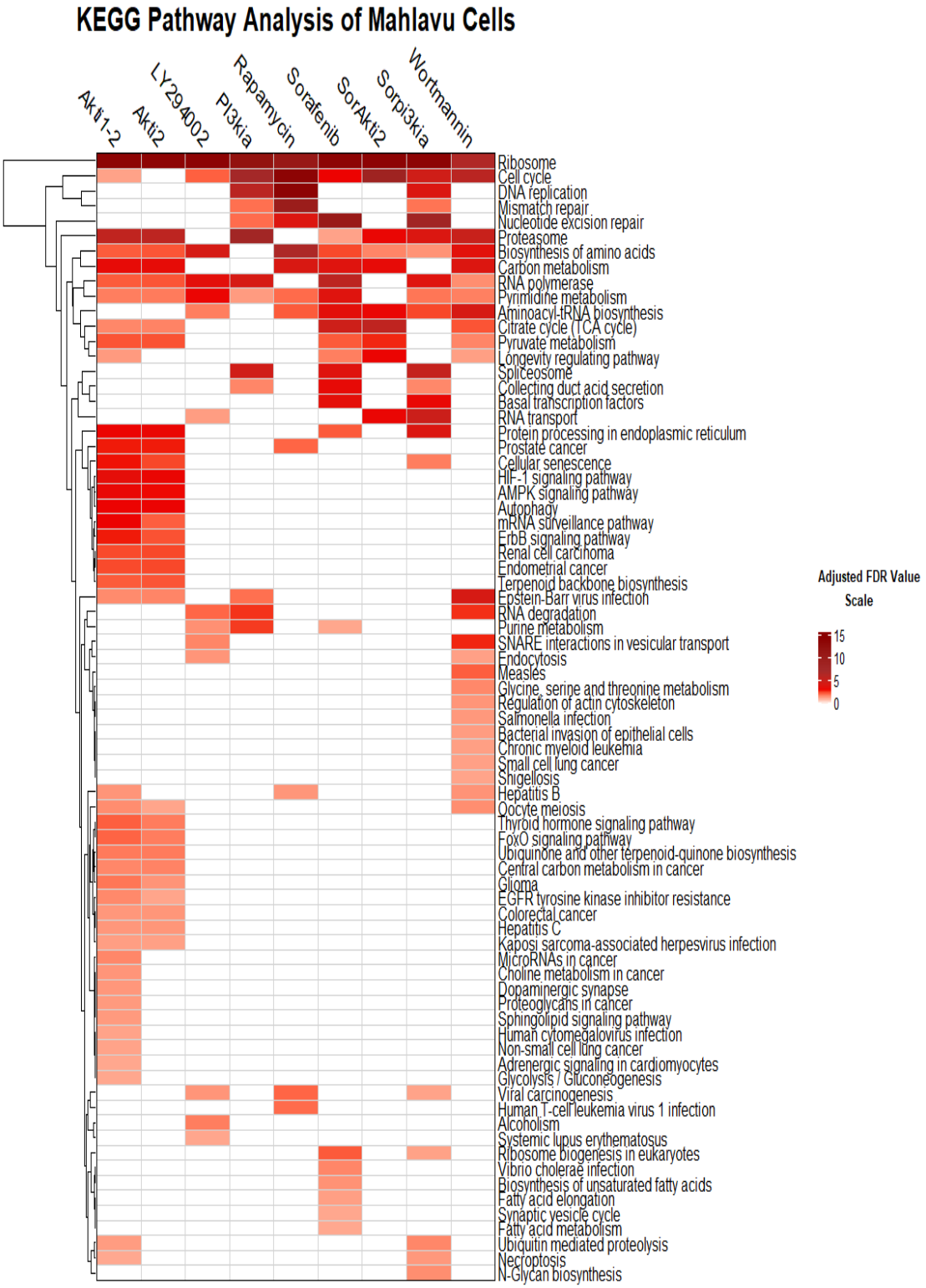

Figure B.4: Heatmap demonstrates enriched KEGG pathway terms for each specific reconstructed Mahlavu network. Functional enrichment terms were listed by a given threshold, FDR ≤ 0.05. The total number of enriched terms in this heatmap is 75. Moreover, we took the negative logarithm base 10 of FDR values of significantly enriched terms. The color intensity, based on adjusted logarithmic scale of FDR values, shows the level of significancy of the corresponding functional enrichments.

Figure B.5: GO molecular function no redundant ORA of Huh7 cells was performed by WebGestaltR. Heatmap demonstrates enriched molecular function terms for each specific reconstructed Huh7 network. Functional enrichment terms were listed by a given threshold, FDR ≤ 0.05. The total number of enriched terms in this heatmap is 55. Afterwards, we took the negative logarithm base 10 of FDR values of significantly enriched terms. The color intensity, based on adjusted logarithmic scale of FDR values, shows the level of significancy of the corresponding functional enrichments. Unless there is any enrichment score for the corresponding specific category of molecular function enrichment terms in the network, white color is depicted for this purpose in the heatmap.

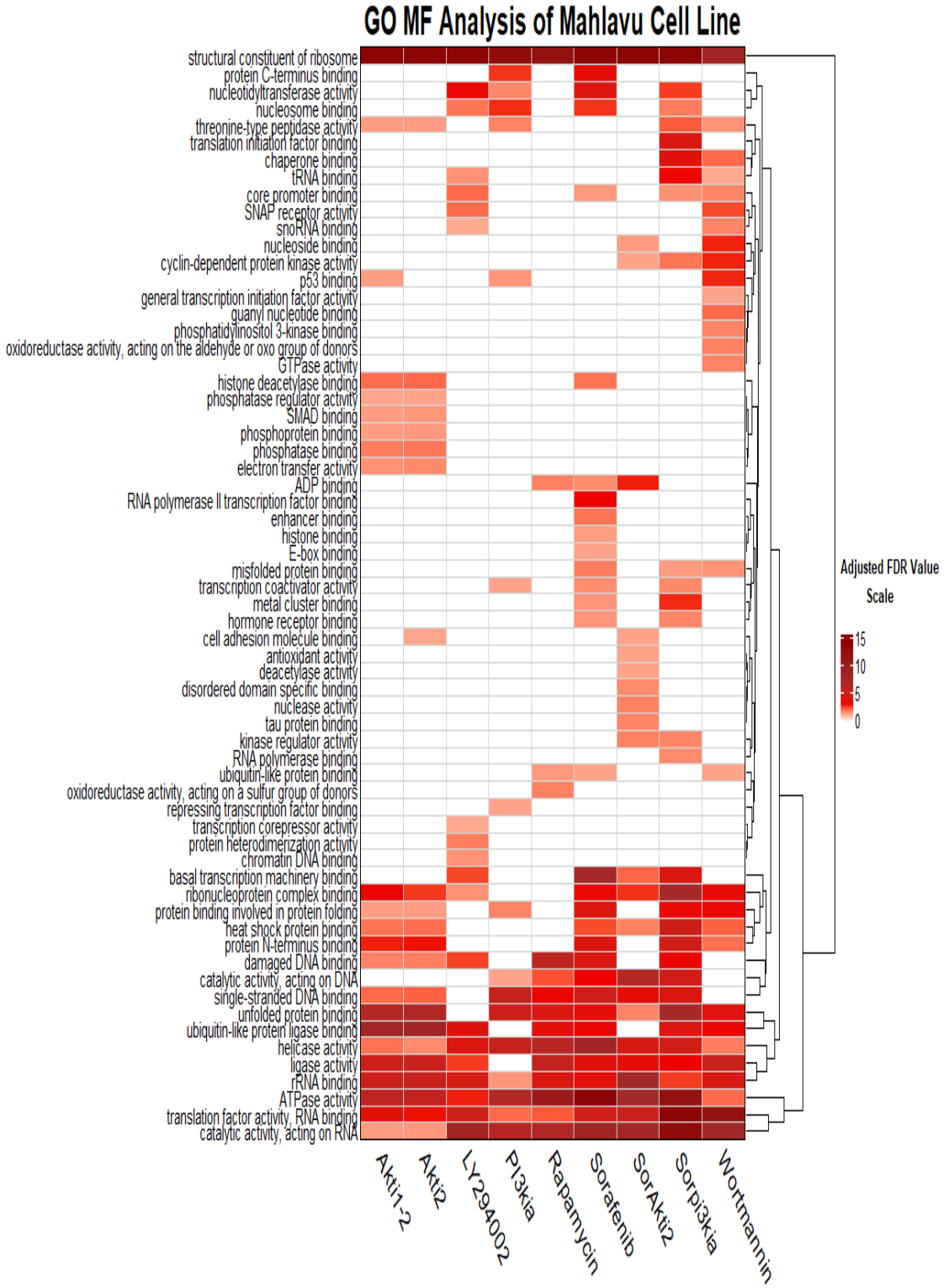

Figure B.6: GO molecular function no redundant ORA of Mahlavu cells was performed by WebGestaltR. Heatmap demonstrates enriched molecular function terms for each specific reconstructed Mahlavu network. Functional enrichment terms were listed by a given threshold, FDR ≤ 0.05. The total number of enriched terms in this heatmap is 64. Following that, we took the negative logarithm base 10 of FDR values of significantly enriched terms. The color intensity, based on adjusted logarithmic scale of FDR values, shows the level of significancy of the corresponding functional enrichments. Unless there is any enrichment score for the corresponding specific category of molecular function enrichment terms in the network, white color is depicted for this purpose in the heatmap.

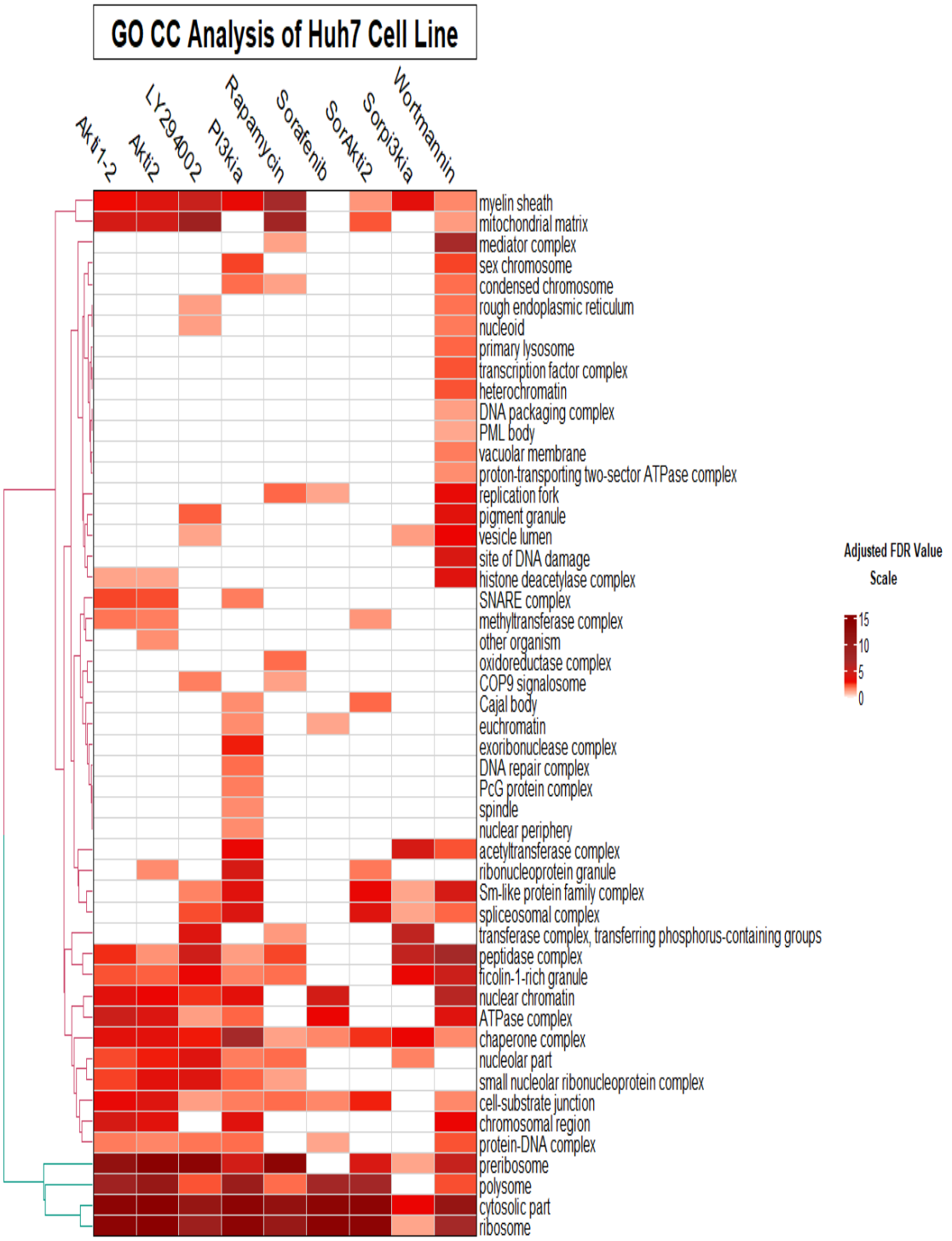

Figure B.7: GO cellular component no redundant ORA of Huh7 cells was performed by WebGestaltR. Heatmap demonstrates enriched cellular component terms for each specific reconstructed Huh7 network. Functional enrichment terms were listed by a given threshold, FDR ≤ 0.05. The total number of enriched terms in this heatmap is 50. Further, we took the negative logarithm base 10 of FDR values of significantly enriched terms. The color intensity, based on adjusted logarithmic scale of FDR values, shows the level of significancy of the corresponding functional enrichments. Unless there is any enrichment score for the corresponding specific category of cellular component enrichment terms in the network, white color is depicted for this purpose in the heatmap.

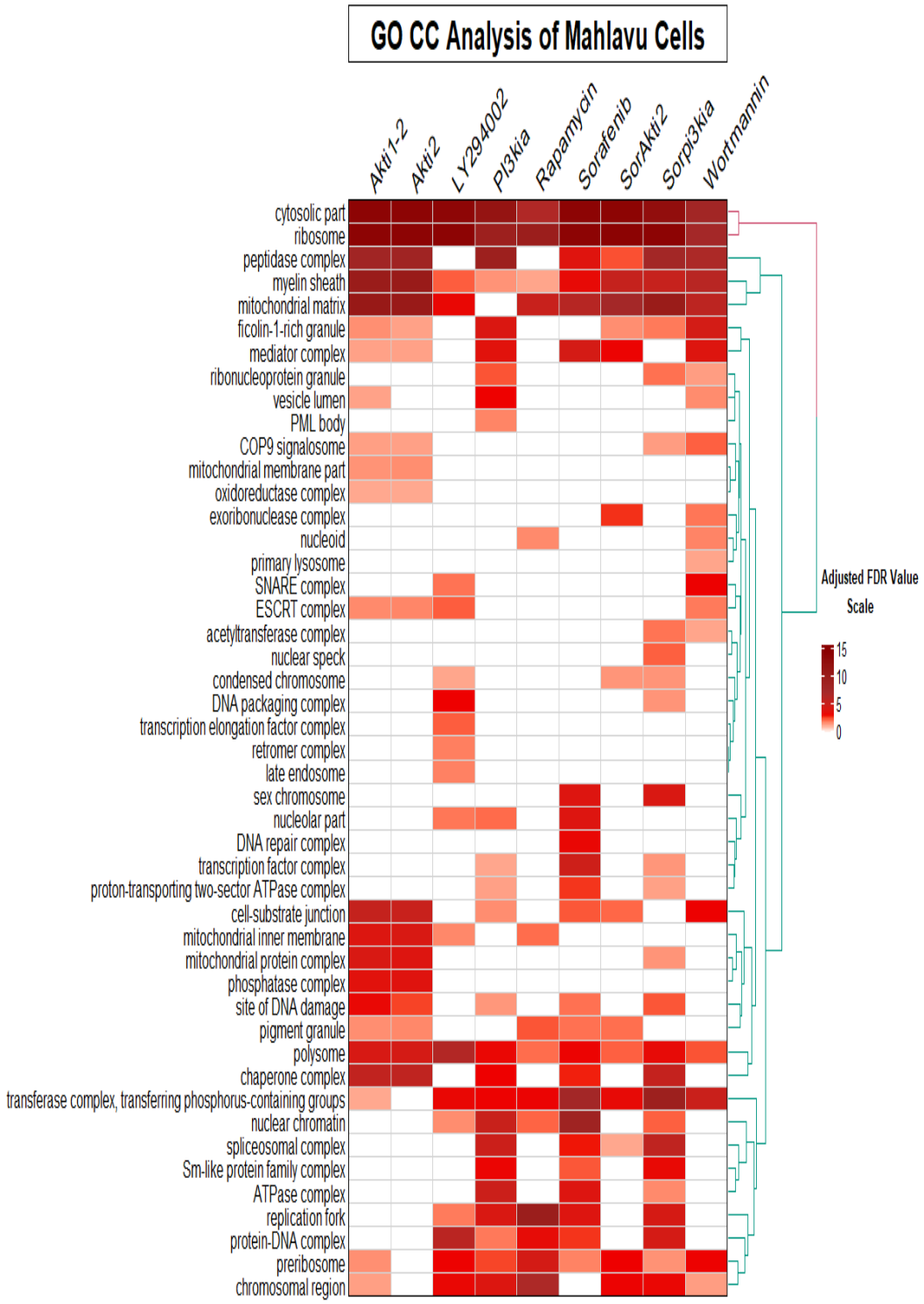

Figure B.8: GO cellular component no redundant ORA of Mahlavu cells was performed by WebGestaltR. Heatmap demonstrates enriched cellular component terms for each specific reconstructed Mahlavu network. Functional enrichment terms were listed by a given threshold, FDR ≤ 0.05. The total number of enriched terms in this heatmap is 47. Furthermore, we took the negative logarithm base 10 of FDR values of significantly enriched terms. The color intensity, based on adjusted logarithmic scale of FDR values, shows the level of significancy of the corresponding functional enrichments. Unless there is any enrichment score for the corresponding specific category of cellular component enrichment terms in the network, white color is depicted for this purpose in the heatmap.